Role of HNF4α in Liver Regeneration, Liver Cancer Pathogenesis and Global Metabolism

By
Ian Huck

Submitted to the graduate degree program in Pharmacology, Toxicology and Therapeutics and the Graduate Faculty of the University of Kansas in partial fulfillment of the requirements for the degree of Doctor of Philosophy.

Chair: Udayan Apte, PhD, DABT

Hartmut Jaeschke, PhD

Tiangang Li, PhD

John Thyfault, PhD, FACSM, FTOS

Steven Weinman, MD, PhD

Date Defended: November 27, 2018

The dissertation committee for Ian Huck certifies that this is the approved version of the following dissertation:

Role of HNF4α in Liver Regeneration, Liver Cancer Pathogenesis and Global Metabolism

_____

Chair: Udayan Apte, PhD, DABT

Date Approved: November 27, 2018

Abstract

Liver is the central metabolic organ and performs many functions necessary for survival. Hepatocyte Nuclear Factor 4 alpha (HNF4α) is a nuclear receptor well characterized for its role in embryonic hepatocyte differentiation and maintenance of the adult hepatocyte phenotype. HNF4α regulates genes involved in many basic hepatocyte functions and deletion or decreased expression of HNF4α results in impaired liver function. More recently, HNF4α has been shown to exhibit tumor suppressor activity and deletion of HNF4α results in hepatocyte proliferation. The objectives of these studies were to characterize the role of hepatic HNF4α in hepatocyte proliferation and metabolism during liver regeneration and to harness HNF4α activity as a prognostic tool in liver cancer.

The remarkable ability of liver to regenerate is possible due to the innate proliferative potential of quiescent adult hepatocytes. Knowing the role of HNF4α in maintaining hepatocyte function and suppressing hepatocyte proliferation, we hypothesized that HNF4α activity and expression may be adjusted to navigate hepatocytes between proliferative and quiescent states during liver regeneration. Using the partial hepatectomy model of liver regeneration, we identified decreased HNF4α activity in livers during the initiation of hepatocyte proliferation. Overexpression of HNF4α delayed hepatocyte proliferation after partial hepatectomy, and we identified Src-kinase as a potential regulator of HNF4α during the initiation of regeneration. Hepatocyte-specific deletion of HNF4α in mice (HNF4α-KO mice) resulted in 100% mortality after partial hepatectomy. RNA-Seq analysis of livers from these mice revealed significant dedifferentiated, and increased activation of proliferative and carcinogenic pathways. Our results show that

HNF4α is required to prevent hepatic failure after liver regeneration, is a critical regulator of termination of regeneration and provide new understanding of HNF4α position in regenerative networks.

Downregulation of HNF4α has been well recognized in the progression of liver disease. We hypothesized that HNF4α activity could be used in the diagnosis and prognosis of liver diseases. Under the assumption that HNF4α activity could best be quantified by its target gene transcription, we identified a set of 44 genes by selecting only those genes that were direct HNF4α targets which were differentially regulated between WT and HNF4α-KO livers in normal and in liver tumors. qPCR analysis was used to validate the signature in mouse models of HNF4α deletion and liver cancer. Using this method, we detected lower HNF4α activity in human cirrhotic samples when compared to HCC samples. While no correlation was observed between disease state and the HNF4α staining pattern in diseased human tissues, the signature was able to accurately classify the severity of samples based on HNF4α activity. Further in silico analysis using human datasets confirmed the signatures ability to diagnose the severity of disease according to HNF4α activity. Lastly, when this analysis was performed on a dataset of human cirrhotic samples, we observed increased survival in a subset of cirrhotic samples with high HNF4α activity as determined by the signature.

The role of HNF4α in regulating carbohydrate and lipid metabolism has been well studied, but how it effects overall global metabolism is not known. We used indirect calorimetry to examine

changes in energy expenditure and substrate utilization between WT and HNF4α-KO mice in fed, fasted, and high fat diet-fed conditions. We observed significant decreases in energy expenditure in HNF4α-KO mice during fed conditions which were exacerbated during high fat diet feeding. The changes were accompanied by significant adipose depletion and hypoglycemia. Our findings bring focus to the central role of liver in metabolism, which is largely regulated by hepatocyte HNF4α.

Altogether, these studies indicate that hepatic HNF4α is a critical regulator of liver regeneration and global metabolism. Further, hepatic HNF4α activity can be used as a prognostic tool in chronic liver diseases such as cirrhosis and cancer.

Table of Contents

Chapter 1. Introduction

Portions of this chapter have been submitted and accepted for publication December 5, 2018. Huck, I., Gunewardena, S., Espanol-Suner, R., Willenbring, H., & Apte, U. (2018). Hepatocyte Nuclear Factor 4 alpha (HNF4alpha) Activation is Essential for Termination of Liver Regeneration. *Hepatology*. doi:10.1002/hep.30405

Portions of this chapter have been previously published as a preprint and have not been peer-reviewed. Huck, I., Morris, E. M., Thyfault, J. P., & Apte, U. (2018). Hepatocyte-Specific Hepatocyte Nuclear Factor 4 alpha (HNF4α) Deletion Decreases Resting Energy Expenditure By Disrupting Lipid and Carbohydrate Homeostasis. *bioRxiv*, 401802. doi:10.1101/401802

1.1. Introduction to HNF4α

1.1.1. Highly conserved nuclear receptor

Hepatocyte Nuclear Factor 4 alpha (HNF4α) is a zinc finger containing nuclear receptor first discovered bound to the transthyretin (TTR) and apolipoprotein CIII (apoCIII) promoter in rat liver extracts (Sladek, Zhong, Lai, & Darnell, 1990). Evidence from simple metazoans like trichoplax, coral and sponges suggest that HNF4α is one of the oldest nuclear receptors conserved during evolution (Baker, 2008; Grasso et al., 2001; Larroux et al., 2006). HNF4α is expressed by all animals (Sladek, 2011), and its DNA binding motifs are highly conserved in livers of chickens, opossums, dogs, mice and humans (Schmidt et al., 2010). HNF4α binds as a homodimer (Chandra et al., 2013) to direct repeat elements within the genome (Fang, Mane-Padros, Bolotin, Jiang, & Sladek, 2012). Functional targets of HNF4α are conserved between mice and humans (Boj et al., 2009).

Reports have shown that myristic acid can bind the HNF4α ligand binding domain (LBD) in HNF4α protein synthesized by bacteria (Dhe-Paganon, Duda, Iwamoto, Chi, & Shoelson, 2002) and linoleic acid can bind HNF4α in mammalian cells and mouse liver during fed, but not fasted conditions (Yuan et al., 2009). However, binding of these fatty acids does not significantly alter HNF4α transcriptional activity. Instead, the authors suggest binding may increase the structural integrity and half-life of the HNF4α protein. The discovery of a strong agonist or antagonist of HNF4α remains elusive.

1.1.2. HNF4α isoforms

Multiple isoforms of HNF4α are produced from 2 promoters and the splicing of RNA and protein. In liver, a P2 promoter activates transcription of fetal HNF4α during embryonic liver development. After birth, the P2 promoter is silenced and a P1 promoter activates transcription of adult HNF4α isoforms (Torres-Padilla, Fougere-Deschatrette, & Weiss, 2001). The P2 promoter is activated by HNF6 and HNF1 during embryonic liver development. Expression of adult HNF4α expression slowly increases throughout embryonic development until a certain threshold, at which point adult HNF4α isoforms silence the P2 promoter in adult liver (Briancon et al., 2004).

The activity of fetal and adult HNF4α isoforms are similar but distinct. Adult and fetal HNF4α isoforms exhibit differential interaction with proteins including CBP, GRIP-1, p300, SMRT and HDACs due to differences in activation function domains between the isoforms (Torres-Padilla, Sladek, & Weiss, 2002). In colorectal cancer cells, P1-driven and P2-driven HNF4α isoforms can bind to different DNA binding motifs, associate with different coactivators and interact with other signaling pathways in a unique manner resulting in mainly tumor suppressor activity from adult isoforms and primarily growth promoting activity from fetal HNF4α (Vuong et al., 2015). While expression of fetal and adult HNF4α isoforms are mutually exclusive in normal liver, both isoforms are expressed in the colon where adult isoforms are primarily expressed in the differentiated colonic crypt and fetal isoforms are expressed in the proliferative compartment. Transgenic mice expressing exclusively fetal isoforms develop colitis and are at higher risk of developing colon cancer (Chellappa et al., 2016). In the pancreas, P2-driven HNF4α is

exclusively expressed (Harries et al., 2008; Tanaka et al., 2006) and P2 isoforms are required for proliferation and expansion of β-cells (Gupta et al., 2007). Moreover, overexpression of P2-driven HNF4α is sufficient to initiate cell cycle in human β-cells (Rieck et al., 2012). In human hepatocellular carcinoma (HCC), adult HNF4α isoform expression is negatively correlated with fetal isoform expression. HCCs expressing high levels of fetal isoforms are associated with decreases survival compared to HCCs with high adult isoform expression (Cai, Lu, Liu, Zhang, & Yun, 2017).

1.2. The Role of HNF4α in Embryonic Liver Development

HNF4α is considered a marker of hepatocyte differentiation. However, its pro-differentiation activity exists long before hepatocytes develop. Examination of differentially expressed genes between different stages of early zygote division have shown that upregulation of networks activated by HNF4α are important for the first division of a single celled zygote (Godini & Fallahi, 2018), although this study did not investigate HNF4α mRNA or protein expression. However, HNF4α is considered to be a marker of primary endoderm since HNF4α mRNA can be detected in primary endoderm at embryonic day 4.5. HNF4α mRNA expression occurs in liver diverticulum and hindgut at day 8.5 and later in the mesonephric tubules, pancreas, stomach, intestine, and metanephric tubules (Duncan et al., 1994). Homozygous loss of HNF4α is embryonically lethal due to impaired gastrulation (Chen et al., 1994), and complementation of HNF4α into HNF4α null embryos restores HNF4α expression in the visceral endoderm and rescues gastrulation (Duncan, Nagy, & Chan, 1997). A later study using this same model system showed that while HNF4α is not required for hepatic specification or the formation of

hepatoblasts, it is required for hepatic expression of gene critical for liver function (albumin, apolipoproteins, aldolaseB, PAH, LFABP, TFN RBP, EPO) as well as the transcription factors HNF1α and PXR (J. Li, Ning, & Duncan, 2000). Livers of hepatoblast-specific HNF4α-KO embryos (generated using alpha fetoprotein-CRE) showed significant disruptions in cell shape and lobule structure, likely caused by decreased expression of E-cadherin and gap junction proteins. These mice also exhibited decreased hepatic glycogen. HNF4α is required for establishing expression of other hepatic transcription factors (HNF1α, HNF1β, FOXA2, HNF6, LRH1, FXR, PXR) (Kyrmizi et al., 2006). Expression of HNF4α is also important for commitment of hepatoblasts to a hepatocyte lineage rather than a cholangiocyte lineage (Zaret & Grompe, 2008). For example, TBX3 suppresses cholangiocyte differentiation through activation of HNF4α (Ludtke, Christoffels, Petry, & Kispert, 2009) and suppression of HNF4α by overactivation of Hippo signaling results in expansion of biliary epithelial cells in livers (Lee et al., 2016).

1.3. The Role of HNF4α in Hepatocyte Differentiation and Liver Function

1.3.1. HNFα and the hepatic transcription factor network

The hepatic transcription factor network (HNF4α, HNF1α, HNF1β, FOXA2, HNF6, LRH1, FXR, PXR) is established by HNF4α in mice during embryonic liver development. Deletion of HNF4α during hepatic specification significantly disrupts the network, and HNF4α contributes to the stability of the network in adult hepatocytes (Kyrmizi et al., 2006). Studies in human hepatocytes have also confirmed HNF4α as a central regulator of the hepatic transcription factor network. Examination of the regulatory network circuitry motifs of six transcription factors

known to be important in hepatocyte biology (FOXA2, HNF4α, HNF1α, HNF6, CREB1, USF1), showed extensive autoregulation, with 5 of the 6 transcription factors binding their own promoter and multiple examples of each transcription factor binding to the promoter of the other transcription factors, resulting in several direct and indirect feed-forward activation loops. In the network examined, HNF4α exerted the most efferent connections to other members of the network. Combinatorial binding of multiple transcription factors at the same promoter was observed, with a significant enrichment in the number of target gene promoters bound by two or more regulators (Odom et al., 2006). Multiple transcription factors binding the same promoter leads to synergistic activation of gene expression and is important for maintaining tissue-specific gene expression (Costa, Kalinichenko, Holterman, & Wang, 2003). Some members of this network are also involved in pancreatic β-cell gene regulation (HNF4α, HNF1α, HNF6) and expression of P1-driven HNF4α in hepatocytes results in major differences in network activity compared to the pancreas, where P2-HNF4α is expressed (Odom et al., 2004). Decreased activity of the network (HNF1α, FOXA2, CEBPα, CEBPβ, PPARα) has been associated with chronic hepatic failure (Guzman-Lepe et al., 2018) and decompensation of cirrhotic livers (T. Nishikawa et al., 2015). Temporary expression of HNF4α in these livers is enough to restore network activity leading to feed-forward activation of HNF4α and recovery of normal hepatic function (T. Nishikawa et al., 2015).

1.3.2. HNF4α in hepatocyte differentiation and liver zonation

In addition to its role in embryonic liver differentiation, HNF4α is critical for many important hepatic functions in adult liver, deeming it the master regulator of hepatocyte differentiation.

HNF4α is required for expression of Ornithine Transcarbamylase (OTC) and argininosuccinate lyase (ASL), which are involved in ureagenesis. HNF4α-KO mice have decreased serum urea and increased serum ammonia (Y. Inoue, Hayhurst, Inoue, Mori, & Gonzalez, 2002). In mouse models of α_1-antitrypsin (AAT) deficiency, accumulation of mutated AAT in the liver is associated with decreased HNF4α expression and defective ureagenesis (Piccolo et al., 2017). HNF4α is also required for the synthesis of transferrin and transferrin receptor 2 which leads to hypoferremia (Matsuo et al., 2015). Synthesis of coagulation factors is dependent on HNF4α and clotting time is prolonged in HNF4α-KO mice (Y. Inoue, Peters, Yim, Inoue, & Gonzalez, 2006). Activation of CYP3A4 by PXR or CAR requires HNF4α (Tirona et al., 2003). HNF4a binds the promoter and activates expression of CYP2C9 and CYP2C19 (Kawashima, 2006). siRNA knockdown of HNF4α in primary human hepatocytes decreases expression of drug metabolizing enzymes and transporters (CYP1A1, CYP2A6, CYP2B6, CYP2C8, CYP2C9, CYP2C19, CYP2D6, CYP2J2, CYP3A4, SULT2A1, UGT1A1, UGT1A9, ABCB1, ABCB11, ABCC2, OATP1B1, OCT1) (Kamiyama et al., 2007). Deletion of HNF4α from hepatocytes in mice disturbs expression of many hepatic phase II enzymes (SULT1A1, SULT1B1, SULT1e1, SULT2a2, SULT5a1, PAPSS1, UGT1a1, UGT1a5, UGT1a9, UGT2a3, UGT2b1, UGT2b36, UGT3a1, UGT3a2, GSTa4, GSTM1, GSTM2, GSTM4, GSTM6, GSTP2), uptake transporters (NTCP, OATP1a1, OATP1a4, OATP1b2, OATP2b1, OAT2, OCT1, OCTN2, SAT1, NPT1, SVCT1) and efflux transporters (MRP3, MRP6, BCRP, MDR1a, MATE1) (Hayhurst, Lee, Lambert, Ward, & Gonzalez, 2001; Lu, Gonzalez, & Klaassen, 2010). The role of HNF4α in regulation of drug metabolizing enzymes and transporters has been extensively reviewed elsewhere (Gonzalez, 2008; Hwang-Verslues & Sladek, 2010; Jover, Moya, & Gomez-Lechon, 2009).

Studies show that HNF4α is involved in the maintenance of liver zonation by suppressing pericentral genes in periportal hepatocytes (Stanulovic et al., 2007) and activation of Wnt/β-catenin displaces HNF4α in liver stem cells allowing them to take on a pericentral phenotype (Colletti et al., 2009). This mechanism is also observed in AAT, when activation of β-catenin and decreased expression of HNF4α perturbs liver zonation (Piccolo et al., 2017).

1.3.3. HNF4α and bile acid metabolism

Hepatic functions related to bile acid metabolism are heavily HNF4α dependent. HNF4α-KO mice have increased serum bile acid levels, decreased hepatic bile acid import, decreased fecal bile acid excretion, increased urinary bile acid excretion, and decreased overall bile acid synthesis. This is due to decreased expression of several enzymes involved in bile acid metabolism including CYP7A1, CYP7B1, CYP8B1 and CYP27A1 (Hayhurst et al., 2001; Y. Inoue, Yu, et al., 2006). HNF4α binding at promoter and enhancer elements results in increased CYP7A1 expression, but PXR activation can inhibit CYP7A1 expression by binding HNF4α and disrupting the transcriptional complex (T. Li & Chiang, 2005). Similarly, PROX1 inhibits CYP7A1 expression by binding to HNF4α at its AF-2 domain (K. H. Song, Li, & Chiang, 2006). CDCA and IL-1β can inhibit CYP7A1 expression by activating JNK signaling which decreases HNF4α expression leading to decreased PGC1α and HNF4α occupancy of CYP7A1 promoter (T. Li, Jahan, & Chiang, 2006). TGFβ can activate SMAD3 and HDACs to epigenetically silence the CYP7A1 promoter. In this mechanism, SMAD3 directly interacts with HNF4α (T. Li

& Chiang, 2007). Glucose-induced activation of AMPK decreases HNF4α protein, but induces CYP7A1 expression by increasing promoter acetylation (T. Li, Chanda, Zhang, Choi, & Chiang, 2010). Expression of bile acid conjugating enzymes (BAT, VLACSR) is HNF4α-dependent, with HNF4α-KO mice exhibiting increased levels of unconjugated bile acids (Y. Inoue, Yu, Inoue, & Gonzalez, 2004). HNF4α binds the promoter and activates CSAD, an enzyme involved in taurine synthesis. SHP activation will suppress CSAD expression by binding to HNF4α in the CSAD promoter (Y. Wang, Matye, Nguyen, Zhang, & Li, 2018). This same method of regulation also occurs on the promoter of CYP7A1, with HNF4α and LRH1 activating CYP7A1 expression and SHP targeting HNF4α on the CYP7A1 promoter to suppress transcription (Kir, Zhang, Gerard, Kliewer, & Mangelsdorf, 2012). CYP7A1 is also suppressed when HNF4α is inhibited after phosphorylation by PKA (Yan et al., 2017). HNF4α coactivates bile acid synthesis genes with other transcription factors, including CAR, EGR1 and C/EBPα to activate CYP2B6 (Benet, Lahoz, Guzman, Castell, & Jover, 2010; K. Inoue & Negishi, 2008).

1.3.4. HNF4α and lipid and carbohydrate metabolism

HNF4α plays a major role in hepatic lipid and carbohydrate metabolism. HNF4α-null drosophila larvae express lower levels of β-oxidation genes, and higher levels of lipid stores. These mutants also exhibit significant mortality after 24 hours of starvation (Palanker, Tennessen, Lam, & Thummel, 2009). Hepatocyte-specific HNF4α-KO mice exhibit hepatic steatosis and depletion of hepatic glucose (Hayhurst et al., 2001; Martinez-Jimenez, Kyrmizi, Cardot, Gonzalez, & Talianidis, 2010; Walesky, Edwards, et al., 2013). Decreased hepatic glycogen is caused by inhibited gluconeogenesis. HNF4α is induced during fasting and is required for activation of

gluconeogenic genes (PEPCK, G6Pase) by PGC-1α (Rhee et al., 2003; Yoon et al., 2001). Also, fructose-1,6-bisphosphatase is coactivated by HNF4α and C/EBPα (Wattanavanitchakorn, Rojvirat, Chavalit, MacDonald, & Jitrapakdee, 2018). Inhibition of HNF4α by DAX1 (Nedumaran et al., 2009) and SULT2B1 (Bi et al., 2018) are mechanisms known to negatively regulate gluconeogenesis.

β-oxidation is an important part of the fasting response. Expression of dominant negative HNF4α in rats decreases expression of CPT1 (Louet, Hayhurst, Gonzalez, Girard, & Decaux, 2002). HNF4α is important for suppressing PPARα-mediated β-oxidation during fed conditions and is a direct activator of PPARα during fasted conditions (Martinez-Jimenez et al., 2010). HNF4α is also required for activation of PPARα by PI3K/AKT signaling (X. Yang et al., 2018). Accumulation of hepatic lipids and cholesterol in HNF4α-KO mice is likely caused by decreased expression of HNF4α target genes involved in VLDL synthesis and packaging (apolipoproteins, MTTP), and increased expression of hepatic HDL importer, CD36 (Hayhurst et al., 2001). This results in decreased serum triglycerides and cholesterol (Hayhurst et al., 2001; L. Yin, Ma, Ge, Edwards, & Zhang, 2011). A similar phenotype is observed in steatosis following HFD feeding where increased oxidative stress decreases APOB expression by promoting cytoplasmic translocation of HNF4α (Yu et al., 2018). Regulation of hepatic lipid homeostasis by HNF4α also occurs through epigenetic mechanisms. An examination of changes to open chromatin sites after high fat diet (HFD) feeding found that majority of sites were bound by HNF4α (Leung et al., 2014). Later, it was confirmed that HNF4α can recruit PROX1-HDAC3 to epigenetically

regulate genes which suppress steatosis. Deletion of HNF4α or this complex increased hepatic triglycerides (TG) (Armour et al., 2017).

1.4. HNF4α and Proliferation

1.4.1. Antiproliferative effects of HNF4α in hepatocytes and other cell types

Recent studies have revealed that HNF4α is antiproliferative in several cell types including hepatocytes. Decreased expression of HNF4α is observed in human renal cell carcinoma (Sel, Ebert, Ryffel, & Drewes, 1996) and expression of HNF4α in HEK293 cells reduces proliferation (Lucas et al., 2005). HNF4α has also been shown to be antiproliferative in pancreatic B-cells (Erdmann et al., 2007), gastric epithelium (Moore, Khurana, Huh, & Mills, 2016) and the proliferative compartment of the colonic crypt (Chellappa et al., 2016). The antiproliferative effects of HNF4α may be limited to P1 isoforms. P2 HNF4α is associated with proliferation in pancreatic β-cell proliferation (Gupta et al., 2007; Rieck et al., 2012), colon cancer cells (Vuong et al., 2015), colon cancer (Chellappa et al., 2016), and hepatocellular carcinoma (S. H. Cai et al., 2017). Hepatocyte-specific deletion of HNF4α in mice results in hepatomegaly and spontaneous hepatocyte proliferation, the product of increased Cyclin D1 expression (Bonzo, Ferry, Matsubara, Kim, & Gonzalez, 2012; Hayhurst et al., 2001; Walesky, Gunewardena, et al., 2013). One mechanism by which HNF4α exerts its antiproliferative effects is the activation of antiproliferative p21 gene (Chiba et al., 2005). HNF4α competes with oncogene c-Myc for a position on the p21 promoter (Hwang-Verslues & Sladek, 2008). Expression of HNF4α was decreased in fast-growing dedifferentiated HCC cell lines compared to slower growing cell lines exhibiting a more differentiated hepatocyte phenotype (Lazarevich et al., 2004). Combined with

the known role of HNF4α in hepatocyte differentiation and function, these data suggest HNF4α is a central regulator of hepatocyte function and quiescence.

1.4.2. HNF4α during liver regeneration

The liver exhibits enormous capacity to regenerate following surgical resection or chemical injury (Michalopoulos, 2017). Two-thirds partial hepatectomy (PH) is a long established model (Higgins & Anderson, 1931) used to study liver regeneration in a variety of species (Mortensen & Revhaug, 2011). After PH, adult hepatocytes enter cell division, undergo proliferation, and return to a quiescent state once the mass of the original liver has been reached (Malato et al., 2011). This feature makes PH an excellent model for studying the innate proliferative potential of adult hepatocytes. Regulation of differentiation and proliferation during this process could both be regulated through modulation of HNF4α activity. No change in HNF4α mRNA has been detected after PH (Flodby et al., 1993), although HNF4α transcriptional activity is suppressed 4 hours post-PH (Jiao, Zhu, Lu, Zheng, & Chen, 2015). One study has reported decreased staining of HNF4α in periportal hepatocytes after PH (Fukuda, Fukuchi, Yagi, & Shiojiri, 2016). However, these three studies contain the extent of what is known about HNF4α during liver regeneration.

1.5. HNF4α and Liver Disease

Extensive evidence exists showing the association between decreased HNF4α and the progression of liver disease. Downregulation of HNF4α protein and its transcriptional targets has

been shown to occur during the development of Non-alcoholic Fatty Liver disease (NAFLD) and Non-alcoholic steatohepatitis (NASH) (Baciu et al., 2017; Yu et al., 2018). Primary hepatocytes cultured on stiff matrix have decreased HNF4α network activity and dedifferentiation (Desai et al., 2016). Expression of HNF4α lessens the severity of fibrosis in rats treated with dimethylnitrosamine or bile duct ligation (Yue et al., 2010) and decreased HNF4α expression is correlated with advanced stages of fibrosis in humans (Guzman-Lepe et al., 2018).

The progression of cirrhosis is also associated with downregulation of HNF4α. Adenoviral delivery of HNF4α reversed the severity of thioacetamide induced cirrhosis in rats by upregulating MMPs (Fan et al., 2013). The transcription factor WT1 can downregulate HNF4α in primary rat hepatocytes, is over expressed in cirrhotic human livers, and is negatively correlated with HNF4α expression in livers with advanced cirrhosis (Berasain et al., 2003). Finally, in rats treated with CCl_4, loss of HNF4α expression occurred in rats with decompensated cirrhosis. This was associated with significant reductions in measures of hepatic function. Reexpression of HNF4α rescued rats with decompensated cirrhosis and restored stability of the hepatic transcription factor network (T. Nishikawa et al., 2015). This study demonstrated that destabilization of the hepatic transcription factor network results in loss of hepatic function leading to decompensation.

Numerous studies have shown the role of HNF4α in promoting an epithelial phenotype (Battistelli et al., 2018; W. Y. Cai et al., 2017; Q. Huang et al., 2017; Ning et al., 2010; Parviz et

al., 2003; Santangelo et al., 2011). Likewise, there is significant evidence for HNF4α to function as a tumor suppressor in hepatocellular carcinoma. Numerous studies have shown decreased expression of HNF4α in human HCCs (W. Y. Cai et al., 2017; Hatziapostolou et al., 2011; Ning et al., 2014; Ning et al., 2010). Irregular staining of HNF4α isoforms has been observed in human HCC (Tanaka et al., 2006) and HCCs expressing high levels of fetal HNF4α exhibit the poorest prognosis (S. H. Cai et al., 2017). Studies from our lab show that deletion of HNF4α promotes the progression of HCC through c-Myc activation. HNF4α-KO mice exhibit higher tumor burden and increased size of tumors (Walesky, Edwards, et al., 2013). Decreased HNF4α expression is observed during the transition from cirrhosis to HCC in humans and mice (Ning et al., 2010). Forced expression of HNF4α in diethylnitrosamine mice from this study prevented the development of HCC by inhibiting β-Catenin signaling and increasing E-cadherin expression.

HNF4α suppresses many procarcinogenic programs activation of these programs after inhibition of HNF4α is a common mechanism driving many HCCs. Human HCCs with an unmutated β-catenin gene retain zone specific gene expression patterns, including gene expression maintained by HNF4α, exhibited decreased aggressiveness, are less advanced and showed longer survival. These findings contrasted with highly aggressive perivenous HCCs exhibiting overactive β-catenin and suppressed of HNF4α transcriptional activity (Desert et al., 2017). Similarly, an inverse relationship between hippo signaling effector YAP and HNF4α was observed in human HCCs. Studies showed that YAP can activate proteasomal degradation of HNF4α while forced expression of HNF4α in mice downregulated YAP and slowed the progression of HCC (W. Y.

Cai et al., 2017). Temporary HNF4α inhibition is enough to permanently activate a positive feedback loop in which STAT3 inhibits HNF4α, resulting in HCC (Hatziapostolou et al., 2011). A negative feedback loop between NF-kB and HNF4α has been identified such that loss of HNF4α expression enhances NF-kB signaling in a model of HCC metastasis (Ning et al., 2014). HNF4α can impart its anti-tumor activity by affecting miRNA expression. HNF4α induces miR-379-656 cluster to transcribes miR-134, which has tumor suppressor activity. HCCs exhibit decreased expression of HNF4α and miR-134 in tumor tissue compared to adjacent non-tumor tissue (C. Yin et al., 2013).

This strong evidence for the role of HNF4α in inhibiting hepatic carcinogenesis has led many to test if restoration of HNF4α expression can be used as a treatment for HCC. Overexpression of HNF4α in Hepa1C1C cells causes cell cycle arrest (Walesky, Gunewardena, et al., 2013). Adenoviral delivery of HNF4α into Hep3B and HepG2 cells decreases expression of stem cell markers and prevents these cells from metastasizing to the liver when injected into mice (C. Yin et al., 2008). Overexpression of HNF4α blocked the formation of DEN-induced HCC in mice (Ning et al., 2010) The tumor suppressor activity of HNF4α is most likely due to its central role in maintaining stability of the hepatic transcription factor network. This was demonstrated when combined expression of HNF4α, HNF1α, and FOXA3 were more effective at inhibiting cancer cell proliferation than when just one of these transcription factors was expressed (Takashima, Horisawa, Udono, Ohkawa, & Suzuki, 2018). Treatment with the flavonoid, Oroxylin A, can indirectly restore HNF4α gene expression and slows HCC tumor growth and increases survival

in mice (Wei et al., 2017). However, while the potential of HNF4α activation for HCC therapy is great, direct agonists of HNF4α have not been developed.

1.6. Purpose and Aims

The role of HNF4α in hepatocyte differentiation and specific liver functions has been well established. However much remains to be understood about how the proliferative capacity of hepatocytes can be kept in check during normal conditions. It is also clear that loss of HNF4α activity is associated with the progression of liver disease and targeting HNF4α would be therapeutically beneficial in some cases, but techniques and tools to use this knowledge in a prognostic or diagnostic setting do not exist. Finally, although we know that a primary function of HNF4α is in hepatic carbohydrate and lipid homeostasis, it is not known how disruption of hepatic HNF4α effects metabolism beyond the liver. This would be especially important to know if HNF4α were to be therapeutically inhibited or activated. The main objective of this dissertation was to use novel models and techniques to further characterize the behavior of hepatic HNF4α in proliferation and metabolism and exploit its activity as a prognostic tool.

Specific Aim 1: Investigate the role of HNF4α on hepatocyte regeneration

- Examine expression and activity of HNF4α during liver regeneration after partial hepatectomy.
- Determine the effect of HNF4α overexpression on initiation of liver regeneration after partial hepatectomy.

- Determine the effect of hepatocyte-specific HNF4α deletion on termination of liver regeneration after partial hepatectomy.

We hypothesized that modulation of HNF4α expression and activity would be required to navigate hepatocyte between quiescent and proliferative states during liver regeneration after partial hepatectomy. Initiation of regeneration would require activation of proliferative pathways normally repressed by HNF4α. Termination of regeneration would require a return to quiescence by inhibiting proliferation and reestablishment of hepatocyte specific gene expression.

Specific Aim 2: Develop HNF4α target gene signature to be used as a prognostic tool for HCC treatment

- Identify genes to include in signature which robustly depict differences in HNF4α activity in normal and diseased conditions.
- Validate this signature in human and mouse tissues.
- Test the ability of the signature to determine disease progression or prognosis in human and mouse datasets.

We hypothesized that decreased HNF4α activity, as measured by target gene expression, would directly correlate with progression of liver disease. We hypothesized that this knowledge could be used to accurately identify HCC advancement and potentially predict which cirrhotic patients would go on to develop HCC.

Specific Aim 3: Investigate the role of hepatic HNF4α on global metabolism

- Characterize the effect of hepatic HNF4α deletion on whole body energy expenditure and substrate utilization.
- Determine the role of HNF4α in regulating whole body metabolism in various metabolic challenges.

We hypothesized that the well described role of HNF4α in hepatic carbohydrate and lipid homeostasis would have a significant effect on systemic energy expenditure and substrate utilization.

Chapter 2. Hepatocyte Nuclear Factor 4 alpha (HNF4α) Activation is Essential for Termination of Liver Regeneration

Portions of this chapter have been submitted and accepted for publication December 5, 2018.

Huck, I., Gunewardena, S., Espanol-Suner, R., Willenbring, H., & Apte, U. (2018). Hepatocyte Nuclear Factor 4 alpha (HNF4alpha) Activation is Essential for Termination of Liver Regeneration. *Hepatology*. doi:10.1002/hep.30405

2.1. Abstract

Hepatocyte Nuclear Factor 4 alpha (HNF4α) is critical for hepatic differentiation. Recent studies have highlighted its role in inhibition of hepatocyte proliferation and tumor suppression. However, the role of HNF4α in liver regeneration is not known. We hypothesized that hepatocytes modulate HNF4α activity when navigating between differentiated and proliferative states during liver regeneration. Western blot analysis revealed a rapid decline in nuclear and cytoplasmic HNF4α protein levels accompanied with decreased target gene expression within 1 hour after 2/3 partial hepatectomy (post-PH) in C57BL/6J mice. HNF4α protein expression did not recover to the pre-PH levels until day 3. Hepatocyte-specific deletion of HNF4α (HNF4α-KO) in mice resulted in 100% mortality post-PH despite increased proliferative marker expression throughout regeneration. Sustained loss of HNF4α target gene expression throughout regeneration indicated HNF4α-KO mice were unable to compensate for loss of HNF4α transcriptional activity. Deletion of HNF4α resulted in sustained proliferation accompanied by c-Myc and Cyclin D1 over expression and a complete deficiency of hepatocyte function after PH. Interestingly, overexpression of degradation-resistant HNF4α in hepatocytes delayed but did not prevent initiation of regeneration after PH. Finally, AAV8-mediated reexpression of HNF4α in hepatocytes of HNF4α-KO mice post-PH restored HNF4α protein levels, induced target gene expression and improved survival of HNF4α-KO mice post-PH. In conclusion, these data indicate that HNF4α reexpression following initial decrease is critical for hepatocytes to exit from cell cycle and resume function during the termination phase of liver regeneration. These results reveal the role of HNF4α in liver regeneration and have implications for therapy of liver failure.

2.2. Introduction

The role of HNF4α in promoting hepatocyte differentiation and inhibiting hepatocyte proliferation was detailed in Chapter 1. Liver has a remarkable capacity to regenerate upon surgical resection, and following viral or drug-induced liver injury. During liver regeneration after 2/3 partial hepatectomy (PH), the most widely used model to study liver regeneration, multiple redundant mechanisms regulate initiation and termination of hepatocyte regeneration (Michalopoulos, 2017). Understanding the mechanisms that govern adult hepatocytes to navigate between quiescent and proliferative states could result in therapeutic targets for inducing hepatocyte proliferation during impaired regeneration or inhibiting excess proliferation during carcinogenesis. Despite its role in maintaining hepatocyte differentiation and quiescence, little is known about the role of HNF4α in hepatocyte regeneration or how decreased HNF4α, a condition commonly found in diseased human livers (W. Y. Cai et al., 2017; Hatziapostolou et al., 2011; T. Nishikawa et al., 2015; Tanaka et al., 2006), would impact regeneration. In this study, we investigated the role of HNF4α in regulation of liver regeneration after PH using wildtype (WT) and HNF4α-KO mice. Our studies revealed that HNF4α is indispensable for survival after PH and a critical component of termination of liver regeneration.

2.3. Materials and Methods

2.3.1. Animal Care and Surgeries.

Animals were housed in facilities accredited by the Association for Assessment and Accreditation of Laboratory Animal Care at the University of Kansas Medical Center under a standard 14-hr dark/10-hr light cycle with access to chow and water *ad libitum.* All studies were approved by the Institutional Animal Care and Use Committee at the University of Kansas Medical Center. PH surgeries were performed and tissue samples obtained as previously described (Borude et al., 2012). Surgeries were performed between 9:00 am and 11:00 am. For liver regeneration in normal conditions, two-month-old male C57BL6/J mice were euthanized at 0, 1, 3, 6, 12, 24 and 48 hr, and 3, 5, 7, and 14 days after PH with 3 mice per time point. To test the effects of Src inhibition on nuclear HNF4α expression, C57BL6/J mice were injected with either the Src-specific inhibitor PP2 (Cayman Chemical, Cat. #13198) dissolved in 1% DMSO or vehicle for 4 days before undergoing PH surgeries. Mice were euthanized 6 hours post-PH and nuclear and cytoplasmic extracts were prepared from fresh liver. To study the effects of HNF4α deletion on liver regeneration, seven days before surgery HNF4α-floxed mice were injected intraperitoneally with AAV8-TBG-eGFP or AAV8-TBG-CRE resulting in WT and hepatocyte-specific HNF4α-KO animals, respectively. These vectors were purchased from Penn Vector Core (Philadelphia, PA) and injected as previously described (Yanger et al., 2013). WT and HNF4α-KO mice were euthanized at 0, 1, 2, 5, 7 and 14 days after PH with 3-5 mice per group. Only two HNF4α-KO mice survived to be included at the 7-day time point. HNF4α reexpression was accomplished by tail vein injection of 2×10^{11} viral genomes/mouse of AAV8-CMV-HNF4α generated in the laboratory of Dr. Holger Willenbring. Male HNF4α-floxed mice were injected with AAV8-TBG-CRE to induce HNF4α deletion and 7 days later were injected with

AAV8-CMV-HNF4α to restore HNF4α expression. Liver and serum samples were collected seven days after AAV8-CMV-HNF4α injection. Next, this system was used to test if HNF4α reexpression could rescue HNF4α-KO mice after partial hepatectomy. WT and HNF4α-KO mice underwent PH 7 days after injection with AAV8-TBG-eGFP or AAV8-TBG-CRE with four mice per treatment. Tail vein injection with reexpression vector or control saline occurred 2 days after surgery to allow for initiation of regeneration. Overexpression of HNF4α was accomplished using Tet-On-HNF4α transgenic mouse line developed at the KUMC Transgenic and Gene Targeting Institutional Facility. These mice contained a reverse tetracycline-controlled transcriptional activator which was constitutively expressed with a C/EBPβ promoter. The existence of a possible feed forward activation loop of C/EBPβ by HNF4α due to strong HNF4α ChIP signal on the C/EBPβ promoter existed in this model (Schmidt et al., 2010). In the presence of the tetracycline-derivative Doxycycline (Dox), this transcription factor binds a tetracycline response element (TRE) upstream of an shRNA-resistant HNF4α gene (kind gift from Dr. Stephen A. Duncan, Medical University of South Carolina). Tet-On-HNF4α were heterozygous for both transgenes. Doxycycline was administered for two weeks prior to surgery by replacing drinking water with a 1 mg/mL Dox in 5% Sucrose solution. Untreated mice were given 5% sucrose solution only. Two mice were used for the untreated 6 hour time point and three to five mice used for all other treatments and time points.

2.3.2. Protein Isolation and Western blotting.

Nuclear and cytoplasmic lysates and RIPA extracts were prepared and used for Western blot analysis as reported (Wolfe et al., 2011). To visualize the extremely low levels of cytoplasmic

HNF4α, SuperSignal West Femto Maximum Sensitivity Chemiluminescent Substrate (ThermoScientific, Cat# 34095) was used. Primary antibodies are provided in Table 2.3.1. Densitometric analysis was performed using Image Studio Lite (LI-COR Biosciences).

Table 2.3.1: Catalog Numbers of Antibodies Used in This Study

Antibody	Catalog no.	Manufacturer
AKT	4691	Cell Signaling Technology
Phospho-AKT (Ser473)	9271	Cell Signaling Technology
β-actin	4970	Cell Signaling Technology
β-Catenin	8480	Cell Signaling Technology
Phospho-β-Catenin (Thr41/Ser45)	9565	Cell Signaling Technology
CDK4	2906	Cell Signaling Technology
Cyclin D1	2978	Cell Signaling Technology
EGFR	4267	Cell Signaling Technology
Phospho-EGFR (Tyr1045)	2237	Cell Signaling Technology
ERK1/2	9102	Cell Signaling Technology
Phospho-ERK1/2 Thr202/Tyr204)	4376	Cell Signaling Technology
GAPDH	2118	Cell Signaling Technology
GSK-3β	9315	Cell Signaling Technology
Phospho-GSK-3β (Ser9)	9323	Cell Signaling Technology
Histone H3	9717	Cell Signaling Technology
Adult HNF4a isoforms	PP-K9218-00	Perseus Proteomics
All HNF4a isoforms	PP-H1415-00	Perseus Proteomics
c-Met	3127	Cell Signaling Technology
c-Myc	5605	Cell Signaling Technology
p38	8690	Cell Signaling Technology
Phospho-p38 (Thr180/Tyr182)	4511	Cell Signaling Technology
PCNA	2586	Cell Signaling Technology

2.3.3. Real Time PCR.

RNA isolation, conversion to cDNA and Real time PCR analysis was performed as previously described (Apte et al., 2009). HNF4α positive and negative target genes were identified based on RNA-Seq analysis comparing gene expression in livers from WT and hepatocyte-specific HNF4α-KO mice (Walesky, Edwards, et al., 2013).. Primer sequences are provided in Table 2.3.2.

Table 2.3.2: Primer Sequences Used in This Study

Gene Name	Forward Primer (5' - 3')	Reverse Primer (5' - 3')
18s	TTGACGGAAGGGCACCACCAG	GCACCACCACCCACGGAATCG
Akr1b7	TTCTGATTCGGTTCCATGTCC	TCCAGTTCCTGTTGAAGCTG
Alas2	TTTAGTATTGGACGCTGCCC	CTTCCTGTCTTGGAGTTCTGAC
ApoA2	GACACCCCTTGTCAGGTCAG	TGGCACATCTCACTTAGCCG
ApoB	CTGCAACCAAGCTGGCATAAG	CCTCCATCCTGAGTTGGACA
c-Myc	GCTGTTTGAAGGCTGGATTTC	GATGAAATAGGGCTGTACGGAG
CcnD1	GCCCTCCGTATCTTACTTCAAG	GCGGTCCAGGTAGTTCATG
Cdkn3	TCGGTTTATGTGCTCTTCCAG	ATATTTTGACAGCTCCCCTCTG
Ces3	TGTATGAGTTTGAGTATCGCCC	CATCTTGCTGAGGTTGGTCT
Cldn1	TCAGATGATGTTTTCCCGATGACCTTT	AAGCACAGTTTGCAGGATCTGGGATG
Cyp2c37	GATGGCAATCAACCATTGC	GCCGATCACATGCTCAATT
Defb1	AATACAAATGCCTTCAACATGGAG	ATCCATCGCTCGTCCTTTATG
Dio1	GTTGCACCTGACCTTCATTTC	CCACGTTGTTCTTAAAAGCCC
Ect2	CGTGTTACCATCTCCTTCTGAG	TCACTCTTGCTTCAACCTGC
Egr1	AGCGCCTTCAATCCTCAAG	TTTGGCTGGGATAACTCGTC
F12	GCCATTTTCCCTTTCAGTACC	TCTTTCACTTTCTTGGGCTCC
Hjurp	AGTACAACCAGCCCTTTGAG	GCCCATTTAATCTGTCAATCACC
Hnf4α Adult Isoforms	GAAAATGTGCAGGTGTTGACCA	AGCTCGAGGCTCCGTAGTGTTT
Slc34a2	CTGGGATCAAATGGTCAGAGAG	GAGCACACGAACAAGTAGAGAA
Ugt2b1	GTCAACTACAGACCTTCTCACTG	CGCATGACATACTCGATCCAG

2.3.4. Staining Procedures.

Paraffin-embedded liver sections (4-μm thick) were used for immunohistochemical staining of proliferating cell nuclear antigen (PCNA) as previously described(Borude et al., 2012). PCNA positive hepatocyte nuclei were quantified by counting three 40x fields per slide for each liver sample.

2.3.5. Serum Bilirubin

Total serum bilirubin was determined using the Total Bilirubin kit from Pointe Scientific (Cat #B7576) according to manufacturer's protocol.

2.3.6. RNA Sequencing and Ingenuity Pathway Analysis.

Equal amounts of RNA was pooled using WT and HNF4α-KO livers (n=3) from day 5 and day 7 post-PH to be used for RNA-Seq and Ingenuity Pathway Analysis (IPA). The Stranded mRNA-Seq was performed using the Illumina HiSeq2500 Sequencing System at the University of Kansas Medical Center – Genomics Core (Kansas City, KS). Total RNA (0.5ug) was used to initiate the Stranded mRNA-Seq library preparation protocol. The mRNA fraction was enriched with oligo dT capture, sized, reverse transcribed into cDNA and ligated with the appropriate indexed adaptors using the TruSeq Stranded mRNA Sample Preparation Kit (Illumina RS-122-2101/2102). Following Agilent Bioanalyzer QC of the library preparation and library quantification using the Roche Lightcycler96 with KAPA SYBR Fast Universal qPCR kit (KAPA Biosystems KK4601), the RNA-Seq libraries were adjusted to a 2nM concentration and pooled for multiplexed sequencing. Libraries were denatured and diluted to the appropriate pM

concentration (based on qPCR results) followed by clonal clustering onto the sequencing flow cell using the TruSeq Paired-End (PE) Cluster Kit v3-cBot-HS (Illumina PE401-3001). The clonal clustering procedure is automated using the Illumina cBOT Cluster Station. The clustered flow cell was sequenced on the Illumina HiSeq 2500 Sequencing System using the TruSeq SBS Kit v3-HS (Illumina FC401-3002). Following collection, sequence data is converted from .bcl file format to FASTQ files and de-multiplexed (if required) into individual sequences for further downstream analysis. RNA sequencing and bioinformatics analysis were performed as previously described in detail (Walesky, Edwards, et al., 2013). An absolute fold change cut off of 3 was used to quantify differentially expressed genes (Table 2.4.1) and to select genes used in Ingenuity Pathway Analysis (IPA, Ingenuity Systems). IPA was used to calculate activation z-scores to predict activation or inhibition of upstream regulators and disease pathways

2.3.7. Statistical Analysis

Results are expressed as mean ± standard error. One Way ANOVA and Student's *t* test was applied to all analyses with $p < 0.05$ being considered significant.

2.4. Results

2.4.1. Decreased HNF4α Protein Expression and Transcriptional Activity During Initiation of Regeneration After Partial Hepatectomy.

First, we investigated the expression and activity of HNF4α in liver regeneration after PH in C57BL/6J mice. We measured protein expression of HNF4α adult isoforms using Western blotting in freshly prepared nuclear (Figure 2.4.1A, 2.4.1C) and cytoplasmic (Figure 2.4.1B) protein extracts. Nuclear HNF4α levels started declining at 1 (hour) hr post-PH reaching the lowest level at 6 hr post-PH. Nuclear HNF4a protein expression started rising at 12 hr, increased higher than the 0 hr levels peaking at 3 days post PH and then declined again to reach the 0 hr levels by 7 days post-PH (Figure 2.4.1A, 2.4.1C). Cytoplasmic HNF4α expression continually declined below 0 hr levels until 12h post-PH, then started to rise but did not return to 0 hr pre-PH levels till 14 days after PH. GAPDH and Histone H3 were used as additional loading controls and to determine the purity of nuclear and cytoplasmic extracts. The expression of adult isoform of HNF4α mRNA did not change over the entire regeneration time course (Figure 2.4.1D).

We assessed HNF4α transcriptional activity by qPCR analysis of its target genes at the 0, 6 and 12 hr time points when nuclear HNF4α protein levels were at their lowest levels. Both positive and negative targets of HNF4α were identified using results from previously published RNA-Seq data (Walesky, Edwards, et al., 2013) and are also known to bind HNF4α in their promoters using previously published ChIP-Seq data (Hoffman et al., 2010). We observed decreased expression of positive target genes (Walesky, Edwards, et al., 2013) (*APOA2*, *APOB*, *CES3*, *CLDN1*, *CYP2C37*, *DIO1*, *F12*, *UGT2B1*) at the 6 and 12-hr time points compared to 0 hr

expression levels (Figure 2.4.1E). qPCR analysis showed induction of HNF4α negative target genes (*AKR1B7*, *CCND1*, *ECT2*, *MYC*) at the 6 and 12 hr time points (Figure 2.4.1F). Together, these data indicate a decrease in HNF4α activity at the onset of regeneration which is consistent with the changes we observed in HNF4α protein expression (Figure 2.4.1A-C).

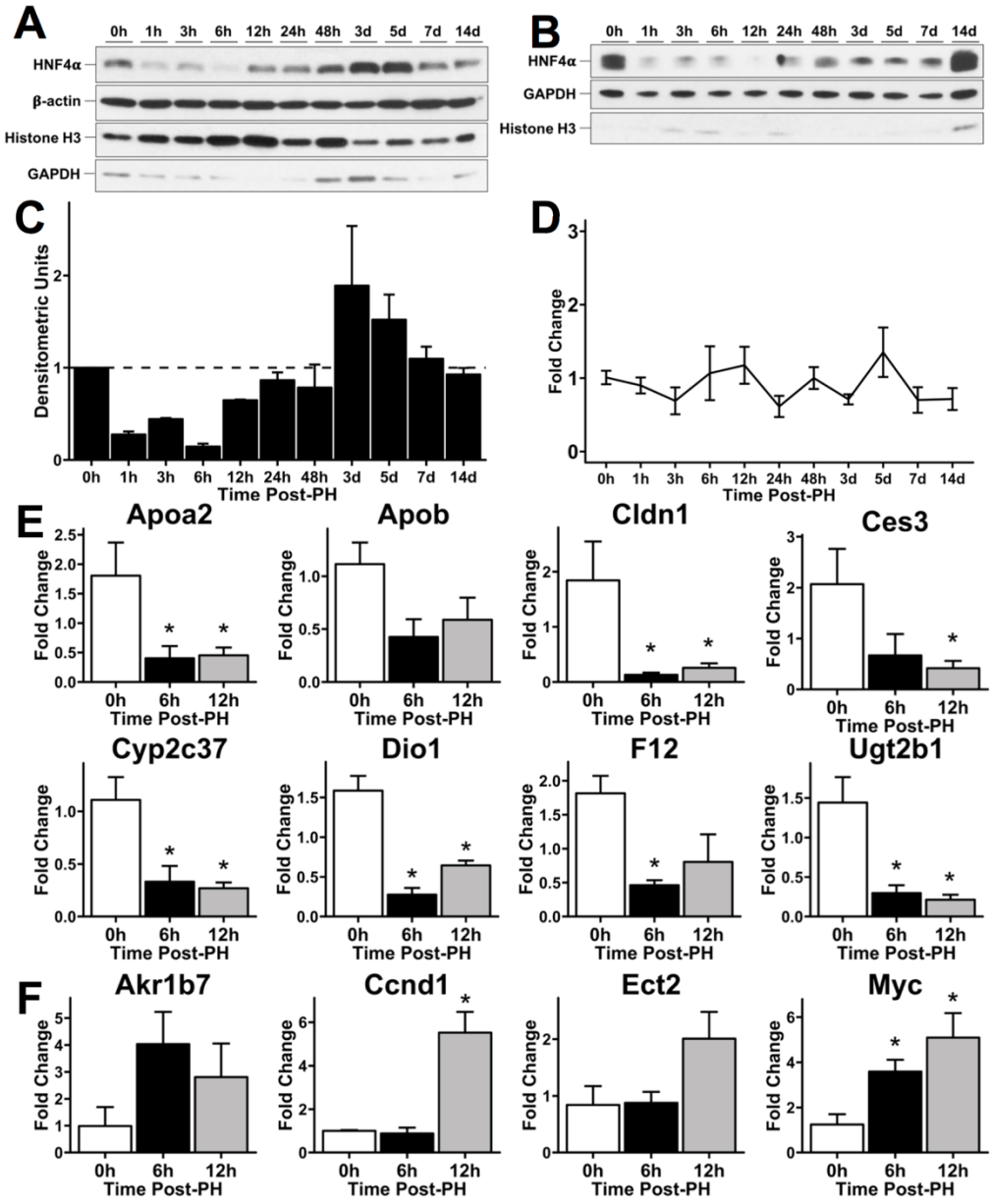

Figure 2.4.1. Decreased HNF4α protein expression and transcriptional activity during initiation of regeneration after partial hepatectomy. Western blot analysis of HNF4α adult isoform in (A) nuclear and (B) cytoplasmic lysates from mouse liver over a time course of 0 – 14 days after 2/3 PH. (C) Densitometric analysis of nuclear HNF4α blot. (D) qPCR analysis of HNF4α adult isoform mRNA over a time course of 0 – 14 days after 2/3 PH. Fold change calculated by comparison to 0 hr time point. qPCR analysis of positively regulated (E) and negatively regulated (F) HNF4α target genes at 0, 6 and 12 hr post-PH. Fold change calculated by comparison to 0 hr time point. *indicate significant difference at $P \leq 0.05$.

2.4.2. Role of Src Kinase in Regulation of HNF4α Expression After PH

Since nuclear HNF4α protein levels decreased during initiation of liver regeneration without changes to HNF4α mRNA expression, we hypothesized that the decrease in nuclear HNF4α was caused by a post-translational regulation of HNF4α protein. Src kinase has been shown to phosphorylate HNF4α leading to its cytoplasmic translocation and degradation (Chellappa, Jankova, et al., 2012). To test this hypothesis, C57BL/6J mice were treated with the Src inhibitor PP2 before undergoing PH. Mice were sacrificed 6 hours post-PH. This timepoint was selected because this is when we observed the lowest levels of nuclear HNF4α in the WT time course. Consistent with our hypothesis, nuclear HNF4α protein was higher in mice treated with PP2 (Figure 2.4.2A). Cytoplasmic HNF4α was not noticeably different in PP2 treated mice compared to Vehicle treated mice. Densitometry for these blots confirms these conclusions (Figure 2.4.2B-C).

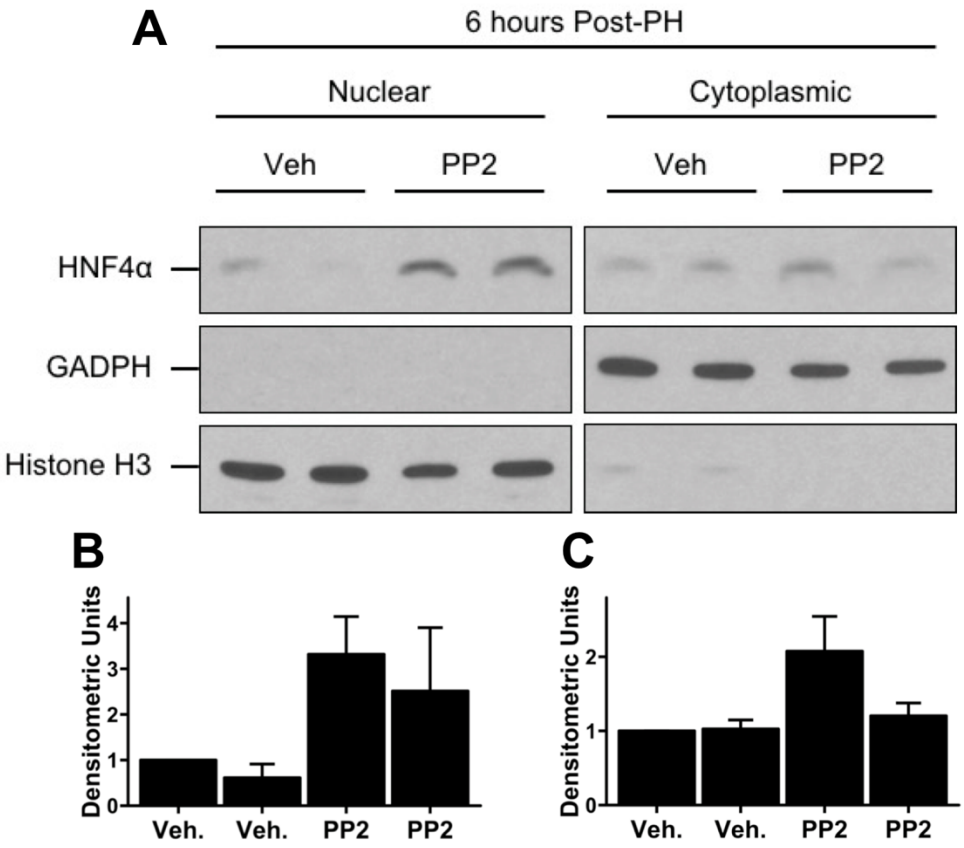

Figure 2.4.2. c-SRC kinase inhibition increases nuclear HNF4α 6 hours after partial hepatectomy. Mice were injected with either 5 mg/kg PP2, a c-SRC kinase specific inhibitor, or vehicle (Veh.) daily for 4 days before undergoing partial hepatectomy and were euthanized 6 hours later. (A) Western blot analysis of HNF4α in nuclear and cytoplasmic extracts from livers 6 hours post-PH. Densitometry for (B) nuclear blot and (C) cytoplasmic blot.

2.4.3. HNF4α Overexpression Delays But Does Not Prevent Hepatocyte Proliferation During Liver Regeneration

We used a Tet-On-HNF4α transgenic mouse system (Das, Tenenbaum, & Berkhout, 2016) to overexpress HNF4α in hepatocytes to test if the anti-proliferative effects of HNF4α would prevent hepatocyte proliferation during the initiation of liver regeneration (Figure 2.4.3). Western blot analysis confirmed increased HNF4α in nuclear lysates from livers of doxycycline (Dox)-treated Tet-On-HNF4α mice at 6 hours post-PH (Figure 2.4.4A). This resulted in fewer PCNA-positive nuclei in Dox-treated mice 6 hours post-PH and increased, although statistically similar, levels of proliferation at 48 hours post-PH. (Figure 2.4.4B-C). Interestingly, Dox treatment inhibited the occurrence of transient steatosis 48 hours post-PH (Figure 2.4.4D). qPCR analysis of HNF4α target genes demonstrated correlation between HNF4α overexpression and increased HNF4α activity. Increased expression of (Figure 2.4.4E) HNF4α positive target genes (*ALAS2, APOA2, CYP2C37, CPT1, HNF4A, UGT2B1*) and decreased expression of (Figure 2.4.4F) HNF4α negative target genes (*CCND1, CDKN3, EGR1*) was observed in DOX treated mice before and after PH.

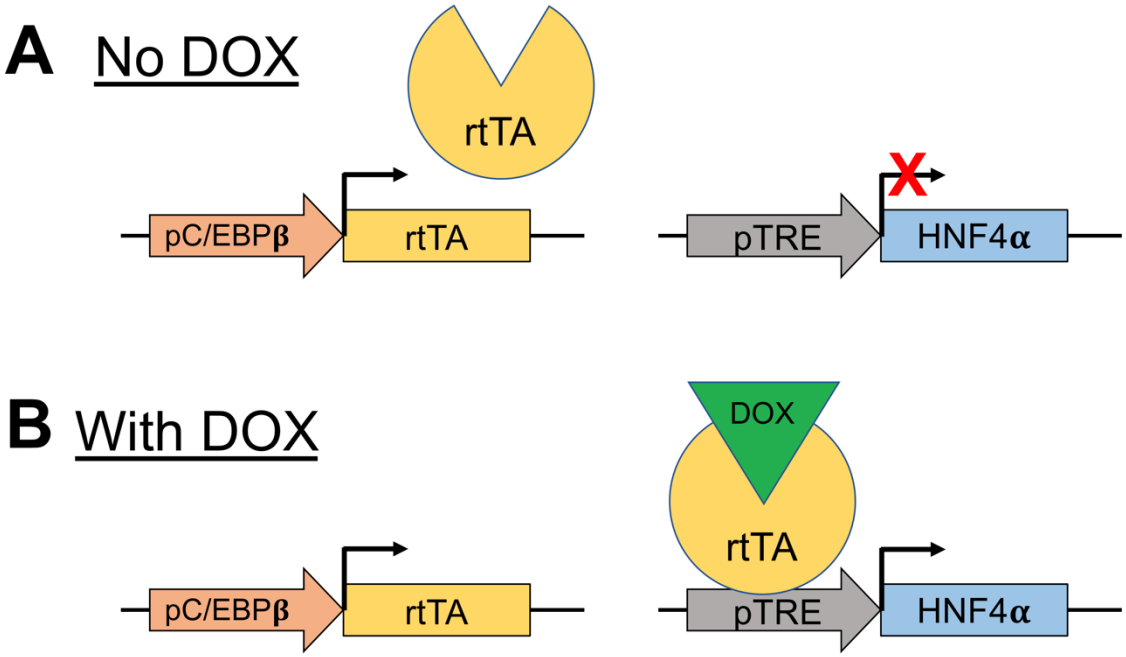

Figure 2.4.3. Schematic depicting mechanism of HNF4α overexpression in Tet-On-HNF4α mouse. (A) In DOX free conditions, rtTA transcription factor is constitutively expressed under a hepatocyte specific C/EBPβ promoter. (B) In the presence of DOX, rtTA transcription factor binds pTRE promoter and activates expression of HNF4α.

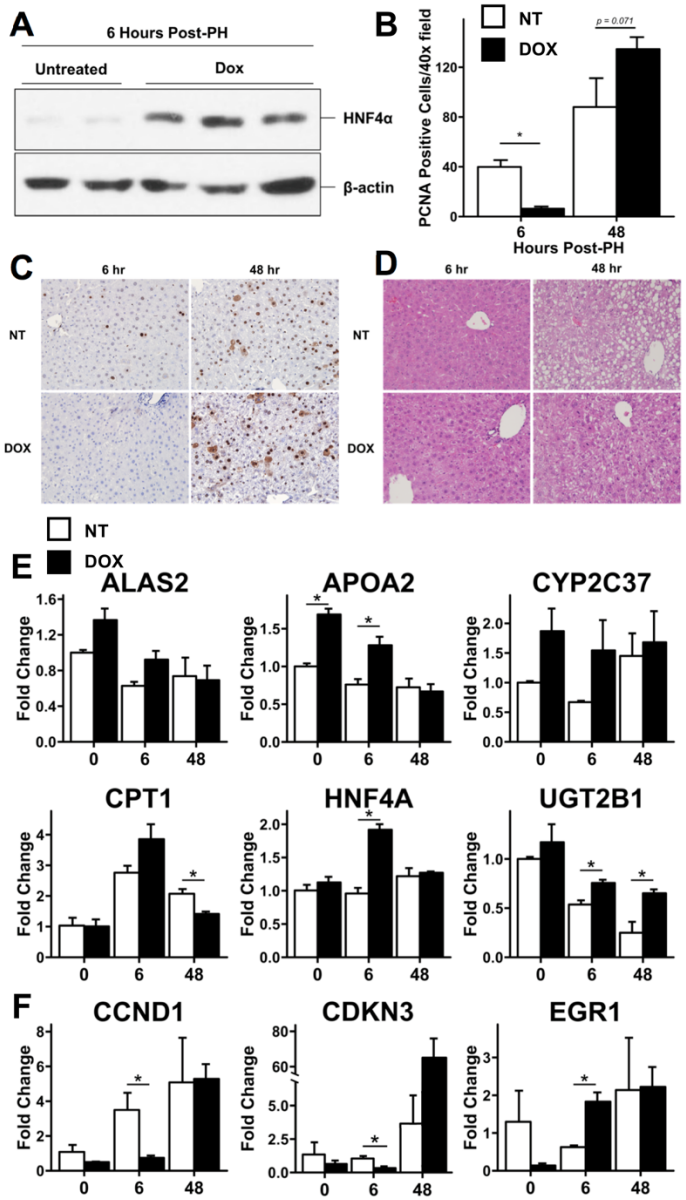

Figure 2.4.4. HNF4α overexpression temporarily delays initiation of liver regeneration. (A) Western blot analysis confirming overexpression of HNF4α in nuclear lysates from livers of untreated (NT) and Dox treated Tet-On-HNF4α mice 6 hrs post-PH. (B) Quantified results for immunohistochemical analysis of PCNA positive nuclei. Representative micrographs (40x) of (C) PCNA stained liver sections and (D) H&E-stained sections from untreated and Dox treated Tet-On-HNF4α mice at 6 and 48 hours post-PH. RT-PCR analysis of HNF4α (E) positive target genes and (F) negative target genes from untreated and Dox treated Tet-On- HNF4α mice at 6 and 48 hours post-PH. * indicate significant difference at $P \leq 0.05$.

2.4.4. Hepatocyte-Specific HNF4α-KO Mice Do Not Survive After PH.

Next, we investigated the effect of hepatocyte-specific HNF4α deletion on liver regeneration after PH. WT and HNF4α-KO mice underwent PH and were euthanized at 1, 2, 5, 7 and 14 days after surgery. HNF4α protein remained undetectable in HNF4α-KO mice throughout the time course after PH (Figure 2.4.5A). We observed 100% mortality in the HNF4α-KO group by day 11 post-PH (Figure 2.4.5B). Interestingly, while liver to body weight ratios were significantly higher in HNF4α-KO mice before PH, the recovery of liver weight was similar between WT and HNF4α-KO groups until 5 days post PH (Figure 2.4.5C). Serum bilirubin was significantly elevated in HNF4α-KO mice at days 1, 2 and 5 post-PH (Figure 2.4.5D). While serum bilirubin in HNF4α-KO animals did decrease over time, this assay could only be performed on surviving mice and most HNF4α-KO mice died before bilirubin could be measured at later time points. Serum bilirubin values were significantly higher in HNF4α-KO mice when summarized as the area under the curve (AUC) for the entire time course after PH.

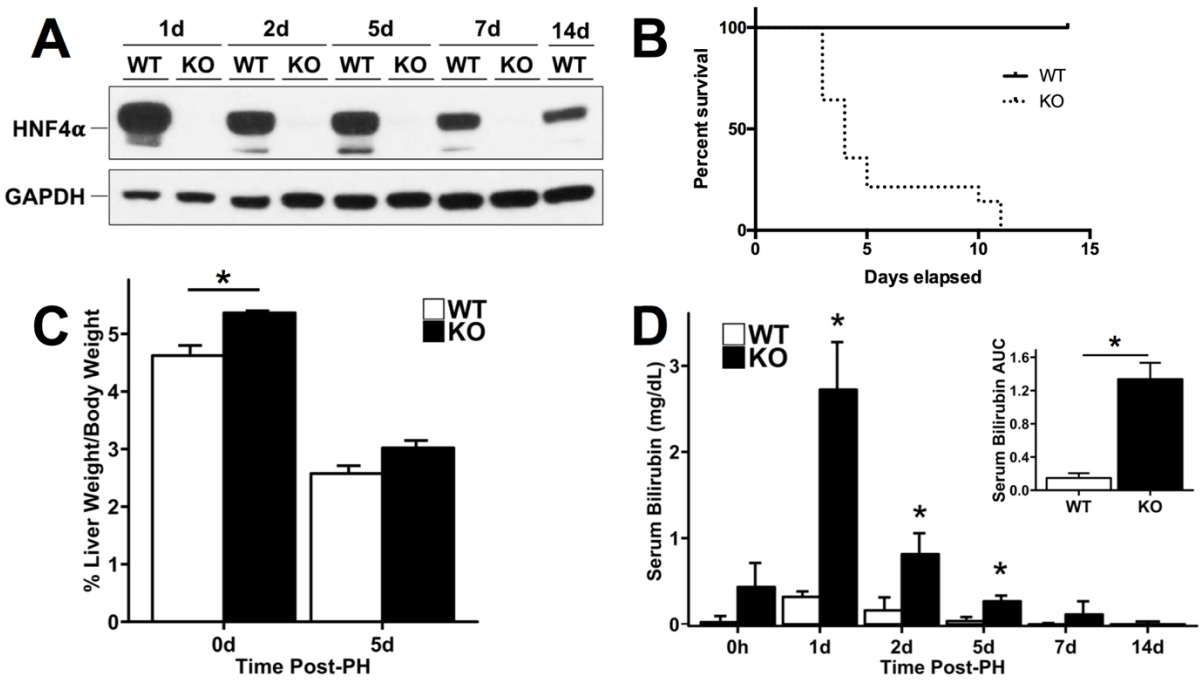

Figure 2.4.5. Complete mortality of HNF4α-KO mice following PH. (A) Western blot of HNF4α confirming efficient KO of HNF4α in pooled liver lysates at all time points post-PH. (B) Kaplan-Meier survival analysis of WT and HNF4α-KO groups after PH. (C) Liver weight to body weight ratios and (D) serum bilirubin levels in WT and HNF4α-KO mice after PH for each time point after PH. Inset represents the area under the curve (AUC) values for bilirubin presented in the main panel. *indicate significant difference at $P \leq 0.05$ between WT and HNF4α-KO.

2.4.5. Sustained Loss of HNF4α Transcriptional Activity In HNF4α-KO Mice 7 Days Post-PH.

We investigated changes in HNF4α target gene expression in WT and HNF4α-KO mice at 7 days after PH, which revealed a significant decrease in expression of positive target genes including *ALAS2, APOA2, APOB, CLDN1, CYP2C37, DIO1, F12 and UGT2B1* (Figure 2.4.6A). Similarly, the expression of the negative targets *AKR1B7, CCND1, CDKN3, DEFB1, ECT2, EGR1, MYC and SLC34A2* was increased at 7 days post-PH (Figure 2.4.6B).

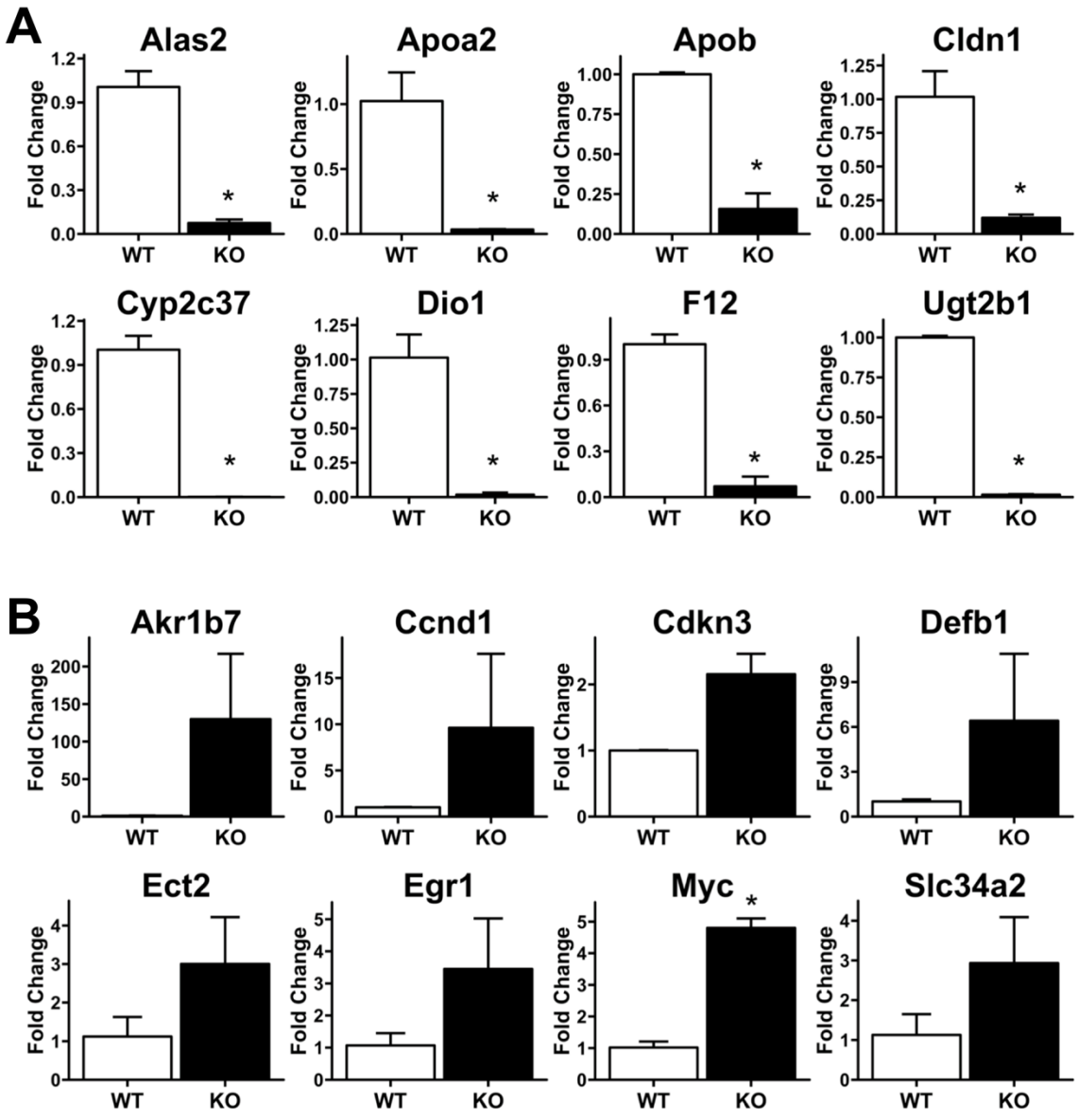

Figure 2.4.6. Sustained Loss of HNF4α Transcriptional Activity In HNF4α-KO Mice 7 Days Post-PH. qPCR analysis of mRNA isolated from frozen liver in WT and HNF4α-KO mice 7 days post-PH. (A) Decreased expression of positive targets of HNF4α and (B) increased expression of negative targets of HNF4α. *indicate significant difference at $P \leq 0.05$ between WT and HNF4α-KO.

2.4.6. Increased Hepatocyte Proliferation in HNF4α-KO Livers Throughout Regeneration. Western blot analysis indicated that protein expression of Cyclin D1, the cyclin involved in driving G0 to G1 and G1 to S cell cycle transition, was significantly increased in HNF4α-KO livers at all time points. The expression of CDK4, the cyclin dependent kinase interacting with Cyclin D1 was lower in HNF4α-KO liver at days 1 and 2 post PH but increased to levels comparable to WT mice by days 5 post PH. Cell proliferation assessed by Western blot and immunohistochemical analysis of PCNA revealed an elevated PCNA level in HNF4α-KO mice at all time points (Figure 2.4.7A). Immunohistochemical analysis of PCNA-positive nuclei per 40x field was significantly higher in HNF4α-KO mice throughput the 7-day time course post PH (Figure 2.4.7B-C).

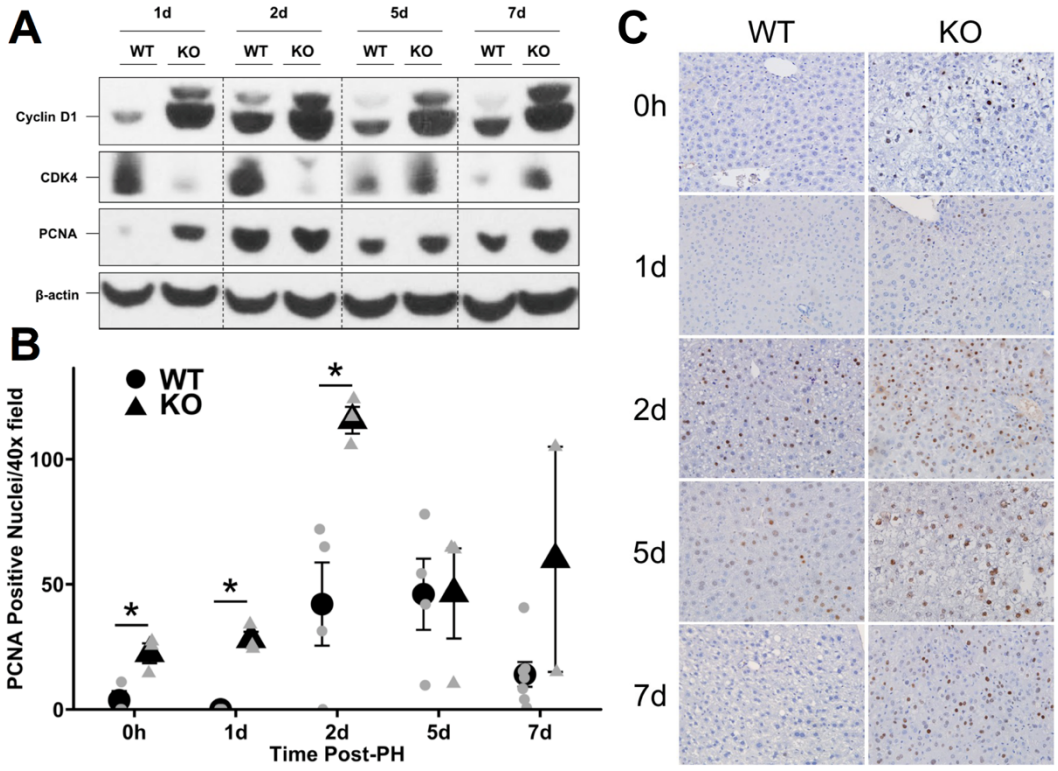

Figure 2.4.7. Increased hepatocyte proliferation in HNF4α-KO livers throughout regeneration. (A) Western blot analysis of Cyclin D1, CDK4, and PCNA over a time course of 0 to 7 days post-PH. (B) Quantification of immunohistochemical analysis for PCNA positive nuclei in liver sections of WT and HNF4α-KO mice throughout time course post-PH. Means for each group indicated in black and values from individual mice indicated in gray. (C) Representative photomicrographs (400x) of PCNA-stained liver sections from WT and HNF4α-KO mice throughout time course post-PH. *indicate significant difference at $P \leq 0.05$ between WT and HNF4α-KO.

2.4.7. Activation of Pro-Proliferative Signaling in HNF4α-KO Mice During Regeneration

We investigated the mechanism of sustained hepatocyte proliferation throughout regeneration in HNF4α-KO mice by Western blot analysis of pathways commonly involved in hepatocyte proliferation. We focused on pathways downstream of primary hepatocyte mitogen signaling as well as those known to activate hepatocyte proliferation in the absence of HNF4α (Paranjpe et al., 2016; Walesky, Edwards, et al., 2013). Most interestingly, we observed complete loss of total EGFR and total c-MET protein expression in HNF4α-KO animals at all time points throughout regeneration (Figure 2.4.8A). Interestingly, it has been shown that signaling through these receptors is required for proliferation to occur after PH (Paranjpe et al., 2016). Next, we examined Wnt/β-catenin pathway members (Figure 2.4.8B). Total β-catenin levels were similar in WT and HNF4α-KO mice before PH and did not change throughout the time course. However, inactive (Thr41/Ser45- phosphorylated) β-catenin was elevated in the WT animals at days 1 and 2 post-PH. Phosphorylated β-catenin was greater in HNF4α-KO compared to WT mice 5 days post-PH. Densitometric analysis of inactive to total β-catenin ratio suggested activation of β-catenin was higher in HNF4α-KO mice at 1 and 2 days post-PH (Figure 2.4.8C). Total GSK-3β levels did not change for both groups throughout the time course. Inactive (ser9-phospho) GSK-3β was higher in both groups at days 1 and 5 post-PH, but no difference was observed between groups. Next, we investigated activation of several MAPK members including AKT, p38 and ERK1/2 (Figure 2.4.8D). No difference in total AKT and total p38 protein levels was observed between groups throughout regeneration. Phosphorylation of AKT was inhibited in the HNF4α-KO mice as compared to WT at days 0, 1 and 5 post-PH but was similar to WT at day 2 after PH. Phosphorylation (activation) of p38 was elevated in HNF4α-KO mice at days 1 and 5 post-PH. Finally, Total ERK1/2 expression was elevated in HNF4α-KO animals at all time

points. Phosphorylation (activation) of ERK1 (upper band) was increased in HNF4α-KO animals compared to WT at all time points. Phosphorylation (activation) of ERK2 (lower band) was inhibited in HNF4α-KO group compared to WT at days 0 and 5 post-PH. ERK2 phosphorylation was elevated in HNF4α-KO group compared to WT at day 7 post-PH. Finally, we measured mRNA expression of known regulator of hepatocyte proliferation and negative target of HNF4α *c-MYC* which was elevated throughout regeneration (Figure 2.4.8E). While c-MYC protein expression was similar between WT and HNF4α-KO animals at day 0, c-MYC expression was elevated in HNF4α-KO animals at all time points post-PH (Figure 2.4.8F-G).

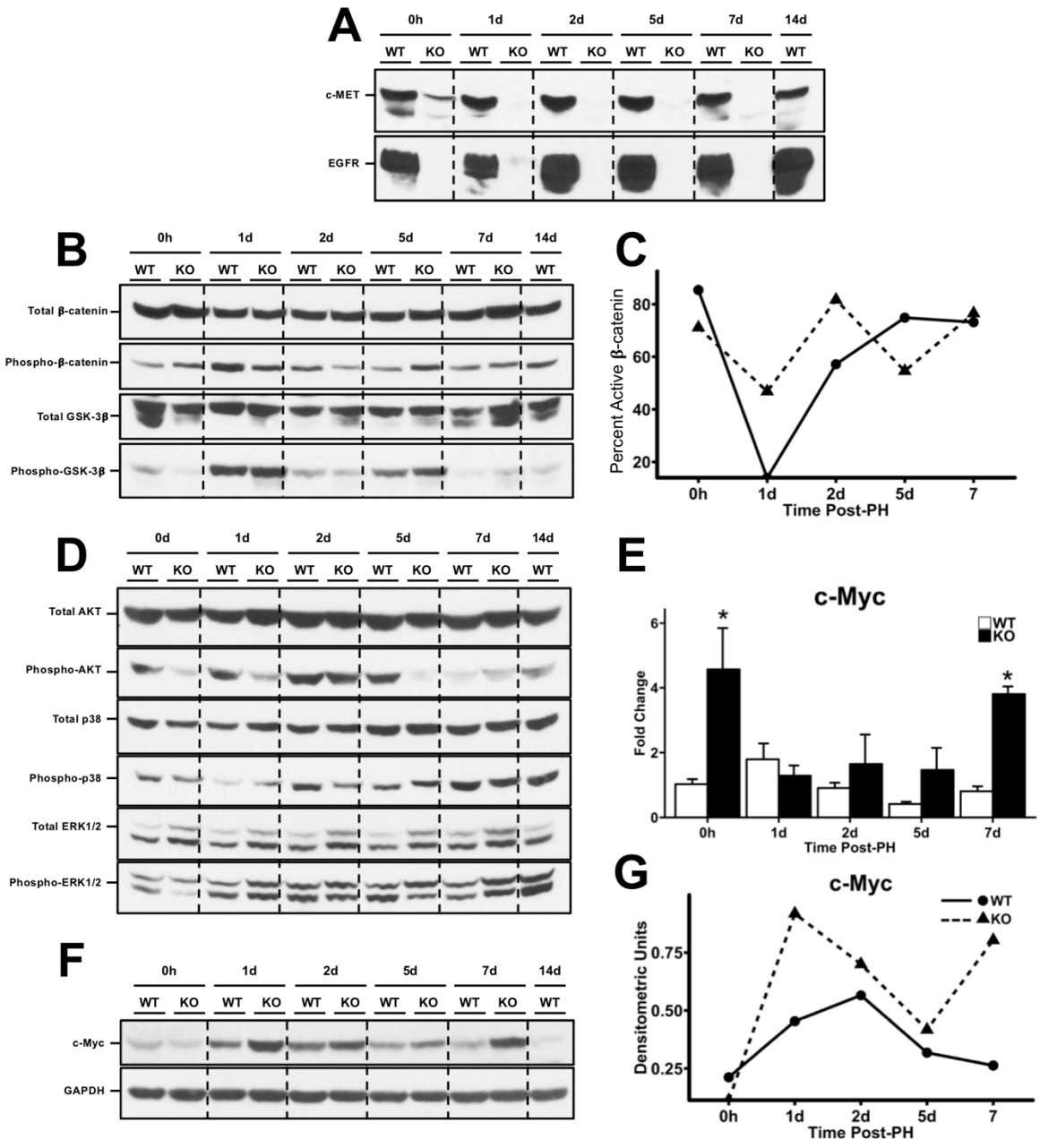

Figure 2.4.8. Activation of pro-proliferative signaling in HNF4α-KO mice during regeneration. Western blot analysis of (A) total EGFR and c-Met, (B) total and phosphorylated β-catenin and total and phosphorylatedGSK3β, (C) line graphs showing densitometric signal of inactive to total β-catenin, (D) Western blots for Total AKT, Phospho-AKT, Total p38, Phospho-p38, ERK1/2, Phospho-ERK1/2, (E) qPCR analysis of c-Myc mRNA from WT and HNF4α-KO livers over time course post-PH, (F) Western blot analysis of c-Myc, (G) and densitometric analysis of c-Myc. *indicate significant difference at $P \leq 0.05$between WT and HNF4α-KO.

2.4.8. RNAseq Revealed Sustained Increase in Pro-Proliferative and Anti-Differentiation Signaling in HNF4α-KO Mice Post-PH

To gain insights in the comprehensive signaling changes in HNF4α-KO livers after PH, we performed RNA-Seq analysis at days 2 and 5 post-PH. These time points were selected to match the peak hepatocyte proliferation (day 2 post PH) and early termination phase of regeneration (day 5 post PH) in the liver regeneration process. Overall, a similar number of genes (~1,000) increased and decreased at day 2 and day 5 after PH in HNF4α-KO mice as compared to WT mice (Table 2.4.1).

Table 2.4.1: Total Number of Gene Expression Changes Occuring in HNF4α-KO Mice Compared to WT Mice At 2 and 5 Days Post-PH.

Number of Gene Expression Changes in HNF4α-KO Mice Post-PH		
	Day 2	**Day 5**
Upregulated	880	1040
Downregulated	1184	1050

Ingenuity Pathway Analysis (IPA) predicted activation and inhibition of transcription factors based on gene expression changes between genotypes. At 2 days post-PH (Table 2.4.2), IPA predicted activation of effectors of proinflammatory signaling (EGR1, IRF3, IRF6, IRF7) and proproliferative transcription factors (JUN, RB1, P300, TCF3) in HNF4α-KO liver. Interestingly, HNF4α-KO also showed activation of TGF-β signaling as indicated by activation of SMAD2 and SMAD4 as well as inhibition of SMAD7 (Fabregat et al., 2016). The transcription factors predicted to be inhibited 2 days post-PH included HNF4α, HNF1A and the HNF4α coactivator PPARGC1A (PGC1A). Furthermore, Estrogen Receptor α (Esrra), which is known to regulate gene expression in coordination with HNF4α and PGC1A (Charos et al., 2012), was also predicted to be inhibited. TAF4, a known HNF4α cofactor which is required for HNF4α transcriptional activity (Alpern et al., 2014), was also inhibited. MED1, which is essential for PPARα activity and required for survival after PH (Jia, Viswakarma, & Reddy, 2014), was inhibited in HNF4α-KO 2 days post-PH. ZBTB20, a known suppressor of hepatocyte proliferation and repressor of alpha-fetoprotein (Weng et al., 2014; Xie et al., 2008), was predicted to be inhibited.

Table 2.4.2: Predicted Activity of Transcription Factors in HNF4□-KO Mice Compared to WT Mice 2 Days Post-PH

Day 2 Post-PH			
Activated Pathways	**Activation z-score**	**Inhibited Pathways**	**Activation z-score**
JUN	3.31	HNF4A	-6.498
EGR1	2.814	HNF1A	-4.428
RB1	2.497	Esrra	-3.357
IRF3	2.42	PPARGC1A	-3.228
FOXO4	2.377	NFIX	-2.433
EP300	2.305	ZBTB20	-2.294
SPI1	2.248	MED1	-2.272
THRAP3	2.219	CLOCK	-2.219
IRF6	2.215	NFIC	-2.2
SMAD4	2.201	GATA2	-2.059
MTA1	2.194	NKX2-3	-2.04
Gm21596/Hmgb1	2.169	E2F1	-2.027
IRF7	2.163	SMAD7	-2.027
SMAD2	2.068	TAF4	-2.008
TCF3	2.022		

At day 5 post-PH (Table 2.4.3), the analysis predicted activation of transcription factor proinflammatory damage associated molecular pattern (DAMP) protein HMGB1 in HNF4α-KO mice indicating sustained inflammatory signaling in HNF4α-KO mice throughout regeneration. The TGFβ effector SMAD2 was also activated at day 5 post-PH. Proliferative marker EP300 was activated at day 5 post-PH. The HNF4α negative target gene and proliferative marker CCND1 was activated in the HNF4α-KO group at day 5 post-PH indicated sustained proliferative signaling compared to WT mice. Activation of SNAI2 was predicted in the HNF4α-KO group at 5 days post-PH. SNAI2 is repressed by HNF4α and is known to promote EMT (Santangelo et al., 2011). PLAG1 is a fetal gene overexpressed in hepatoblastomas (Juma, Damdimopoulou, Grommen, Van de Ven, & De Groef, 2016) and was predicted to be activated in the HNF4α-KO group at day 5. Activation of TRIM24, a transcription factor with oncogenic activity (Appikonda, Thakkar, & Barton, 2016), was predicted at day 5 post PH in the HNF4α-KO mice. Transcription factors including HNF4A, HNF1A, PPARGC1A, and Esrra were inhibited at day 2 post-PH and continued to be inhibited at day 5 post-PH. Inhibition of SIRT2 was observed at 5 days post-PH in HNF4α-KO mice consistent with its known role in sharing many of the same target genes as HNF4α(Palu & Thummel, 2016). PPARGC1B is a known coactivator of PPARGC1A and was inhibited. NCOA2 and EBF1, known tumor suppressors(Armartmuntree et al., 2018; O'Donnell et al., 2012), were inhibited in HNF4α-KO mice day 5 post-PH. NFIX, a transcription factor known to inhibit development of HCC(Hu et al., 2018), was inhibited. Finally, the master regulators of sterol and lipid metabolism, SREBF1 and SREBF2, were inhibited 5 days post-PH.

Table 2.4.3: Predicted Activity of Transcription Factors in HNF4α-KO Mice Compared to WT Mice 5 Days Post-PH.

Day 5 Post-PH			
Activated Pathways	**Activation z-score**	**Inhibited Pathways**	**Activation z-score**
Gm21596/Hmgb1	2.767	HNF4A	-6.471
EP300	2.565	HNF1A	-4.641
TRIM24	2.554	SREBF2	-4.603
SMAD2	2.401	SREBF1	-3.768
CCND1	2.307	PPARGC1A	-3.045
SNAI2	2.1	Esrra	-2.887
ANKRD42	2	IRF7	-2.476
PLAG1	2	SIRT2	-2.449
		NFIX	-2.433
		PPARGC1B	-2.424
		BCL6	-2.229
		EBF1	-2.177
		ZEB1	-2.077
		NCOA2	-2.028

IPA analysis also predicted activity of diseases and organ function based on gene expression differences between WT and HNF4α-KO mice at 2 and 5 days post-PH. The comparison at day 2 post-PH (Table 2.4.4) predicted HNF4α-KO mice would exhibit activation of pathways involving inflammation, tumorigenesis and wound healing. Inhibited functions included numerous basic liver processes such as transport, metabolism and synthesis of cholesterol, lipids, bile acids and xenobiotics.

Table 2.4.4: Predicted Activation or Inhibition of Diseases and Functions in HNF4α-KO Mice Compared to WT Mice 2 Days Post-PH.

Day 2 Post-PH			
Activated Functions	**Activation z-score**	**Inhibited Functions**	**Activation z-score**
homing of cells	2.502	metabolism of retinoid	-3.653
hematopoiesis of phagocytes	2.308	metabolism of vitamin	-3.527
energy homeostasis	2.165	metabolism of tretinoin	-3.398
myelopoiesis of leukocytes	2.095	transport of lipid	-3.371
chemotaxis	2.073	metabolism of xenobiotic	-3.073
liver lesion	2.065	flux of lipid	-3.006
tumorigenesis of tissue	2.015	transport of steroid	-2.997
		flux of cholesterol	-2.974
		fatty acid metabolism	-2.925
		efflux of cholesterol	-2.843
		efflux of lipid	-2.77
		uptake of lipid	-2.753
		metabolism of terpenoid	-2.683
		transport of cholesterol	-2.68
		synthesis of terpenoid	-2.632
		uptake of bile salt	-2.578
		esterification of cholesterol	-2.551
		export of molecule	-2.537
		production of retinoid	-2.396
		hydroxylation of lipid	-2.241
		transport of rosuvastatin	-2.236
		uptake of fexofenadine	-2.219
		tonic-clonic seizure	-2.219
		synthesis of lipid	-2.139

This pattern continued at day 5 post-PH (Table 2.4.5). Activated functions continued to be related to cell proliferation, tumorigenesis and inflammation. Additionally, functions related to embryonic organ tissue development were activated in the HNF4α-KO group. Functions related to transport and metabolism of lipids, cholesterol and vitamins remained inhibited in HNF4α-KO mice 5 days post-PH.

Table 2.4.5: Predicted Activation or Inhibition of Diseases and Functions in HNF4α-KO Mice Compared to WT Mice 5 Days Post-PH.

Day 5 Post-PH			
Activated Functions	**Activation z-score**	**Inhibited Functions**	**Activation z-score**
sepsis	2.95	uptake of lipid	-3.472
stimulation of cells	2.891	metabolism of vitamin	-3.031
proliferation of cancer cells	2.783	metabolism of retinoid	-2.832
development of genitourinary system	2.698	metabolism of xenobiotic	-2.559
proliferation of tumor cells	2.574	metabolism of amino acids	-2.449
tumorigenesis of tissue	2.555	fatty acid metabolism	-2.38
immediate hypersensitivity	2.547	weight gain	-2.344
development of urinary tract	2.541	transport of lipid	-2.212
inflammation of absolute anatomical region	2.494	flux of lipid	-2.204
neoplasia of epithelial tissue	2.414	secretion of hormone	-2.107
assembly of cells	2.409	flux of cholesterol	-2.055
growth of malignant tumor	2.383		
development of body trunk	2.373		
inflammation of liver	2.3		
endothelial cell development	2.289		
inflammation of organ	2.253		
acute phase reaction	2.219		
development of epithelial tissue	2.184		
development of abdomen	2.17		
abnormality of lower limb	2.157		
inflammation of body cavity	2.14		
formation of mammary gland	2.043		

formation of gland	2.043	
development of exocrine gland	2.017	
activation of epithelial cells	2.008	
stimulation of carcinoma cell lines	2	

2.4.9. Reexpression of HNF4α Restores Hepatocyte Quiescence and Gene Expression and Extends Survival of HNF4α-KO Animals Post-PH

Next we tested if reexpression of HNF4α in hepatocytes by intravenous injection of AAV8-CMV-HNF4α could rescue HNF4α-KO mice after PH by restoring HNF4α transcriptional activity after cell division. First we reexpressed HNF4α in HNF4α-KO mice and measured HNF4α target gene expression. HNF4α reexpression increased total c-MET and total EGFR protein expression to WT levels and reduced cyclin D1 expression to WT levels (Figure 2.4.9A). Hepatocyte proliferation was assessed by immunohistochemical analysis of PCNA positive nuclei. High levels of hepatocyte proliferation were observed in the HNF4α-KO group. HNF4α reexpression resulted in decreased hepatocyte proliferation compared to HNF4α-KO mice (Figure 2.4.9B-C). Finally, we reexpressed HNF4α in HNF4α-KO mice 2 days post-PH. This treatment improved survival compared to HNF4α-KO mice (Figure 2.4.9D).

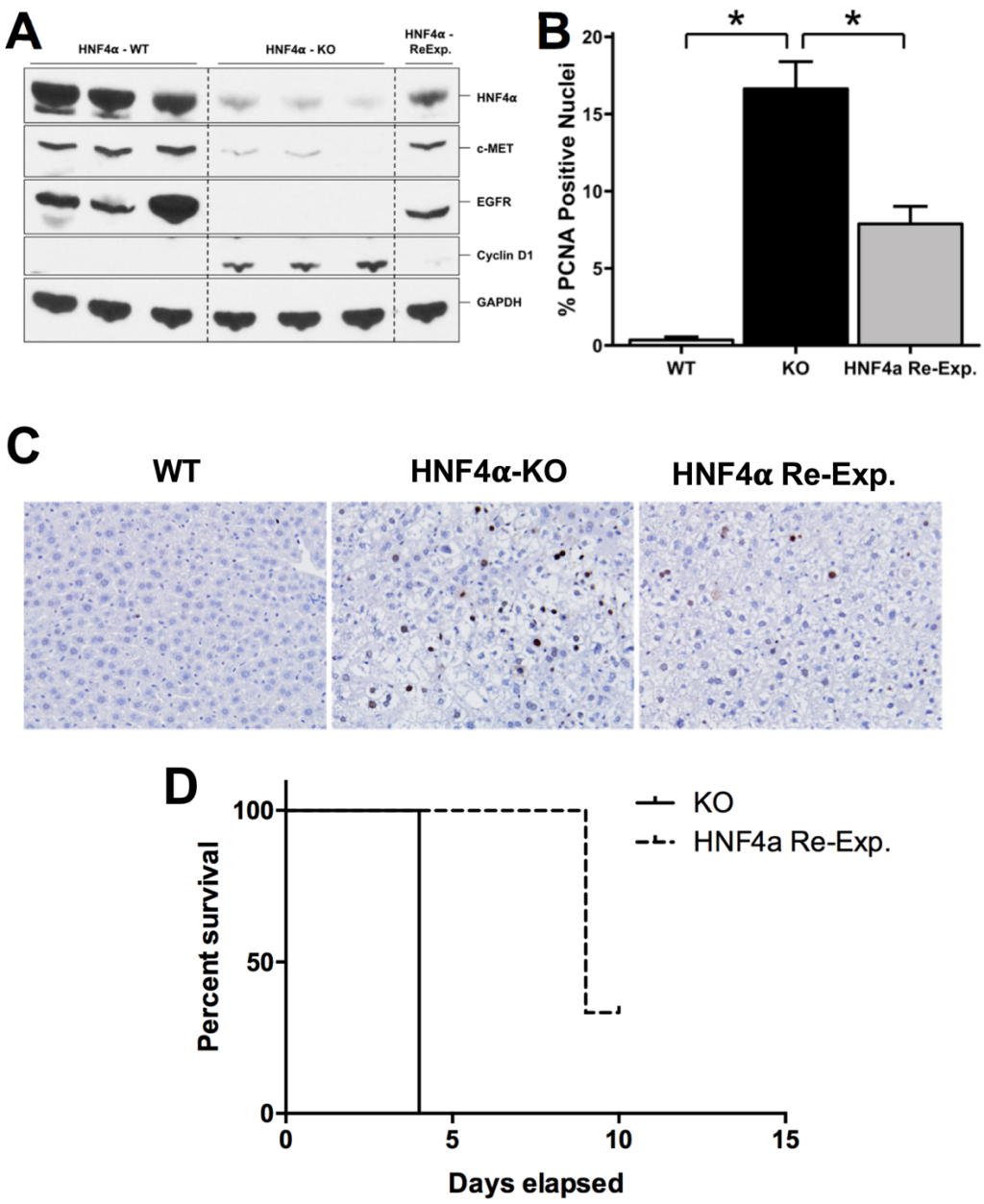

Figure 2.4.9. Reexpression of HNF4α restores hepatocyte quiescence and gene expression and extends survival of HNF4α-KO animals post-PH. (A) Western blot analysis of HNF4α, Cyclin D1, c-Met and EGFR in WT, HNF4α-KO and HNF4α-Reexp. mice, (B) Immunohistochemical analysis of PCNA positive nuclei in liver sections from WT, HNF4α-KO and HNF4α-Reexp. mice, (C) Representative photomicrographs (40x) of PCNA-stained liver sections, (D) Kaplan-Meier survival analysis of WT and HNF4α-Reexp mice after PH. * indicate significant difference at $P \leq 0.05$.

2.5. Discussion

HNF4α is the master regulator of hepatocyte differentiation because it is required for hepatocyte differentiation during embryonic liver development and it maintains hepatocyte specific gene expression in adult hepatocytes (Gonzalez, 2008; Kyrmizi et al., 2006; Morimoto et al., 2017). HNF4α also exerts strong anti-proliferative effects on hepatocytes and decreased HNF4α expression and activity results in loss of quiescence, which can lead to HCC (W. Y. Cai et al., 2017; Hatziapostolou et al., 2011; Walesky, Edwards, et al., 2013). Despite being recognized as one of the strongest anti-proliferative proteins in the liver, the role of HNF4α during liver regeneration is not known. We investigated the role of HNF4α in liver regeneration after PH, where adult hepatocytes exit the physiological quiescent state and enter the cell cycle before returning to the quiescent state once liver regeneration has been completed. We hypothesized that decreased HNF4α expression and function would occur during the initiation of regeneration to alleviate the antiproliferative effects of HNF4α as quiescent hepatocytes enter the cell cycle during the initiation of liver regeneration. Indeed, we observed decreased nuclear and cytoplasmic levels of HNF4α occurring within hours after surgery. This decreased protein expression was not due to changes in transcription of the HNF4α gene because there were no changes in HNF4α mRNA post-PH. Decreased periportal HNF4α staining after PH has been previously reported (Fukuda et al., 2016). However, HNF4α expression during liver regeneration has never been studied in a time course at this level of resolution until now. Posttranslational modifications (PTMs) of HNF4α which result in decreased nuclear localization are known (Z. Wang, Salih, & Burke, 2011; Yokoyama et al., 2011), and phosphorylation of HNF4α by PKC or Src can lead to proteasomal degradation of HNF4α (Chellappa, Jankova, et al., 2012; K. Sun

et al., 2007). We investigated how inhibiting one of these phosphorylation mechanisms, Src, would affect nuclear HNF4α expression 6 hours post-PH, when HNF4α was observed to be at its lowest levels in normal mice. Mice treated with a Src inhibitor exhibited higher levels of nuclear HNF4α compared to vehicle treated mice, providing evidence that phosphorylation of HNF4α by Src could be the mechanism through which HNF4α is removed from the nucleus after PH. Src and PKC are both activated by EGF through EGFR making this mechanism of HNF4α phosphorylation relevant to liver regeneration. However, little remains known about post-translational regulation of HNF4α in the liver and future studies are needed to map the impact of individual PTMs on HNF4α and characterize how inhibition of Src, PKC and other kinases might change HNF4α activity in liver regeneration and other conditions. Decreased nuclear expression of HNF4α protein after PH resulted in decreased transcriptional activity as measured by its target genes, which play a critical role in liver physiology (Walesky, Edwards, et al., 2013). Our observations independently reproduce a microarray study describing decreased HNF4α target gene expression 4 hours post-PH (Jiao et al., 2015). This highlights functional differences between quiescent and proliferating hepatocytes and suggests restoring HNF4α in hepatocytes responding to chronic injury could successfully restore hepatic function (T. Nishikawa et al., 2015; Yue et al., 2010).

Next, we hypothesized that overexpressing HNF4α in hepatocytes at time points after PH when HNF4α levels were normally decreased would prevent hepatocytes from proliferating and halt or delay initiation of liver regeneration. Interestingly, our experiments with Tet-On driven HNF4α expression demonstrated significantly decreased hepatocyte proliferation 6 hours post-PH and an

almost statistically significant increase in proliferation 48 hours post-PH. Decreased proliferation 6 hours post-PH was likely driven by decreased expression of proproliferative HNF4α negative target genes CCND1 and CDKN3. These data suggest that rapid down regulation of HNF4α after PH may accelerate hepatocyte cell cycle entry, but is not absolutely necessary for initiation of cell cycle progression after PH. It also suggests activation of compensatory proliferative pathways which can activate liver regeneration despite increased HNF4α expression, highlighting the redundant nature of pro-regeneration pathways. It is also possible that HNF4α overexpression resulted in delayed initiation because the mechanism responsible for HNF4α degradation was still active and more time was needed to degrade the overexpressed protein. Inhibiting the mechanism responsible for HNF4α degradation, such as Src kinase, might be a better strategy to study the effects of increased HNF4α expression during initiation of liver regeneration once those mechanisms are established. One interesting observation from the HNF4α overexpression study was the lack of steatosis in HNF4α overexpressing mice, which is known to occur after PH (Shteyer, Liao, Muglia, Hruz, & Rudnick, 2004). This might be caused by increased expression of apolipoproteins such as APOA2 which are well established HNF4α target genes. These data indicate that the initial loss of HNF4α could be mechanistically involved in the transient steatosis observed following PH and those mechanisms may be independent of initiation of cell proliferation.

The most striking observation from our studies is 100% mortality in HNF4α-KO mice following PH within 11 days secondary to loss of hepatic function. HNF4α is required for ureagenesis and liver-specific HNF4α-KO mice have increased serum ammonia and decreased serum urea (Y.

Inoue et al., 2002). Several HNF4α-KO mice exhibited loss of righting reflex prior to death, a symptom of hepatic encephalopathy (data not shown). Decreased hepatic function further manifested as elevated bilirubin levels in HNF4α-KO mice after PH and a significant deficiency of hepatocyte differentiation gene expression at 7 days post PH in HNF4α-KO mice as compared to the WT mice. In contrast, a significant increase in nuclear HNF4α expression was observed in the control mice (Figure 2.4.1) at days 3 and 5 after PH, the time points when the cell proliferation decreases and redifferentiation starts. The fact that HNF4α-KO hepatocytes were not able to compensate for loss of HNF4α function (as measured by target gene expression) further supports the role of HNF4α as a master regulator of hepatic differentiation. Taken together, these data clearly demonstrate that HNF4α-mediated differentiation of the newly divided hepatocytes is an essential part of the termination of regeneration and failure to redifferentiate can lead to cell and animal mortality.

Another important observation in our studies was the complete loss of c-MET and EGFR expression in HNF4α-KO mice which could contribute to the death observed in HNF4α-KO mice after PH. Recent studies have shown that c-MET deletion combined with EGFR inhibition results in death of mice without any disturbance to the liver (Tsagianni et al., 2018). These mice exhibited decreased serum albumin, decreased blood glucose and poor expression of hepatic genes involved in urea synthesis, lipid metabolism and carbohydrate metabolism. Microarray analysis of these mice found HNF4α to be the top prediction in a list of inhibited transcription factors. This study shows that baseline signaling through c-MET and EGFR is required for hepatocyte function in the quiescent liver and combined with our data is evidence of a positive

regulation feedback loop between EGFR, c-MET and HNF4α in normal liver. A combined loss of EGFR, c-MET and HNF4α observed in the HNF4α-KO mice could have resulted in loss of several redundant survival mechanisms at once, leading to death after PH.

It is known that signaling induced by primary hepatic mitogens HGF and EGF family members (EGF, TGFα etc.) via their cognate receptors c-MET and EGFR is essential for liver regeneration after PH (Paranjpe et al., 2016). Mice with deletion of c-MET and inhibition of EGFR do not exhibit any hepatocyte proliferation after PH (Paranjpe et al., 2016). However, HNF4α-KO mice seem to be an exception to this rule. Despite the loss of c-MET and EGFR expression in HNF4α-KO mice, hepatocyte proliferation occurred at high levels before PH and a surge of proliferation was observed at the same time as peak proliferation in WT mice before returning to baseline levels, although remaining higher than WT levels. Two important conclusions can be made from this observation. First, increased proliferation in HNF4α-KO mice before and after PH is consistent with our previous findings that HNF4α is anti-proliferative in hepatocytes (Walesky, Gunewardena, et al., 2013). Second, although proliferation is higher in HNF4α-KO mice before PH, the surge of additional proliferation that occurs in response to PH in the HNF4α-KO mice suggests some pro-proliferative pathways involved in regeneration remain intact in HNF4α-KO mice. Furthermore, the occurrence of a regenerative response in HNF4α-KO mice, which do not express EGFR or c-MET, is the product of activation of a pro-proliferative pathway that is normally repressed by HNF4α. To address the alternate mechanisms at play, we investigated several known pathways including Wnt/β-catenin pathway and MAPK signaling. Whereas, significantly higher β-catenin signaling

was observed in HNF4α-KO mice as evident by decrease in phosphorylated (inactive) β-catenin, this was observed only during the early time points. Similarly, the AKT, p38 and ERK-1/2 pathways also revealed only moderate differences between WT and HNF4α-KO mice after PH, which cannot explain the sustained proliferation of hepatocytes in HNF4α-KO mice. However, we observed a significant activation of c-Myc in HNF4α-KO mice consistent with previous studies showing activation of c-Myc in the absence of HNF4α (Walesky, Edwards, et al., 2013). Also, the role of c-Myc in liver regeneration and cancer is well documented. Our studies show that HNF4α-KO hepatocytes lose two of the primary mitogenic pathways, namely c-MET and EGFR, but proliferation continues mainly via c-Myc activation.

It is well known that deletion of hepatic HNF4α increases liver to body weight ratios, which consistent with our observations in HNF4α-KO mice before PH (Bonzo et al., 2012; Hayhurst et al., 2001). However, despite exhibiting increased hepatocyte proliferation throughout the time after PH, there were no differences in recovery of liver weight between WT and HNF4α-KO mice. Liver mass is a product of cell number and cell size. Increased proliferation would contribute to increased cell number, but restoration of cell size after PH involves the nutrient, protein and water content of hepatocytes to return to normal levels. Considering the importance of HNF4α activity in hepatocyte function, it is likely that the processes required to restore cell size would take a longer time in HNF4α-KO mice, but HNF4α-KO mice die before this can be achieved. Thus we cannot determine if regeneration in HNF4α-KO mice would overshoot target liver mass due to excess proliferation.

The RNAseq analysis further revealed mechanisms that drive continued proliferation and also the mechanisms that lead to liver failure and death of the HNF4α-KO mice after PH. We investigated days 2 post-PH, the time points with peak proliferation, and 5 days post-PH the time point when termination of regeneration begins. At both time points, the HNF4α-KO livers exhibited a proinflammatory and profibrotic transcriptional profile. Elevated inflammation in HNF4α-KO mice was not caused by hepatocellular injury, as there was no difference in ALT levels or histopathological changes between groups (data not shown). However, previous studies have reported elevated bile acid levels in HNF4α-KO livers, which could cause increased inflammatory signaling (Hayhurst et al., 2001). Furthermore, many HNF4α negative target genes such as EGR1 are pro-inflammatory. IPA analysis also supported our findings of dedifferentiation and loss of hepatocyte function in HNF4α-KO mice. IPA predicted consistent inhibition of several prominent hepatocyte functions in HNF4α-KO at day 2 and day 5 post-PH. However, we observed a shift in the characteristics of activated functions between the two time points. Most of the activated functions in HNF4α-KO mice at day 2 included those involved in inflammation. However, the activated functions in HNF4α-KO mice at day 5 included many more functions involved in proliferation, tumorigenesis and a developmentally immature phenotype in addition to inflammation. Furthermore, HNF4α-KO mice at day 5 were predicted to express higher levels of known oncogenes (TRIM24, SNAI2, PLAG1) which were not activated at day 2. This transformation from an abnormal regenerative response to the beginnings of a pathological condition raise the question of how hepatocytes with poor expression of HNF4α may respond to chronic or intermittent low level liver injury. The decreased expression of HNF4α expressed in many liver diseases and HCC may be an example of the innate regenerative capability of the liver contributing to the progression of liver disease.

We observed that reexpression of HNF4α in HNF4α-KO mice using the AAV8 resulted in restoration of quiescence and the expression of c-MET and EGFR. However, when the HNF4α construct was introduced after PH, we did not observe complete prevention of death. This may be due to the timing of HNF4α reexpression (two days after PH may be too early), the possibility that dividing cells may have decreased sensitivity to AAV8 and that the dividing cells may reject AAV8-mediated introduction of exogenous material. Nevertheless, following HNF4α reintroduction into HNF4α-KO mice after PH did significantly increase survival time compared to HNF4α-KO counterparts included in this experiment and those used in the deletion time course. Even if HNF4α reexpression was not 100% efficient in dividing hepatocytes, delayed mortality due to partial restoration of hepatic function through HNF4α expression supports hepatic failure being the cause of death in these animals.

In summary, our studies are the first to examine and manipulate HNF4α expression over multiple time points throughout the initiation, progression and termination of liver regeneration after partial hepatectomy. Our findings suggest downregulation of HNF4α may contribute to hepatocyte cell cycle entry during initiation of regeneration. More importantly, reestablishment of HNF4α activity during termination of regeneration is absolutely required for termination of regeneration and resumption of hepatocyte function. This study uncovers new evidence of HNF4α mediated expression of EGFR and c-MET and demonstrate that HNF4α-KO mice are capable of mounting a regenerative response despite lacking these receptors. Furthermore, regeneration in the absence of HNF4α results in a dedifferentiated, pro-carcinogenic hepatocyte

phenotype. These results confirm the role of HNF4α as a major player in hepatocyte proliferation and differentiation during liver regeneration.

Chapter 3. Using HNF4α Gene Signature to Determine Hepatocellular Carcinoma Disease Progression

3.1. Abstract

Hepatocellular carcinoma (HCC) is the major hepatic malignancy and third leading cause of cancer related deaths in the world with extremely limited treatment options. An important issue is lack of tools to determine the disease progression from the non-malignant stages such as liver cirrhosis to cancer and further progression of disease from early stage cancer to later stage HCC are limited. Recent studies have identified role of Hepatocyte Nuclear Factor 4α (HNF4α) in inhibition of hepatocyte proliferation and HCC pathogenesis. Here we report that HNF4α activity as measured by using a specific HNF4α target gene signature can be used as an excellent predictive tool in HCC disease progression. We identified a specific HNF4α gene expression signature using RNAseq-ChIPseq data obtained from hepatocyte specific HNF4α knockout (HNF4αKO) mice, which was further refined for use in human samples. Validation studies were performed using HNF4αKO mice and diethylnitrosamine-initiated cholic acid promoted mouse HCCs. We initially performed an *in silico* analysis using three independent gene expression data sets consisting of a total of 102 individual human samples. Cluster analysis performed using HNF4α gene signature was successful in distinguishing Cirrhotic-non-HCC from cirrhotic-with HCC with >80% specificity; differentiate between normal, cirrhotic non-HCC, dysplastic nodules, early stage HCC and advanced HCC with >85% specificity and distinguish HCC from paired non-tumor tissues with 100% specificity. Further studies with two independent sets of human samples (n=26 total) of various stages of HCC disease progression corroborated the *in silico* analysis. Finally, survival analysis performed on a total of 365 HCC samples indicated that the HNF4α target gene signature was able to clearly distinguish cases with shorter survival, which had significantly lower HNF4α activity. These data indicate that loss of HNF4α is a

critical factor in HCC and HNF4α function as measured by target gene expression is a potential predictive biomarker in HCC pathogenesis in humans.

3.2. Introduction

The role of HNF4α in hepatocyte differentiation and proliferation, along with its activity in liver disease is detailed in Chapter 1. In the liver, hepatocyte-specific deletion of HNF4α results in hepatomegaly, spontaneous hepatocyte proliferation and promotion of DEN-induced liver cancers (Bonzo et al., 2012; Walesky, Edwards, et al., 2013; Walesky, Gunewardena, et al., 2013). Globally, there are 850,000 new cases of Hepatocellular Carcinoma (HCC) every year (Torre et al., 2015) and it is the second leading cause of cancer related deaths worldwide ("Global, regional, and national age-sex specific all-cause and cause-specific mortality for 240 causes of death, 1990-2013: a systematic analysis for the Global Burden of Disease Study 2013," 2015). Disease prevalence and limited treatment options made HCC the leading indication among liver transplant registrants and recipients in 2015 (J. D. Yang et al., 2017). It is known that 3-5% of cirrhotic patients will develop HCC each year (Villanueva et al., 2010) and HCC is a leading cause of death among cirrhotic patients (Sangiovanni et al., 2004). Overwhelming demand on organ donation networks as well as decreased quality of donor livers has resulted in a shortage of available livers (Habka, Mann, Landes, & Soto-Gutierrez, 2015). When following the BCLC staging and treatment schedule, early detection and accurate prognosis is critical for curative treatment of HCC (Josep M. Llovet, Burroughs, & Bruix, 2003). This can be accomplished by screening patients likely to develop HCC, such as those with cirrhosis, or by the molecular classification of diagnosed HCCs (Bruix, Han, Gores, Llovet, & Mazzaferro, 2015). Predicting which cirrhotic patients will develop HCC would lead to improved outcomes and decreased consumption of donor liver supply.

The prevalence of data linking decreased HNF4α expression with progression of liver cancer led us to hypothesize that the development and advancement of HCC occurs with a corresponding decrease in HNF4α expression and activity. Here, we report the identification of an HNF4α target gene signature and demonstrate its ability to measure HNF4α activity in human and mouse liver tissue and gene expression datasets. This signature revealed a pattern of decreased HNF4α activity that correlated with progression of HCC. Our results demonstrate the potential of this gene signature to refine current screening protocols and prognostic algorithms in the treatment of HCC.

3.3. Materials and Methods

3.3.1. Animals and Generation of Global Gene Expression Datasets

The generation of hepatocyte specific conditional HNF4α-KO mice and induction of HCCs in the HNF4α-KO mice has been previously published (Walesky, Edwards, et al., 2013). Two RNAseq datasets were generated. First, differentially expressed genes (DEGs) in the livers of WT and HNF4α-KO mice were identified using RNAseq as previously published (Walesky, Edwards, et al., 2013). The second RNAseq dataset was generated using HCCs isolated from WT and HNF4α-KO mice (three tumors per genotype) as described before (Walesky, Edwards, et al., 2013). Additionally, a published HNF4α chromatin immunoprecipitation sequencing dataset (ChIPseq) for mouse liver was used for the analysis (Hoffman et al., 2010). These three datasets were used to determine the HNF4α target gene signature.

3.3.2. Identification of HNF4α Target Gene Signature

The strategy used to identify genes included in the HNF4α target gene signature is illustrated in Figure 3.4.1A. First, RNA-Seq analysis of normal liver tissue from WT and hepatocyte-specific HNF4α mice identified 829 genes with a minimum 2-fold difference in expression between groups (Dataset 1). This dataset selected for genes that are directly and indirectly regulated by HNF4α. Next, RNA-Seq analysis performed on liver tumor tissue from WT and hepatocyte-specific HNF4α-KO mice identified 2152 genes with a minimum 2-fold difference in expression between groups (Dataset 2). The genes from Dataset 1 and Dataset 2 were compared to Dataset 3 which contained genes identified in a previously published HNF4α ChIP-Seq dataset (Hoffman et al., 2010). This identified genes that were directly regulated by HNF4α by selecting for genes

with a HNF4α binding site within 5kb of the transcription start site and was termed Dataset 4, which contains 323 genes were found in common between Dataset 1-3. Further, to reduce the number of genes in the signature such that analysis of signature expression can be conducted using a 96-well Taqman-based qPCR approach and to account for differences between human and mouse gene expression, Dataset 4 was refined using IPA analysis to identify genes. The resulting 44 genes contained in Dataset 5 identified the HNF4α Target Gene Signature.

3.3.3. Confirmation of HNF4α Target Gene Signature

For confirmation of target gene signature, total hepatic mRNA from WT and HNF4α-KO mice were used as described before (Walesky, Gunewardena, et al., 2013). For further analysis of the gene signature, used mRNA samples generated in a recently published HCC study in our laboratory where we had investigated the role of bile acids in promoting DEN-induced liver cancer (L. Sun et al., 2016). The experimental design included four groups including Controls (DEN- CA-), 0.2% cholic acid alone (DEN- CA+), DEN alone no cholic acid (DEN+ CA-) and DEN+ cholic acid (DEN+ CA+). The treatment protocols, tissue collection methods, and results from this study have been previously published (L. Sun et al., 2016).

3.3.4. Human Samples

All human liver, RNA, and paraffin embedded sections were obtained from the University of Kansas Medical Center Liver Tissue Bank. Samples were obtained with informed consent from patients in accordance with ethical and institutional guidelines. The Institutional Review Board at the University of Kansas Medical Center approved this study.

3.3.5. qPCR

Total RNA was harvested from frozen livers using the TRIzol method according to manufacturer's protocol (Life Technologies, Carlsbad, CA). Quality and quantity of isolated RNA was determined using a NanoDrop 1000 Spectrophotometer (ThermoScientific). RNA was converted to cDNA as previously described (Apte et al., 2009). Expression of HNF4α transcripts in human samples were determined using an Applied Biosystems StepOnePlus Real-Time PCR System with SYBR Green PCR Master Mix (Applied Biosystems, Foster City, CA) as previously described (Beggs et al., 2016). Human primers were designed as follows: HNF4α, 5′-aagccgtccagaatgagc-3′ (forward) and 5′-aatgtcgccgttgatccc-3′ (reverse), GAPDH, 5′-tgatgacatcaagaaggtggtgaag-3′ (forward) and 5′-tccttggaggccatgtgggccat-3′ (reverse). Fold change in gene expression was calculated using the $2^{-\Delta\Delta Ct}$ method (Livak & Schmittgen, 2001).

For HNF4α gene signature analysis, Ct values of genes included in the HNF4α target gene signature were determined using a custom made TaqMan Gene Expression Assays containing species specific primers for each gene in the signature (Applied Biosystems, Foster City, CA). Each TaqMan array had 44 genes and 4 housekeeping internal controls in duplicates. The ΔCt values of signature genes were calculated by subtracting the geometric mean of Ct values from 4 housekeeping control genes (18S, GAPDH, HPRT, GUSB) (Vandesompele et al., 2002) from the Ct values of each signature gene.

3.3.6. Hierarchical Clustering and Heatmaps

Expression of HNF4α signature genes was analyzed using hierarchical clustering modules from GenePattern (Reich et al., 2006). The HierarchicalClustering module uses algorithms originally published in 1998 (Eisen, Spellman, Brown, & Botstein, 1998) and later improved (de Hoon, Imoto, Nolan, & Miyano, 2004). Raw values used for the clustering process were -ΔCt values for each gene. Module settings were specified such that column and row distance was determined by calculating Euclidean distance measurement. The clustering method used was pairwise complete-linkage. Rows were mean-centered and normalized. Files generated using this module were used by the HierarchicalClusteringViewer module to generate heatmaps and dendrograms.

3.3.7. Immunohistochemistry

Paraffin-embedded human liver sections were stained with hematoxylin-eosin using an autostainer (model CV 5030, Leica Microsystems, Buffalo Grove, IL). Additional sections were used for immunohistochemical detection of HNF4α using a staining procedure that has previously been described (Wolfe et al., 2011) with a modification to the antigen retrieval step. Instead of boiling, slides submerged in citrate buffer were subjected to autoclave treatment. The primary antibody used for HNF4α detection (PP-H1415-00, Perseus Proteomics Inc., Tokyo, Japan) was diluted 1:500 and incubated on samples overnight at 4°C.

3.4. Results

3.4.1. Validation of HNF4α Target Gene Signature

To test the ability of the HNF4α target gene signature (Figure 3.4.1A, Dataset 5) to detect HNF4α activity, we used qPCR to measure signature gene expression in WT (CRE+ CO and CRE- CO), tamoxifen (TAM) control (Cre- CO) and HNF4α-KO mice (CRE+ TAM). Group average -ΔCt values were used to generate the heatmap (Figure 3.4.1B). Expression of signature genes was decreased in the HNF4α-KO group compared to all control groups. The column dendrogram shows three WT samples, including the TAM control, clustering together away from the HNF4α-KO group. Fold change values for each gene when compared to the CRE+ CO group are found in Table 3.4.1. Gene names have been replaced with numbers due to ongoing patent application, which prevents us from describing them. Together, these data demonstrate the ability of the HNF4α target gene signature to measure HNF4α activity.

Table 3.4.1: Fold change values of HNF4α target signature genes as compared to CRE+ mice treated with corn oil. Gene expression was measured using custom made Taqman qPCR plates.

Gene #	**CRE+ TAM**	**CRE- TAM**	**CRE- CO**	**CRE+ CO**
1	0.115	0.600	0.476	1
2	0.104	0.523	0.480	1
3	0.083	0.533	0.666	1
4	0.151	0.620	0.796	1
5	0.065	0.427	0.883	1
6	0.023	0.255	0.615	1
7	0.008	0.137	0.693	1
8	0.150	0.586	1.278	1
9	0.099	1.066	1.591	1
10	0.145	0.921	1.717	1
11	0.092	0.789	1.750	1
12	0.448	0.587	1.038	1
13	0.030	0.077	0.513	1
14	0.252	0.446	0.750	1
15	0.095	1.532	1.158	1
16	0.164	1.546	1.218	1
17	0.235	1.512	1.109	1
18	0.094	1.764	0.905	1
19	0.277	1.295	0.915	1
20	0.037	1.334	0.731	1
21	0.028	1.494	0.730	1
22	0.036	1.246	0.619	1
23	0.285	1.047	0.861	1
24	0.022	1.130	0.641	1
25	0.112	1.036	0.847	1
26	0.250	1.050	0.940	1
27	0.040	1.290	0.909	1
28	0.036	1.452	1.063	1
29	0.084	0.793	0.634	1
30	0.130	0.958	0.739	1
31	0.246	0.938	0.765	1
32	0.023	1.060	1.044	1
33	0.076	0.948	1.003	1
34	0.098	0.998	1.038	1
35	0.034	0.737	0.831	1
36	0.056	1.820	0.538	1
37	0.120	2.104	0.980	1
38	0.117	2.312	1.009	1
39	0.212	2.124	0.959	1
40	0.238	1.698	0.877	1
41	0.146	1.065	0.319	1
42	0.265	8.375	1.522	1
43	2.838	0.639	2.174	1
44	8.601	2.566	10.559	1

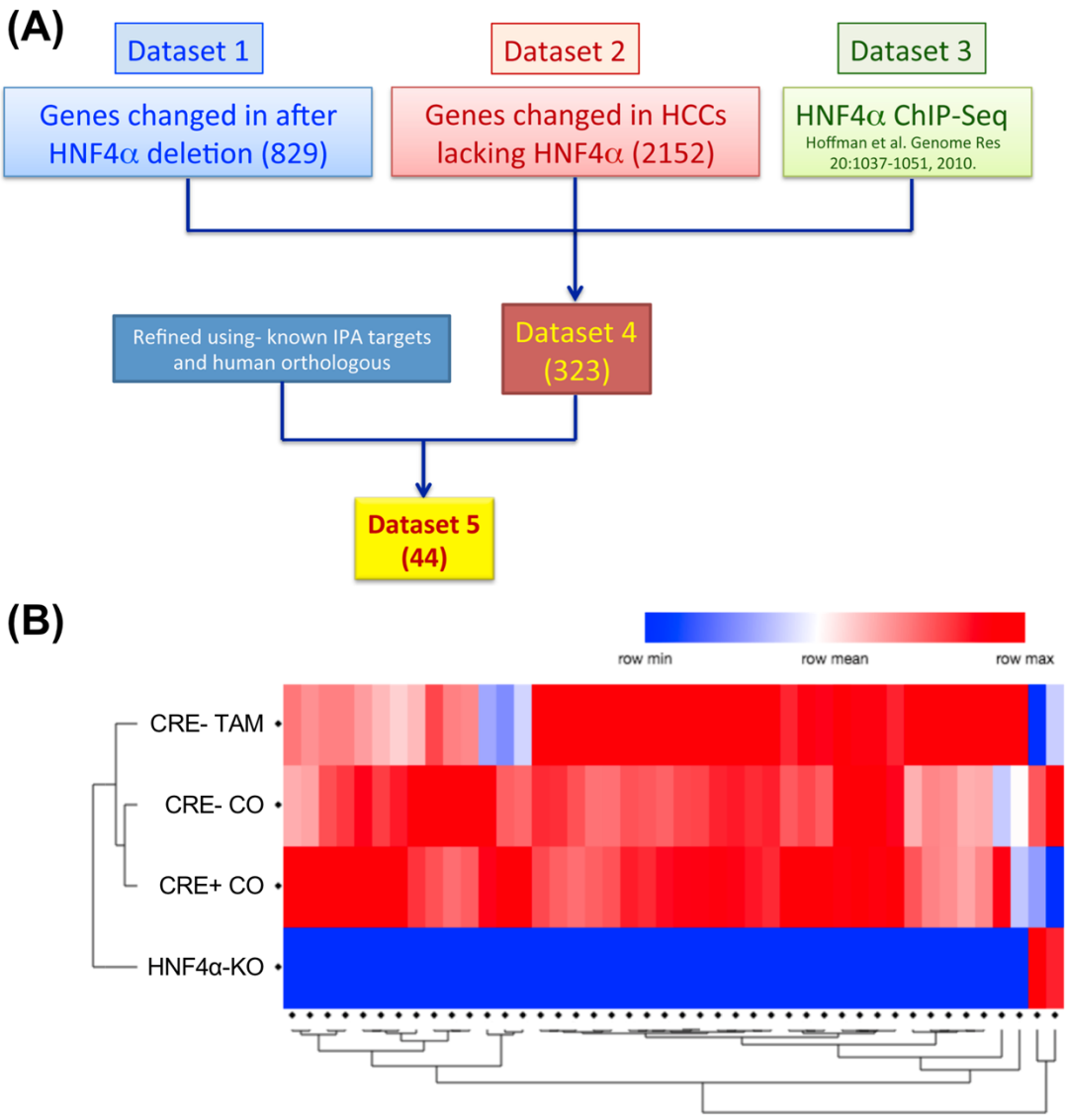

Figure 3.4.1. Identification and Validation of HNF4α Target Gene Signature. (A) Schematic representing method used to identify 44 target genes included in the signature. Quantity of genes included in each dataset are indicated in parentheses. (B) Heatmap comparing expression of signature genes from HNF4α-KO mice (CRE+ TAM) to WT control mice (CRE- CO, CRE+ CO, CRE- TAM).

3.4.2. HNF4α Target Gene Signature Analysis in Cholic Acid-Promoted HCC

We hypothesized that progression of HCC to more advanced forms would correlate with a decrease in HNF4α activity. To test this, we used mRNA samples generated in a recently published HCC study in our laboratory (L. Sun et al., 2016) where we had investigated the role of bile acids in promoting DEN-induced liver cancer. The experimental design included four groups: Controls (DEN- CA-), 0.2% cholic acid alone (DEN- CA+), DEN alone no cholic acid (DEN+ CA-) and DEN+ cholic acid (DEN+ CA+). Out of the four groups, only DEN alone (DEN+ CA-) and DEN+Cholic acid (DEN+ CA+) mice had shown liver tumors. The DEN+ CA+ group had much higher number of tumors, which were advanced HCCs. Control groups (DEN- CA+, and DEN- CA-) had normal liver histology and did not develop HCC (L. Sun et al., 2016). qPCR analysis of HNF4α signature gene expression showed high levels of HNF4α activity in DEN- CA- and DEN- CA+ groups. DEN+ CA- and DEN+ CA+ groups clustered together and showed low levels of signature gene expression. However, DEN+ CA+ treated animals, the group with the most severe tumor progression, had the lowest levels of HNF4α gene signature expression (Figure 3.4.2).

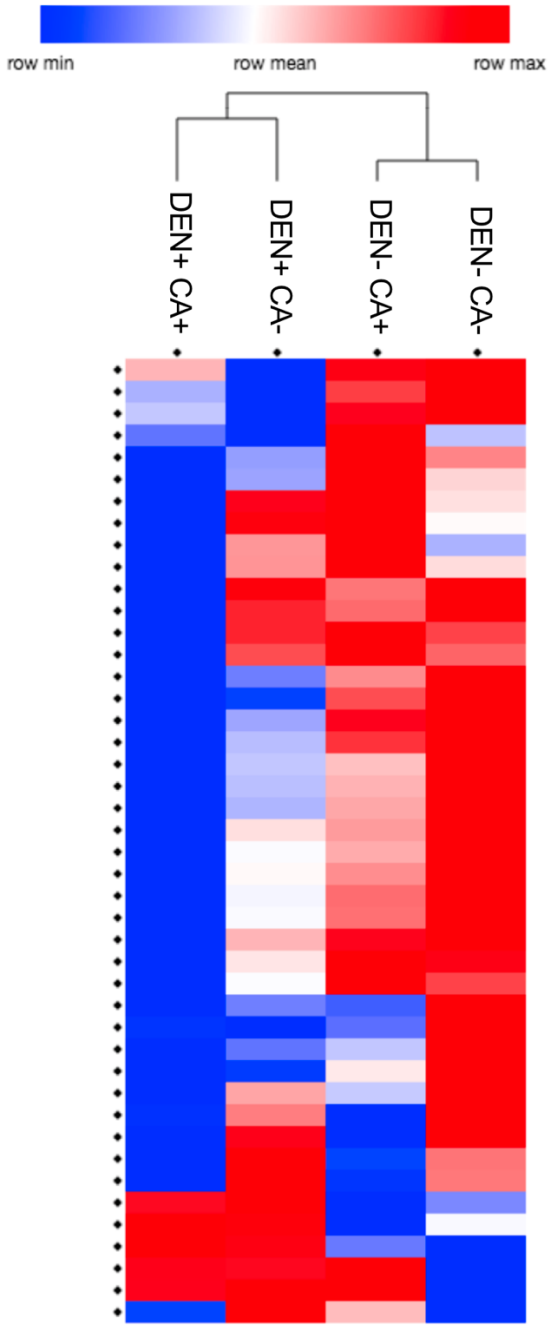

Figure 3.4.2. Decreased Expression of HNF4α Signature Genes Correlates with Advancement of HCC Severity in Mice. Hierarchical clustering of signature expression patterns indicates decreased HNF4α activity in mice with DEN-induced HCC (DEN+ CA-, DEN+ CA+) when compared to untreated mice (DEN- CA-) or mice treated with only cholic acid (DEN- CA+). A further decrease in activity was observed in mice with cholic acid promoted HCCs (DEN+ CA+).

3.4.3. In Silico Analysis of HNF4α Target Gene Signature Expression in Human Samples

Next, we tested if decreased HNF4α activity in human samples, as measured by signature gene expression, would correlate with advancement of HCC. We analyzed expression of signature genes in publicly available human liver cancer data sets (Yildiz et al., 2013). The first data set consisted of 37 samples consisting of cirrhotic liver or HCC (Figure 3.4.3A). Clustering analysis identified 2 clusters with opposite expression patterns. The first cluster, outlined in red, expressed high levels of signature genes (73% or 19/26), which were primarily cirrhotic samples. The second cluster, outlined in blue, expressed low levels of signature genes (91% or 10/11) and had primarily of HCC samples. The second data set consisted of patient-paired normal liver and tumor tissue from 10 human patients (Figure 3.4.3B). Clustering analysis identified 2 clusters with opposite expression patterns. The first cluster, outlined in red, expressed high levels of signature genes and contained primarily (90% or 9/10) the paired normal liver tissue. The second cluster, outlined in blue, expressed low levels of signature genes and contained primarily (90% or 9/10) tumor tissue.

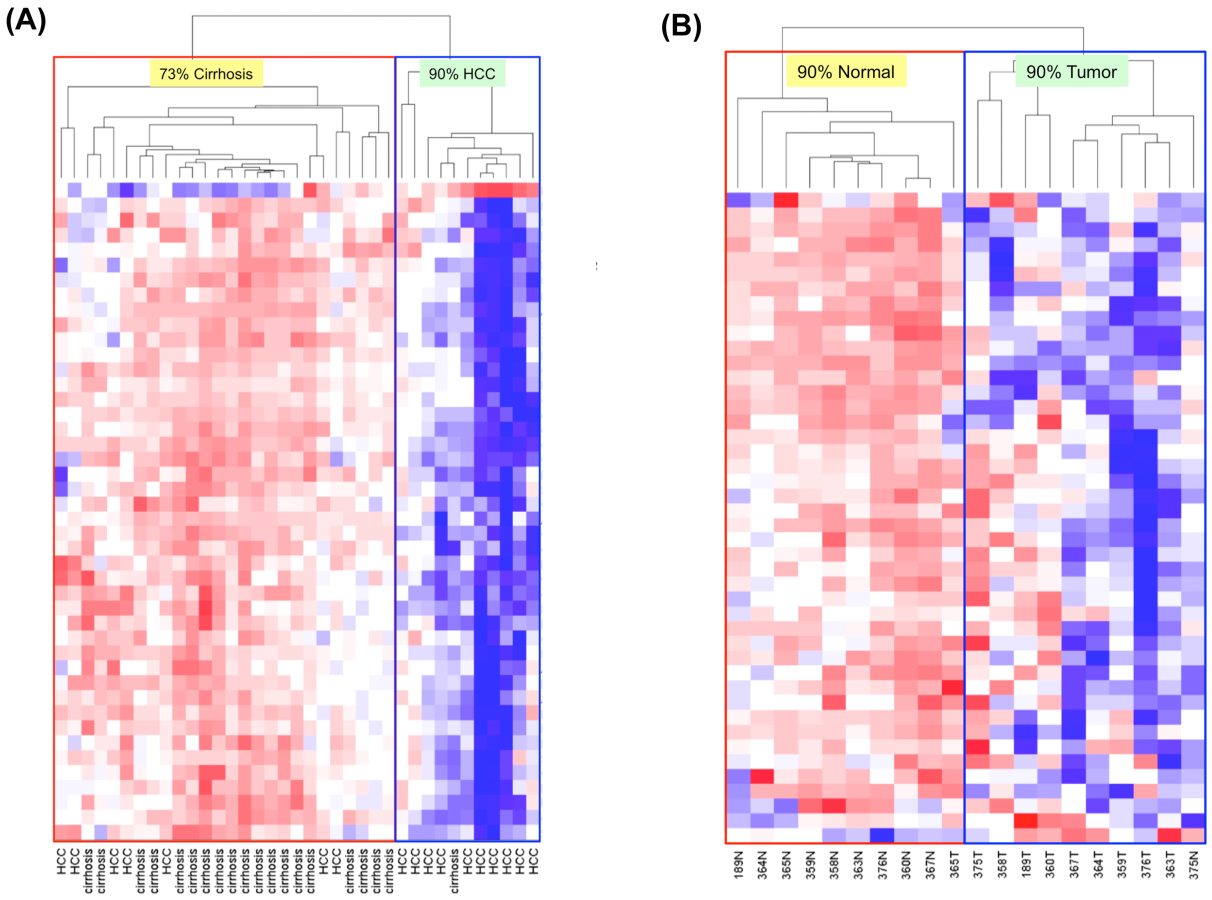

Figure 3.4.3. Expression of HNF4α Signature Genes Distinguishes HCC Samples from Cirrhotic or Normal Tissue Expression Patterns. (A) Comparison of signature gene expression in a dataset of 37 human cirrhosis and HCC samples revealed decreased HNF4α activity is observed in cluster consisting primarily HCC samples. (B) Hierarchical clustering of signature expression patterns in sample set of 10 patient-paired normal and liver tumor tissue distinguished between normal tissue (high expression) from liver tumor tissue (low expression).

The third data set consisted of 75 human samples of various histopathological findings including normal liver, cirrhotic liver tissue, low-grade dysplasia, high-grade dysplasia, very early HCC, early HCC, advanced HCC, and very advanced HCC (Figure 3.4.4) (Wurmbach et al., 2007). Clustering analysis identified 2 clusters with opposite expression patterns. The first cluster, outlined in red, expressed high levels of signature genes and only 2% (1/44) of the samples included in this cluster belonged to advanced HCC while the remainder belonged to normal liver, cirrhotic liver, low grade dysplasia, high grade dysplasia, or very early HCC. Within the first cluster was a subcluster with very high expression of signature genes (outlined with purple dotted line in the figure) that consisted exclusively of samples from normal liver tissue. The second cluster, outlined in blue, expressed low levels of signature genes and 52% (16/31) of the samples in this cluster belonged to advanced or very advanced HCC while the remainder belonged to early or very early HCC. Within the second cluster was a subcluster, outlined with green dotted line, with very low expression of signature genes. In this subcluster, 90% (9/10) of the samples belonged to advanced or very advanced HCC.

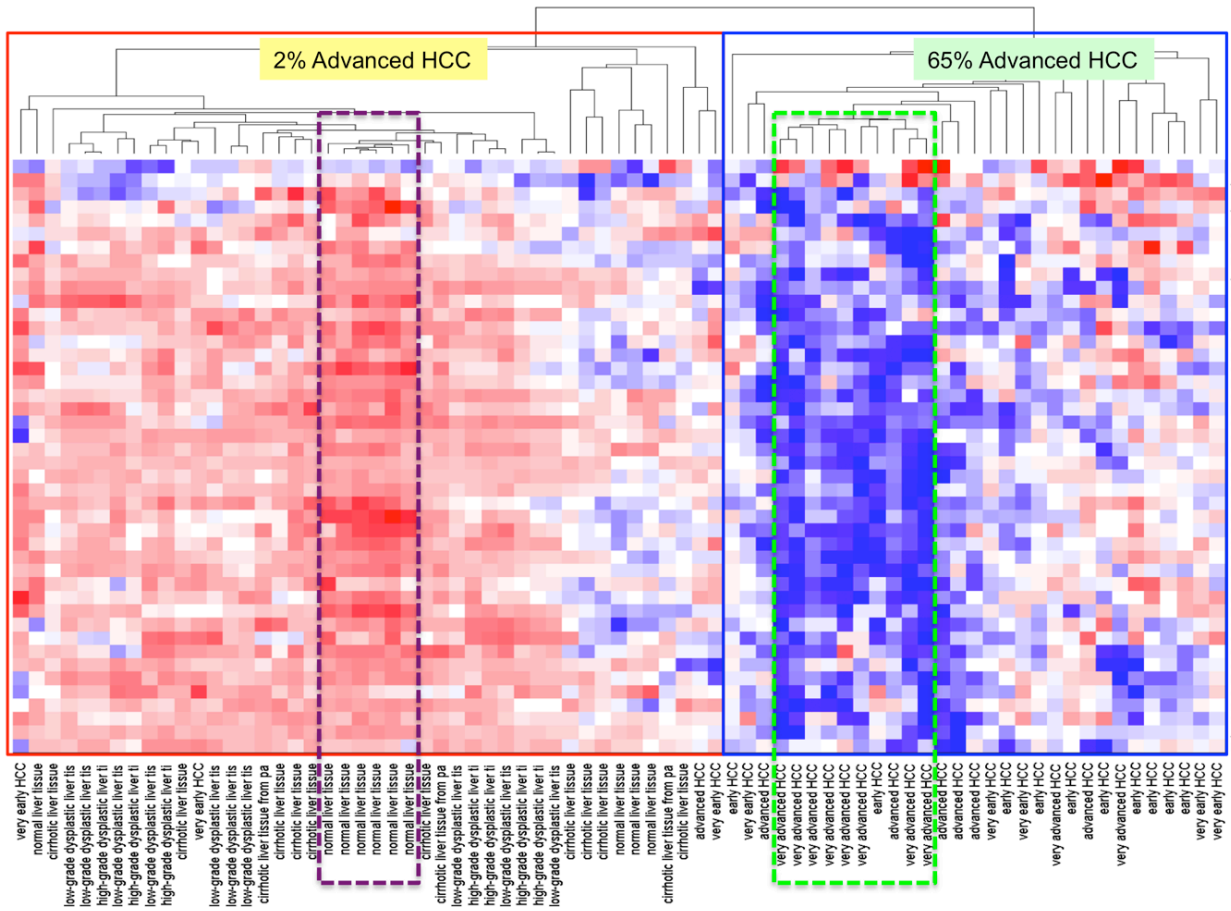

Figure 3.4.4. Decreased HNF4α Activity Correlates with Advancement of Human HCC. Hierarchical clustering of signature gene expression in 75 human samples revealed increased HNF4α activity in cluster of normal liver and pre-HCC samples (red outline) and decreased HNF4α activity in cluster consisting primarily of HCC (blue outline). A subcluster with very high HNF4α activity (dotted purple outline) included only normal liver samples and a subcluster with very low HNF4α activity (dotted green outline) included primarily very advanced HCC samples.

3.4.4. In Vivo Analysis of HNF4α Target Gene Signature Expression in Human Cirrhotic and HCC Samples

To further confirm the *in silico* data, we measured expression of HNF4α mRNA and HNF4α gene signature in a set of 5 cirrhotic liver and 5 HCC human patient samples. Expression of HNF4α mRNA was variable within each group (Figure 3.4.5A). Next, we performed TaqMan based qPCR analysis of the HNF4α gene signature followed by cluster analysis of the data. Clustering analysis of gene signatures identified 2 clusters with opposite expression patterns (Figure 3.4.5B). The first cluster, outlined in red, expressed high levels of signature genes. 3 of 4 samples in this cluster belonged to cirrhotic samples. The second cluster, outlined in blue, expressed low levels of signature genes. 4 of 6 samples in this cluster belonged to HCC samples. On average, expression of signature genes was lower in HCC samples than cirrhotic samples (Figure 3.4.5C).

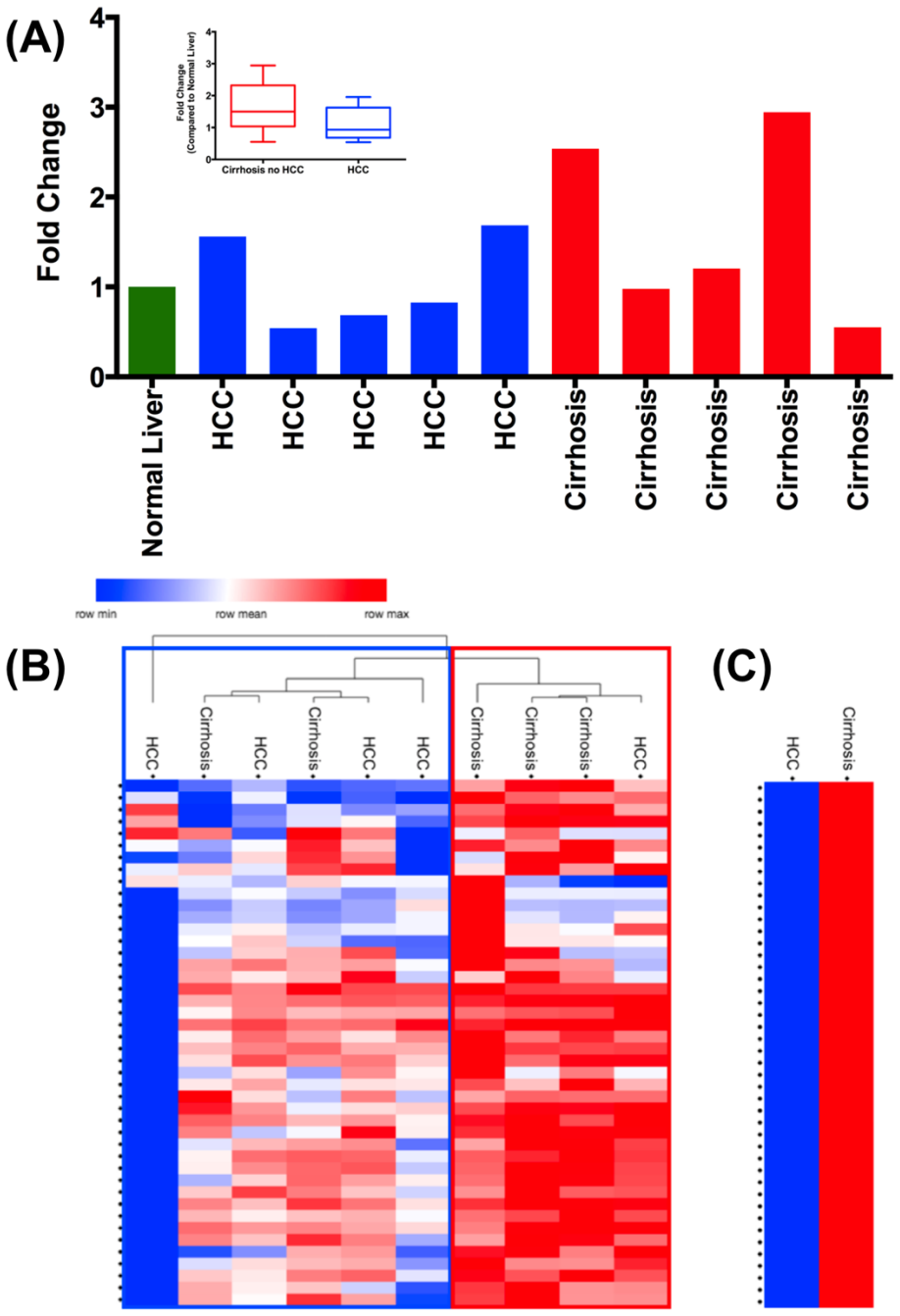

Figure 3.4.5. Decreased HNF4α Activity in HCC Compared to Cirrhotic Samples. In a sample set of 5 cirrhotic and 5 HCC human samples (A) various levels of HNF4α mRNA expression was detected but was lower on average in samples with HCC. (B) Increased HNF4α activity was observed in a cluster of 75% cirrhotic samples (red outline) and decreased HNF4α was observed in a cluster of 60% HCC samples (blue outline). (C) HNF4α activity was lower on average in HCC samples compared to cirrhotic samples.

3.4.5. Correlation of HNF4α Target Gene Signature Expression with Histological Progression of HCC in Human Samples

Next, we tested whether decreased HNF4α target gene signature expression would correlate with histological progression of HCC. Dr. Maura O'Neil, a board-certified pathologist used histological features from H&E stained sections to classify 16 human liver samples into discrete stages of HCC progression. From least advanced to most advanced disease, the stages were "Regenerative Nodule", "Dysplasia", "Well-Differentiated HCC", and "Moderately-Differentiated HCC". Duplicate sections from the same samples were stained for HNF4α immunohistochemistry, which revealed a variety of staining patterns (Figure 3.4.6A). The normal tissues showed strong nuclear staining only in hepatocytes. The patient samples showed various patterns including decreased nuclear staining, both nuclear and cytoplasmic staining, only strong cytoplasmic staining and almost complete loss of HNF4α staining. Although many of the staining patterns were abnormal when compared to normal liver, no correlation was found between HNF4α staining pattern and stage of HCC progression. We obtained total RNA from the same samples, which was used to measure expression of HNF4α signature genes using TaqMan arrays. The data showed that dysplastic nodules had most 'normal' gene expression pattern while the regenerative nodules has a significantly decreased HNF4α target gene expression. Further, downregulation of a majority of signature genes was observed in well-differentiated and moderately differentiated HCC. The moderately differentiated HCC samples exhibited the most significant decrease in HNF4α target gene expression. Finally, the HNF4α staining patterns did not correlate with signature outcomes.

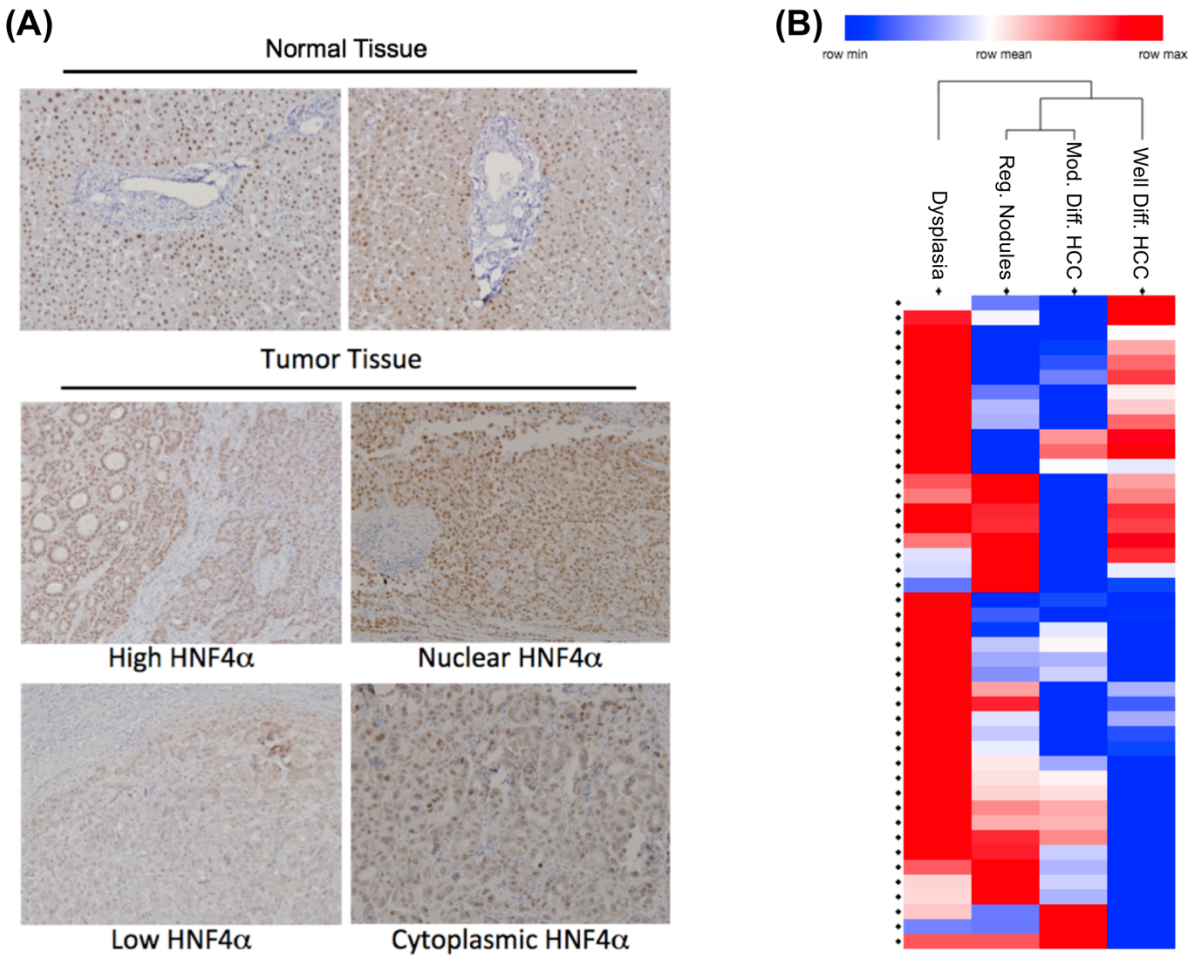

Figure 3.4.6. HNF4α Target Gene Signature Correlates with Histological Staging of HCC Better than HNF4α Staining. In a sample set of 16 human tumor samples of various stages in advancement (A) immunohistochemical staining for HNF4α revealed a variety of staining patterns among the samples which did not correlate with tumor staging. (B) HNF4α activity was decreased in well differentiated and moderately differentiated HCCs compared to samples with lesser advancement.

3.4.6. HNF4α Gene Signature is Correlated With Clinical Outcome.

To determine if final clinical outcome of HCC is correlated with HNF4α gene signature, we performed cluster analysis of expression data and survival data of 365 independent HCC cases obtained from the TCGA database. Cluster analysis (Figure 3.4.7A) distributed the samples in two main clusters, one with significantly higher HNF4α target gene expression (group 1, blue, 279 samples) and second with a significantly lower HNF4α gene expression pattern (group 2, yellow, 86 samples). A Kaplan-Meier plot of the groups showed that Group 1, which had significantly higher HNF4α target gene signature showed significantly better survival ($p=0.0001$) over 3500 days (9.5 years).

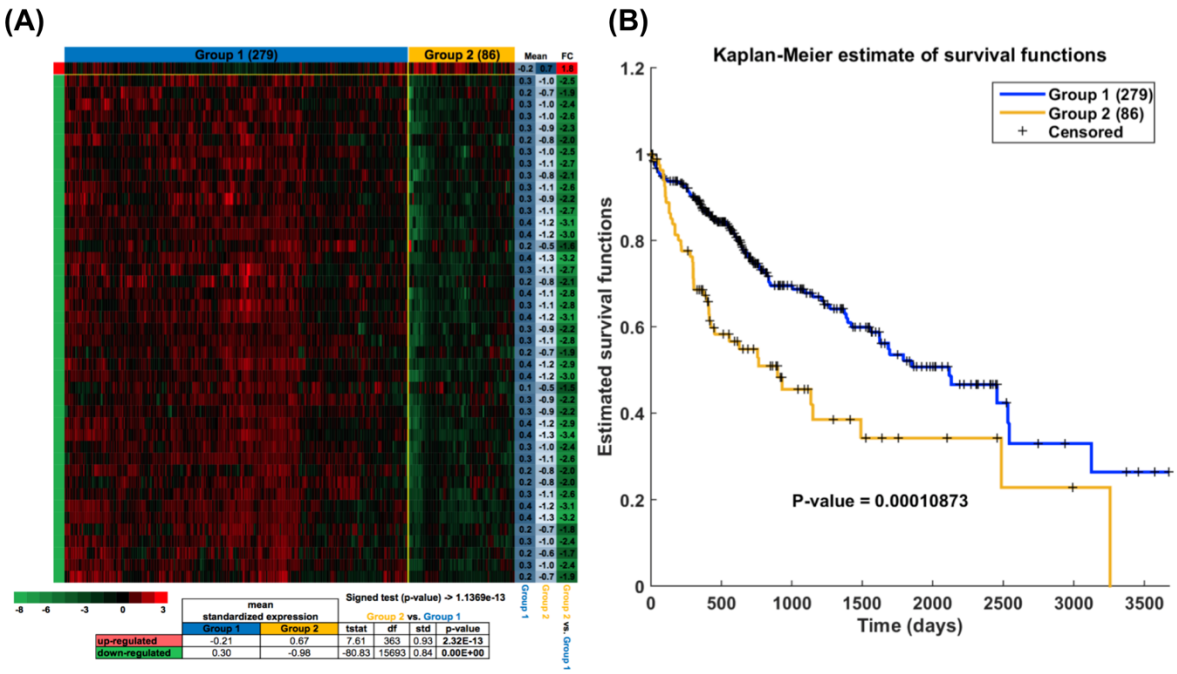

Figure 3.4.7. High Expression HNF4α Signature Genes is Predictive of Survival. (A) 365 human samples were divided into 2 groups using K-means clustering. Group 1 consisted of samples with high HNF4α activity and Group 2 consisted of samples with low HNF4α activity. (B) Kaplan-Meier plot of these groups indicated significantly decreased survival of Group 2 compared to Group 1 over the course of 9.5 years.

3.5. Discussion

There is substantial evidence that HNF4α expression is downregulated in cancers of the gut, kidney and liver (W. Y. Cai et al., 2017; Chellappa, Jankova, et al., 2012; Chellappa, Robertson, & Sladek, 2012; Hatziapostolou et al., 2011; Ning et al., 2010; Sel et al., 1996; Tanaka et al., 2006; Walesky, Edwards, et al., 2013; C. Yin et al., 2008). Further, studies in rodent models have shown that HNF4α reexpression may be used as 'differentiation therapy' in HCC. Whereas these studies indicate that HFN4α is an anti-tumor nuclear receptor, the exact mechanisms are not known. Furthermore, if HNF4α can be used as a prognostic tool in cancer pathogenesis has not been investigated. The hypothesis driving this study was that a decrease in HNF4α activity occurs during disease progression from normal liver to cirrhosis and further to HCC and also during further progression of HCC to more advanced stages. Evidence showing loss of HNF4α activity drives HCC pathogenesis comes from a variety of sources. Decrease in HNF4α expression results in decrease of hepatocyte differentiation, which could be further related to increased rates of proliferation and increased HCC aggressiveness (Lazarevich et al., 2004). By identifying the HNF4α target gene signature, our objective was to develop a tool that could measure HNF4a activity so that the loss of HNF4α activity that occurs during HCC progression could be observed.

We defined HNF4α activity as expression of HNF4α target genes. By defining HNF4α activity as expression of HNF4α target genes, we could measure activity independently of changes in mRNA transcript sequence or antigen availability, which can confound results obtained using qPCR or antibody detection of protein, such as IHC or western blotting. Our studies indicate that

measuring HNF4α protein or mRNA expression does not reflect HNF4α activity. We observed a variety of HNF4α staining patterns, none of which correlated with either HNF4α activity measured by target gene expression or the HCC pathogenesis. The varied staining pattern may be due to either posttranslational modification of HNF4α protein or due to presence of more than isoforms of HNF4α or the combination of both. Multiple post-translational modifications are known for HNF4α but it is not known how those might affect activity. Also, multiple mRNA transcripts code for different isoforms of HNF4α and differences in activity between these isoforms is not well understood in the liver.

We used an unbiased, global approach to identify the genes contained in the signature. Because HNF4α regulates 60% of all hepatocyte specific genes, the challenge with this approach was to select only for those genes that are direct targets with significant and reliable changes in expression based on HNF4α activity that are also relevant to the pathogenesis and advancement of HCC. Comparing gene expression changes between WT and HNF4α-KO normal livers, we identified novel positive and negative target genes of HNF4α. We were specifically interested in circumstances where decreased HNF4α activity led to HCC formation. Not all cancers will exhibit decreased expression of HNF4α, but we wanted to identify the patterns of gene expression characteristic of cancers with low HNF4α activity. Analysis of gene expression changes between WT and HNF4α-KO HCC tumors selected for direct and indirect targets whose expression is dependent on HNF4α in the cancer setting. Genes common between both of these analyses were robust direct and indirect HNF4α targets. These common genes were compared to HNF4α ChIP-Seq data to select for direct targets of HNF4α. HNF4α operates as part of a hepatic transcription factor network to maintain hepatocyte gene expression, which allows

HNF4α to indirectly control expression of many genes. These indirect targets are susceptible to expression changes caused by changes in activity from other transcription factors. By identifying direct HNF4α targets, the genes contained in the signature are not susceptible to this type of interference and can be considered a direct output of HNF4α function. In order for analysis of signature genes to take place using qPCR, the 323 gene signature was refined using IPA analysis to identify genes known to be involved in HCC. The signature was developed using mice, so only genes that were also found in humans were included in the final 44 gene signature. 42 of the 44 signature genes are activated by HNF4α. The 2 negative targets, ITGA2 and CYP39A1, were included as inverse verification of HNF4α activity.

Our analysis HCCs observed in the DEN-initiated cholic acid promoted HCC confirmed the ability of the signature to measure HNF4α activity and confirmed the hypothesis that decreased HNF4α activity occurs with advancement of HCC. We then tested this hypothesis using human gene expression data sets *in silico*. Clustering analysis of HNF4α gene signatures was capable of distinguishing cirrhotic samples from HCC samples based on the decreased HNF4α activity found in the latter (Figure 3.4.3A). The same was true when applied to patient-paired normal liver and tumor samples (Figure 3.4.3B). Finally, human HCCs of more advanced stage show the lowest HNF4α activity compared to normal or less advanced HCCs (Figure 3.4.4). From these analyses, we can conclude that HNF4α activity is lower in HCC than in normal liver, cirrhotic liver, and less advanced HCC.

Our data indicate that HNF4α activity is lower in HCC samples than cirrhotics on average. Whereas variation in signature expression patterns is expected, our data shows that the loss of HNF4α activity will lead to loss of hepatocyte function resulting in liver decompensation. This is consistent with previous findings that overexpression of HNF4α can improve survival in rodent studies (T. Nishikawa et al., 2015).

Our analysis also examined how expression of signature genes correlated with HNF4α protein staining and disease progression as determined by histology. Previous studies have reported dysregulated HNF4α staining patterns in HCC. Accurate staging of HCC currently relies on histological analysis of biopsy material. We observed decreased HNF4α activity in sample groups with HCC. Previous studies have reported dysregulated HNF4α staining patterns in HCC. We observed similar variations in HNF4α staining in our samples, but these staining patterns did not correlate with disease stage or HNF4α activity.

Finally, the most important finding of our study was that HNF4α gene signature analysis was clearly able to predict patient outcome. Our data shows that patients with higher target gene expression indicating significantly higher HNF4α activity have a substantially longer survival over a 9.5 year period. These data indicate that these patients are better able to maintain liver function and may be able to cope better with treatments. Use of the HNF4α target gene signature could be used to address some of the weaknesses present in current HCC treatment strategies. The BCLC therapeutic strategy and staging system is a widely accepted, evidence-based

algorithm used to determine treatment for HCC patients based on tumor stage (Bruix et al., 2015; J. M. Llovet, Bru, & Bruix, 1999; J. M. Llovet et al., 2016). This staging system uses Child-Pugh and ECOG scores as well as size and number of tumor nodules to determine HCC stage. These scoring systems rely on outputs of liver function and patient well-being and do not take into consideration the molecular drivers of the disease. Classification of HCCs based on HNF4α activity might result in more accurate staging methods or therapies targeting restoration of HNF4α transcriptional activity. Our results show more advanced HCCs have less HNF4α activity than less advanced HCCs. In patients diagnosed with HCC, those with low HNF4α activity could be given higher priority for curative therapies such as liver transplantation. HCCs must be diagnosed during the asymptomatic "Very Early" or "Early" stages if curative therapy is to be an option. Thus, screening of patients most at risk of developing HCC could improve chances of early diagnosis when the HCC is in a curable stage.

Due to study design, we cannot claim that decreased HNF4a activity is predictive of which cirrhotic patients will progress to HCC. However, we did observe lower levels of HNF4α activity in HCCs compared to cirrhotic patients in Figure 3.4.3 to Figure 3.4.5, indicating that loss of HNF4a activity does occur in some cirrhotic patients that develop HCC. Cirrhotic patients face risk of developing HCC as well as decompensating. Loss of HNF4α activity can promote progression to either of these disease states. Use of the signature in cirrhotic patients could be a screening method to identify patients at higher risk of developing HCC and decompensating. Our data suggest follow up studies could be done to determine if low HNF4α signature gene expression is predictive of HCC development or decompensation in cirrhotic patients.

Here we present a novel target gene signature capable of measuring HNF4α activity in humans and mice. The method used to develop this signature could be used to develop target gene signatures for other transcription factors. Measurement of HNF4α signature genes in a variety of scenarios revealed decreased HNF4α activity occurring in HCC compared to normal tissue. We also observed decreased HNF4α activity in HCCs of increasing advancement. This study offers evidence that classification of HCCs based on HNF4α activity may refine current HCC staging systems and provide additional tools for screening and diagnosis. Decreased HNF4α activity occurs in a majority of HCCs and restoration of HNF4α activity may be a new therapeutic strategy.

Chapter 4. Role of HNF4α in Systemic Energetics During Feeding Challenges

Portions of this chapter have been previously published as a preprint and have not been peer-reviewed. Huck, I., Morris, E. M., Thyfault, J. P., & Apte, U. (2018). Hepatocyte-Specific Hepatocyte Nuclear Factor 4 alpha (HNF4α) Deletion Decreases Resting Energy Expenditure By Disrupting Lipid and Carbohydrate Homeostasis. *bioRxiv*, 401802. doi:10.1101/401802

4.1. Abstract

Hepatocyte Nuclear Factor 4 alpha (HNF4α) is required for hepatocyte differentiation and regulates expression of genes involved in lipid and carbohydrate metabolism including those that control VLDL secretion and gluconeogenesis. Whereas previous studies have focused on specific genes regulated by HNF4α in metabolism, its overall role in whole body energy utilization has not been studied. In this study, we used indirect calorimetry to determine the effect of hepatocyte-specific HNF4α deletion (HNF4α-KO) in mice on whole body energy expenditure (EE) and substrate utilization in fed, fasted, and high fat diet (HFD) conditions. HNF4α-KO had reduced resting EE during fed conditions and higher rates of carbohydrate oxidation with fasting. HNF4α-KO mice exhibited decreased body mass caused by fat mass depletion despite no change in energy intake and evidence of positive energy balance. HNF4α-KO mice were able to upregulate lipid oxidation during HFD suggesting that their metabolic flexibility was intact. However, only hepatocyte specific HNF4α-KO mice exhibited significant reduction in basal metabolic rate and spontaneous activity during HFD. Consistent with previous studies, hepatic gene expression in HNF4α-KO supports decreased gluconeogenesis and decreased VLDL export and hepatic β-oxidation in HNF4α-KO livers across all feeding conditions. Together, our data suggest deletion of hepatic HNF4α increases dependence on dietary carbohydrates and endogenous lipids for energy during fed and fasted conditions by inhibiting hepatic gluconeogenesis, hepatic lipid export, and intestinal lipid absorption resulting in decreased whole body energy expenditure. These data clarify the role of hepatic HNF4α on systemic metabolism and energy homeostasis.

4.2. Introduction

The role of HNF4α in hepatic lipid and carbohydrate metabolism has been well recognized and was described in Chapter 1. Alterations in these pathways following HNF4α knockout would likely alter systemic metabolism but this has not been examined. The previous investigations have focused on the role of HNF4α in metabolism by examining hepatic gene expression, histology and serum metabolites. Despite its powerful effect on hepatic glucose and lipid metabolism, the exact role of hepatic HNF4α on systemic energy metabolism and substrate utilization patterns has not been examined. Here we used metabolic stressors of fasting and high fat diet (HFD) feeding combined with indirect calorimetry to examine how targeted hepatic deletion of HNF4α in adult mice effects systemic energy metabolism.

4.3. Materials and Methods

4.3.1. Animal Care and Tissue Preparation

All animal studies were approved by and performed in accordance with the Institutional Animal Care and Use Committee (IACUC) at the University of Kansas Medical Center. All mice were housed in temperature-controlled conditions (23°C) with a 07:00-21:00 h light phase and 21:00 to 07:00 h dark phase. Two to three-month-old male homozygous HNF4α-floxed mice on C57BL/6J background were injected intraperitoneally with AAV8-TBG-eGFP or AAV8-TBG-CRE resulting in wild-type (WT) and hepatocyte-specific deletion of HNF4α (HNF4α-KO). These vectors were purchased from Penn Vector Core (Philadelphia, PA) and injected as previously described (Yanger et al., 2013). Liver was harvested, weighed and flash frozen in liquid nitrogen at time of euthanasia.

To study the effects of HNF4α deletion in fed and fasted conditions (Figure 4.4.1, Figure 4.4.3, Table 4.4.1), HNF4α-floxed littermates were injected with AAV8 to generate WT (n=4) and KO (n=4) groups and were housed individually for one week before entering metabolic cages. While in the cages mice were given *ad libitum* access to normal chow (PicoLab Rodent Diet 20 #5053, LabDiet, St. Louis, MO) for 6.5 days. Chow was removed, and mice were subjected to a 12-hour fasting challenge beginning at the start of the dark cycle. Chow was returned to the cages and mice were given 48 hours of *ad libitum* access to chow before euthanasia and tissue collection.

To study the change in energy metabolism and body composition during the process of HNF4α deletion (Figure 4.4.2, Table 4.4.2), HNF4α-floxed littermates were housed individually for 5 days before entering metabolic cages. Mice were then acclimatized for 2 days to the indirect calorimetry cage conditions before being injected with AAV8 to generate WT (n=3) and HNF4α-KO (n=4) groups. Mice remained in the cages for 7 days post injection before euthanasia and tissue collection.

To study the effects of HNF4α deletion in high fat diet (HFD) conditions, HNF4α-floxed littermates were individually housed, injected with AAV8 to generate WT (n=4) and HNF4α-KO (n=4) groups and fed a control diet containing normal fat content (10% kcal from fat, Cat.# D12110704, Research Diets, Inc., New Brunswick, NJ) for 1 week before entering indirect calorimetry cages. Mice were fed control diet for an additional 3 days in the indirect calorimetry cages before switching to a HFD (60% kcal from fat, catalog# D12492, Research Diets, Inc., New Brunswick, NJ) for 4 days before euthanasia and tissue collection. HFD was replaced every 2 days to prevent spoilage.

To study the role of HNF4α on energy metabolism during liver regeneration after partial hepatectomy (PH), HNF4α-floxed littermates were injected with AAV8 and individually housed for 4 days before entering metabolic cages. Mice were acclimatized for 2 days to the indirect calorimetry cage conditions before data collection started. Data were collected for 1 day prior to PH and 7 days after PH before euthanasia and tissue collection.

4.3.2. Indirect Calorimetry

Indirect Calorimetry analysis was performed at the University of Kansas Medical Center Metabolic Obesity Phenotyping Facility using a Promethion continuous indirect calorimetry system (Sable Systems International, Las Vegas, NV) as previously described (Fletcher et al., 2018). Macros available from the manufacturer were used to calculate total energy expenditure (TEE) based on the Weir equations (Weir, 1949) and respiratory quotient (RQ) by VCO_2/VO_2. To calculate resting energy expenditure (REE), the Promethion designed macro pulled out the lowest 30 min period of EE (light cycle) which was then extrapolated to a 24 hour period. The difference between TEE and REE was used to determine non-resting energy expenditure (NREE). Food was weighed before and after each experiment to determine food consumption. The mass of food consumed was used to determine energy intake (EI) based on the manufacturer provided values for metabolizable energy from each diet type and comparisons were made using body mass as a covariate for EI. Energy Balance (EB) was calculated by subtracting daily total energy expenditure from EI. These calculations were performed as previously described (Morris et al., 2014). Food hoppers were equipped with a sensor to determine food hopper interaction and manufacturer designed macros used this data to determine hourly feeding bouts. Activity was determined using the XYZ Beambreak Activity Monitor (Sable Systems, Las Vegas, NV) and is expressed as the sum of X and Y beam breaks per time period. Mice were given 2 days to acclimatize to new cages before data was recorded.

4.3.3. Serum Analysis

Blood glucose was measured with a glucometer using blood collected via retroorbital sinus at time of euthanasia. Serum was isolated and commercially available kits were used to measure β-Hydroxybutyrate (#2440-058, Stanbio), serum triglycerides (#T7532-500, Pointe Scientific) and serum free fatty acids (#MAK044, Sigma-Aldrich).

4.3.4. Body Composition Analysis

Body composition was performed prior to placement in indirect calorimetry cages and again before euthanasia using the EchoMRI-900 instrument (EchoMRI, Houston, TX). Mice were weighed by hand before entering indirect calorimetry cages, at injection times, before diet changes and before euthanasia. Fat-free mass was calculated by subtracting fat mass from body mass. Percent fat and percent fat free mass was calculated by dividing fat or fat free mass by body mass. Change in fat and fat-free mass was calculated by subtracting the value obtained at the start of the experiment from the value obtained before euthanasia.

4.3.5. RT-PCR Analysis

RNA from frozen liver was isolated using Trizol method and reverse transcribed to cDNA as previously described (Apte et al., 2009). Fold change values were calculated in comparison to WT-fed mice using the ddCt method as previously described (Livak & Schmittgen, 2001). Table 4.3.1 contains primer sequences used in this study.

Table 4.3.1: Primer Sequences Used in This Study

	Forward Primer (5' - 3')	**Reverse Primer (5' - 3')**
g6pase	CCGGTGTTTGAACGTCATCT	CAATGCCTGACAAGACTCCA
pepck	TGCGGATCATGACTCGGATG	AGGCCCAGTTGTTGACCAAA
pdk4	AGATTGACATCCTGCCTGACC	TCTGGTCTTCTGGGCTCTTCT
cpt1	GGACTCCGCTCGCTCATTC	GAGATCGATGCCATCAGGGG
cd36	ATGGGCTGTGATCGGAACTG	GTCTTCCCAATAAGCATGTCTCC
mttp	CAAGCTCACGTACTCCACTGAAG	TCATCATCACCATCAGGATTCCT

4.3.6. Statistical Analysis

Statistical analysis was performed using IBM SPSS Statistics Version 25. One Way ANOVA or Student's t test was applied where indicated with $p < 0.05$ being considered significant. Analysis of energy expenditure and energy intake with body mass as a covariate was performed as previously described (Morris et al., 2014) and in accordance with published protocols (Speakman, Fletcher, & Vaanholt, 2013).

4.4. Results

4.4.1. Hepatocyte-Specific HNF4α-KO Mice Exhibit Decreased Resting Energy Expenditure During Fed Conditions.

HNF4α-KO mice on a chow diet exhibited decreased total energy expenditure (TEE) at multiple time points throughout the dark and light cycle (Figure 4.4.1A). TEE and resting energy expenditure (REE) were also significantly lower in HNF4α-KO mice when data was summarized throughout the 24-hour cycle (data not shown). However, energy expenditure is influenced to a significant degree by body mass and multiple methods have been proposed for eliminating the contributing of body mass when comparing energy expenditure in organisms of different size (Tschop et al., 2011). To account for the impact of body mass on energy expenditure, TEE, REE, and non-resting energy expenditure (NREE) were calculated and analyzed with body mass used as a covariate (Figure 4.4.1B). In this experiment, random distribution of littermates into treatment groups resulted in individual differences in body mass, with some HNF4α-KO mice weighing more than their WT littermates. Since these mice also exhibited decreased unadjusted TEE, adjusting means with body mass as a covariate actually underestimated the decrease in EE in HNF4α-KO mice. The correction of EE with body mass as a covariate resulted in the adjusted TEE between WT and HNF4α-KO mice to be similar (Figure 4.4.1B). However, REE values, which were adjusted for body mass, were significantly reduced in HNF4α-KO mice (Figure 4.4.1B). There were no differences in adjusted NREE between genotypes (Figure 4.4.1B). Respiratory quotient (RQ) in HNF4α-KO and WT mice was similar throughout the 24-hour cycle (Figure 4.4.1C). RQ remained similar between WT and HNF4α-KO mice when the data was quantified for the entire light or dark cycle (Figure 4.4.1D, Left Panel). However, delta RQ, representing the difference in RQ between light and dark cycles, was

greater in HNF4α-KO mice and was nearly statistically significant with $p = 0.06$ (Figure 4.4.1D, Right Panel). Activity was measured by total X and Y beam breaks. No significant differences in activity were observed between WT and HNF4α-KO mice at any time point during the 24-hour cycle (Figure 4.4.1E) or when mean hourly beam breaks were summarized per light/dark cycle (Figure 4.4.1F). Daily energy intake (EI) was similar between groups (Figure 4.4.1G). Daily energy balance was similar between groups (Figure 4.4.1H). In summary, on a chow diet the hepatocyte-specific HNF4α-KO mice exhibited decreased resting energy expenditure. This occurred with only minor differences in substrate utilization and no differences in spontaneous activity or energy intake between WT and HNF4α-KO mice.

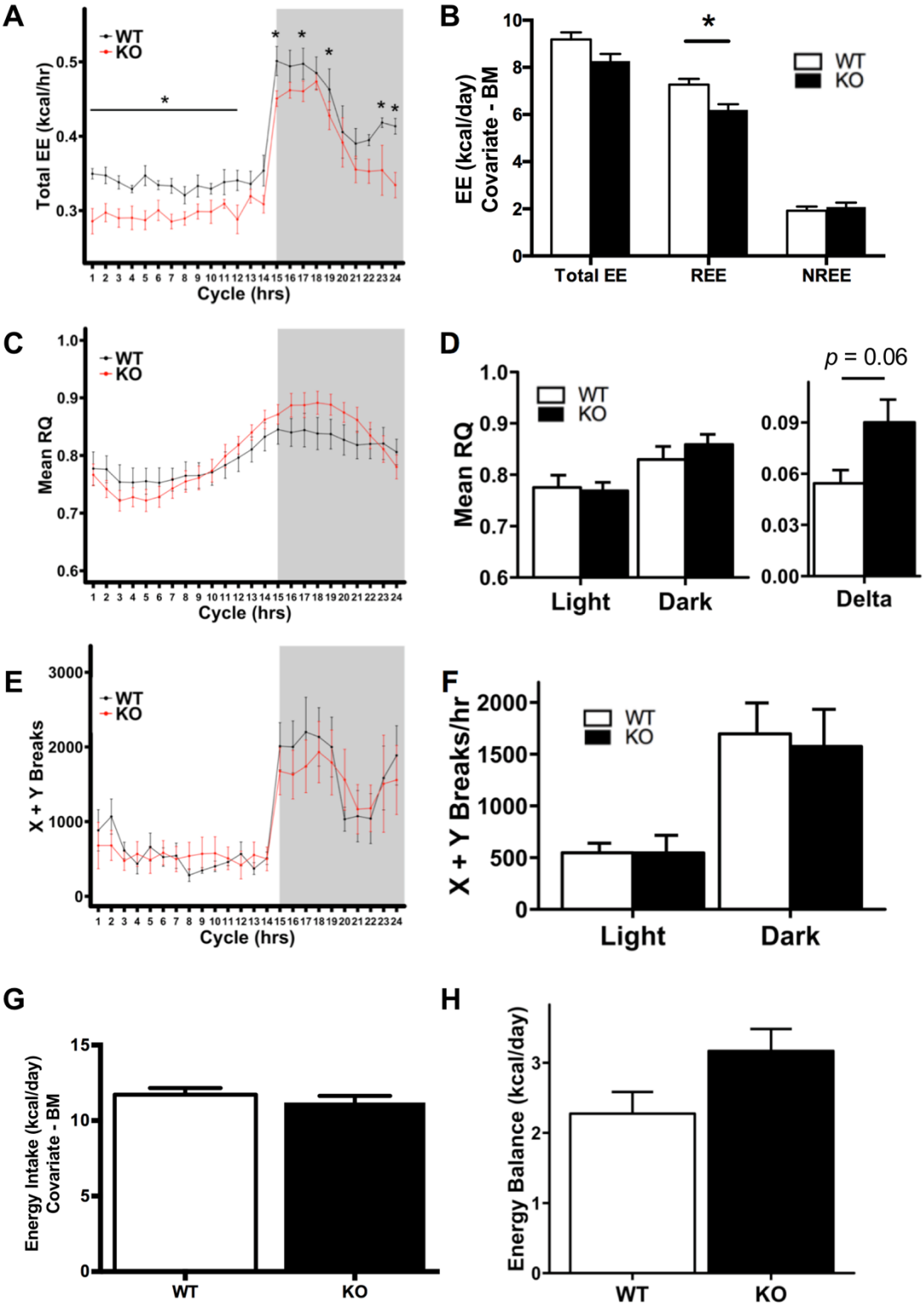
A
WT
KO
Total EE (kcal/hr)
Cycle (hrs)
B
EE (kcal/day)
Covariate - BM
Total EE
REE
NREE
C
Mean RQ
Cycle (hrs)
D
p = 0.06
Mean RQ
Light
Dark
Delta
E
X + Y Breaks
Cycle (hrs)
F
X + Y Breaks/hr
Light
Dark
G
Energy Intake (kcal/day)
Covariate - BM
H
Energy Balance (kcal/day)

Figure 4.4.1: Hepatocyte-specific HNF4α-KO mice exhibit decreased resting energy expenditure during fed conditions. Indirect calorimetry performed on WT and hepatocyte-specific HNF4α-KO mice during 4.5 days of *ad libitum* normal chow feeding. (A) Mean hourly total energy expenditure in WT and HNF4α-KO mice over a 24-hour cycle. Raw values have not been adjusted for body mass differences. (B) Daily total energy expenditure, resting (REE) and non-resting (NREE) energy expenditure in WT and HNF4α-KO mice. Means adjusted with body mass (BM) used as a covariate for energy expenditure. (C) Mean RQ over a 24-hour cycle. (D, Left Panel) Mean RQ summarized by light and dark cycles. (D, Right Panel) Delta depicts the difference in RQ between light and dark cycles. (E) Activity of WT and HNF4α-KO mice expressed as the total X and Y beam breaks for each hour over a 24-hour cycle. (F) Activity of WT and HNF4α-KO mice expressed as the total X and Y beam breaks per hour and summarized per light and dark cycle. (G) Daily energy intake in WT and KO mice with BM used as a covariate. (H) Daily energy balance in WT and KO mice. Gray background indicates dark cycle time point. Values are means ± SEM. Statistical significance determined by one-way ANOVA between WT and KO with * indicating significance with $p < 0.05$ between WT and HNF4α-KO.

As mentioned previously, individual differences in body mass existed between mice, but there were no significant differences in mean body mass between WT and HNF4α-KO groups (Table 4.4.1). There were no significant differences in food consumption (Table 4.4.1). HNF4α-KO mice had significantly less fat mass at the end of the experiment and lost a significant amount of fat mass over the 9 days of analysis compared to WT mice (Table 4.4.1). Fat-free mass was significantly greater in HNF4α-KO mice (Table 4.4.1). HNF4α-KO mice had significantly lower blood glucose compared to WT mice (Table 4.4.1).

Table 4.4.1: Body composition, food consumption and blood glucose data for WT and HNF4α-KO mice fed normal chow. Body mass, fat mass, and blood glucose were measured immediately before euthanasia. Food consumption values depict the mass of normal chow consumed during the entire feeding period and are presented as absolute values. Change in fat mass was calculated for each mouse by subtracting the total fat mass at the start of indirect calorimetry analysis from the fat mass measured immediately before euthanasia. Fat free mass was calculated by subtracting fat mass from body mass using values obtained immediately before euthanasia. Values are means ± SEM. Statistical significance determined by Student's t-test with * indicating significance with $p < 0.05$ between WT and HNF4α-KO.

	WT	**KO**
Body Mass (g)	22.35 ± 0.52	23.45 ± 0.21
Food Consumption (g)	24.38 ± 0.36	24.13 ± 1.08
Fat Mass (g)	1.83 ± 0.13	1.16 ± 0.22*
Change in Fat Mass (g)	0.25 ± 0.05	-0.17 ± 0.16*
Fat Free Mass (g)	20.53 ± 0.61	22.29 ± 0.15*
Blood Glucose (mg/dL)	195.00 ± 12.54	102.25 ± 7.82*

4.4.2. Changes in Energy Expenditure Observed During Hepatocyte-Specific HNF4α Deletion Time Course.

In the experiments from Figure 4.4.1, mice were injected with AAV8 vector and 1 week was allowed for cre recombinase to induce HNF4α deletion before the mice were placed in the indirect system for a 2 day acclimation period. This 9-day time span between viral treatment and data collection produced uncertainty as to whether the reduced REE observed in HNF4α-KO mice was ultimately caused by deletion of HNF4α from hepatocytes, or was a compensatory response to long-term HNF4α deletion. To address this issue, we adjusted the timing of our study so HNF4α-floxed mice were placed into the indirect calorimetry cages for 2 days before being injected with AAV8. EE, RQ and activity was measured for a 7-day time course following injection of AAV8 into mice. If the decreased REE phenotype observed in HNF4α-KO mice was a direct result of HNF4α deletion, we expected REE to be the same between groups prior to AAV8 injection and REE to steadily decrease in mice injected with AAV8-TBG-CRE. As expected, TEE was similar between groups before AAV8 injection. However, TEE began to decrease in HNF4α-floxed mice after AAV8-TBG-CRE injection (Figure 4.4.2A), most notably during the light cycle. REE was calculated for WT and HNF4α-KO mice for the initial two days at the start of deletion and the final two days before euthanasia with body mass used as a covariate. REE in WT mice did not change over the experiment time course, but there was a significant decrease in HNF4α-KO over the deletion time course. (Figure 4.4.2B). Although statistically significant differences in REE between WT and HNF4α-KO at both time points were not observed, the trend of decreased REE during HNF4α deletion suggests that the decline in REE would continue in HNF4α-KO mice and become statistically significant over a longer time course, like what was observed in Figure 4.4.1.

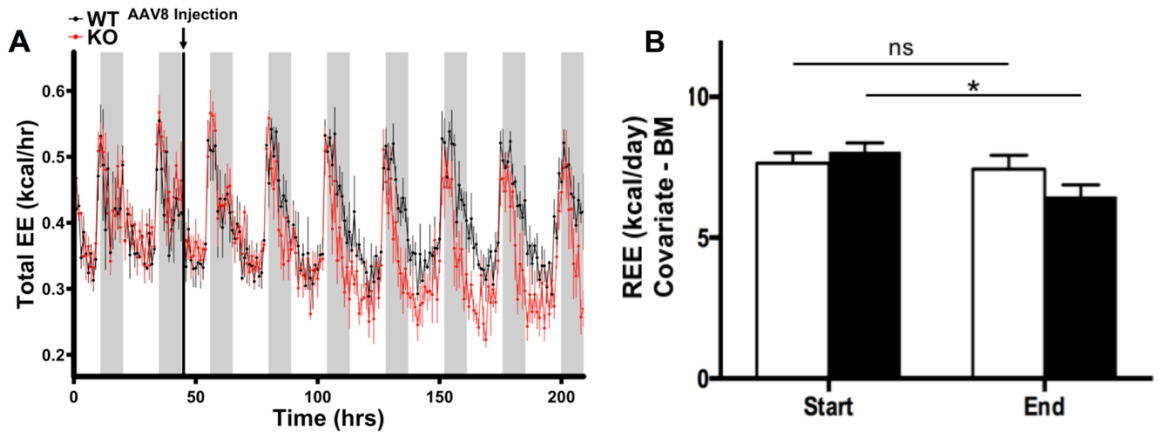

Figure 4.4.2. Changes in energy expenditure observed during hepatocyte-specific HNF4α deletion time course. Indirect calorimetry performed on HNF4α-floxed mice before and 7 days after injection with AAV8-TBG-eGFP(WT) or AAV8-TBG-CRE (HNF4α-KO). (A) Mean hourly total energy expenditure (EE) for WT and HNF4α-KO mice before and after AAV8 injection. Raw values have not been adjusted for body mass differences. (B) Resting EE (REE) in WT and HNF4α-KO mice at the start (first 2 days) and end (final 2 days) of the deletion time course. Means adjusted with body mass (BM) used as a covariate for energy expenditure. Gray background indicates dark cycle time point. Values are means ± SEM. Statistical significance determined by one-way ANOVA between WT and KO or between time points with * indicating $p < 0.05$ between WT and HNF4α-KO.

Food consumption was similar between treatments (Table 4.4.2). Body mass at time of euthanasia was similar between treatments, but HNF4α-KO mice lost significantly more body mass compared to WT mice from the time of AAV8 injection to euthanasia (Table 4.4.2). The decrease in body mass primarily occurred through a decrease in fat mass. Total fat mass was significantly lower in HNF4α-KO mice compared to WT at euthanasia and HNF4α-KO mice lost more total fat mass over the deletion time course compared to WT mice (Table 4.4.2). Fat-free mass was similar between treatments (Table 4.4.2).

Table 4.4.2: Body composition data for WT and HNF4α-KO mice in acute deletion study. Body mass and fat mass were measured at the end of the deletion time course immediately before euthanasia. Food consumption values depict the mass of normal chow consumed throughout the entire deletion time course and are presented as absolute values. Change in fat mass was calculated for each mouse by subtracting the total fat mass measured before AAV8 injection from the fat mass measured immediately before euthanasia. Fat free mass was calculated by subtracting fat mass from body mass using the values obtained immediately before euthanasia. Values are means ± SEM. Statistical significance determined by Student's t-test with * indicating significance with $p < 0.05$ between WT and HNF4α-KO.

	WT	**KO**
Body Mass (g)	26.10 ± 0.83	24.78 ± 0.49
Change in Body Mass (g)	-0.17 ± 0.38	-1.40 ± 0.24*
Food Consumption (g)	32.37 ± 0.92	33.35 ± 3.24
Fat Mass (g)	1.70 ± 0.24	1.00 ± 0.13*
Change in Fat Mass (g)	-0.04 ± 0.03	-0.59 ± 0.08*
Fat Free Mass (g)	24.40 ± 0.69	23.77 ± 0.40

4.4.3. HNF4α-KO Exhibit Elevated RQ During Fasting

WT and HNF4α-KO mice were subjected to a 12-hour fasting challenge to determine how this would differently impact EE and substrate utilization. We found no significant differences in TEE between WT and HNF4α-KO mice at any time points throughout the fasting challenge (Figure 4.4.3A). The TEE, REE and NREE summarized throughout the 12 hour fast and adjusted using body mass as a co-variate also did not reveal differences (Figure 4.4.3B). However, we did find pronounced differences in substrate utilization in the HNF4α-KO mice compared to WT. HNF4α-KO mice had a much slower shift in lowering RQ during the fast compared to WT, suggesting a defect in the ability to upregulate the utilization of lipids for energy (Figure 4.4.3C). This metabolic inflexibility phenotype was likely due to a decreased availability of fatty acids from lipolysis as we observed depletion of adipose tissue after HNF4α deletion (Table 4.4.1, Table 4.4.2) and found reduced circulating FFA after fasting (Figure 4.4.5A). In addition, reduced fatty acid utilization could also occur because of reduced fat oxidation in the liver due to reduced CPT-1 expression, which is known to be reduced with HNF4α deletion (Figure 4.4.5B). Activity was not different between groups (Figure 4.4.3D).

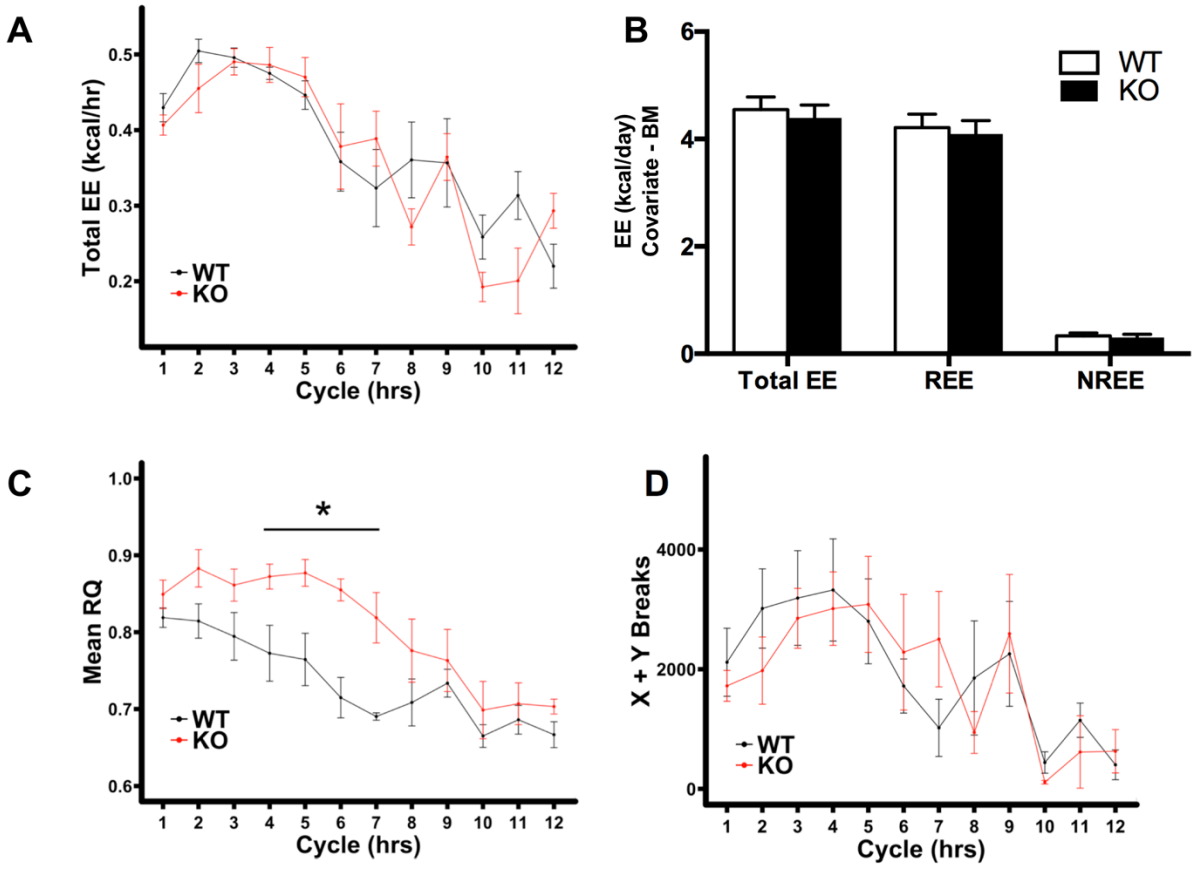

Figure 4.4.3. HNF4α-KO mice exhibit elevated RQ during fasting. (A) Mean hourly total energy expenditure (EE) during 12-hour fast. Raw values have not been adjusted for body mass differences. (B) Total EE, resting EE (REE) and non-resting EE (NREE) during 12-hour fast. Means adjusted with body mass (BM) used as a covariate for energy expenditure. (C) Mean hourly RQ during 12-hour fast. (D) Activity during 12-hour fast expressed as total X and Y beam breaks per hour. Values are means ± SEM. Statistical significance determined by one-way ANOVA with * indicating $p < 0.05$ between WT and HNF4α-KO.

4.4.4. HNF4α-KO Mice Exhibit Decreased Energy Expenditure, Decreased RQ, Decreased Activity and Loss of Body Mass During Acute High Fat Diet (HFD) Challenge.

The metabolic inflexibility displayed by the HNF4α-KO mice to a fasting challenge suggested hepatic HNF4α deletion reduces whole body capacity for lipid utilization. To test the ability of HNF4α to obtain energy from lipids, we monitored energy expenditure, substrate utilization, activity and body composition in WT and HNF4α-KO mice before and after the initiation of a diet containing 60% kcal from fat (HFD). HNF4α-KO mice tended to have lower total EE before HFD feeding. However, total EE was reduced further in HNF4α-KO mice upon HFD feeding (Figure 4.4.4A). Significant reductions in total EE, REE and NREE were observed in HNF4α-KO mice when body mass was used as a covariate (Figure 4.4.4B). Contrary to the metabolic inflexibility observed in HNF4α-KO mice during the fasting challenge, RQ of both groups decreased at the same rate upon initiation of HFD feeding. Further, RQ of HNF4α-KO mice was lower than WT mice at several time points throughout HFD feeding suggesting HNF4α-KO mice had greater capacity for or increased reliance on dietary lipid utilization when consuming a HFD (Figure 4.4.4C-D). Dark cycle activity was significantly reduced in HNF4α-KO mice compared to WT when measured by total X and Y beam breaks (Figure 4.4.4E) as well as feeding bouts (Figure 4.4.4F). Feeding bouts were determined by a manufacturer provided macro, and say more about activity than food consumption, since food intake rate and total food consumption as determined by macros was similar between groups (data not shown). Furthermore, food was weighed by hand at the start and end of the experiment and while HNF4α-KO mice consumed significantly less HFD (Table 4.4.3), energy intake was similar between groups when body mass was used as a covariate for food consumption (Figure 4.4.4G). Energy balance was similar between groups and positive in both groups (Figure 4.4.4H). Body

mass of WT and HNF4α-KO mice was similar at start of HFD feeding and at euthanasia (Table 4.4.3). However, HFD feeding led to significantly different changes in body mass with a 7.7% increase in WT body mass and a 6.2% decrease in HNF4α-KO body mass (Table 4.4.3). While comparison of body mass between groups revealed no significant differences, the changes in body mass occurring during HFD feeding were significant for both genotypes and were confirmed using the in-cage body mass sensors (Figure 4.4.4I).

HNF4α-KO mice contained significantly less fat mass than WT mice after HFD feeding (Table 4.4.3). Comparison of the change in fat mass before and after HFD was similar between groups (Table 4.4.3). Fat free mass was similar between WT and HNF4α-KO mice (Table 4.4.3). Blood glucose was significantly lower in HNF4α-KO mice compared to WT mice, reflective of impaired gluconeogenesis (Table 4.4.3).

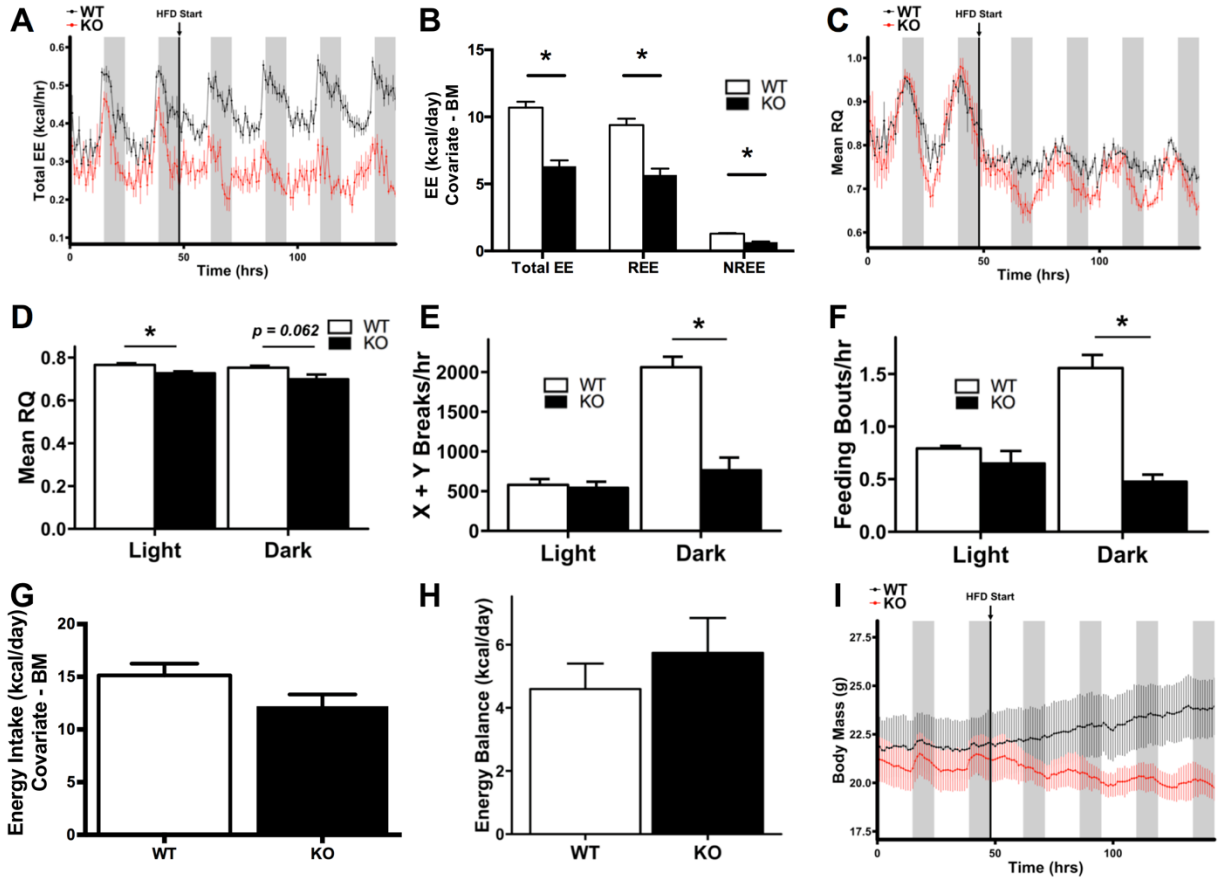

Figure 4.4.4. HNF4α-KO mice exhibit decreased energy expenditure, decreased RQ, decreased activity and loss of body mass during acute high fat diet (HFD) challenge. (A) Mean hourly total energy expenditure (EE) during the transition from normal chow to HFD. Raw values have not been adjusted for body mass differences. (B) Total EE, resting EE (REE) and non-resting EE (NREE) in WT and HNF4α-KO mice fed HFD. Means adjusted with body mass (BM) used as a covariate for energy expenditure. (C) Mean hourly RQ during transition from normal chow to HFD. (D) Mean RQ during HFD summarized by light and dark cycles. (E) Activity in HFD fed WT and HNF4α-KO mice during light and dark cycles expressed as the total X and Y beam breaks per hour. (F) Hourly feeding bouts during light and dark cycle in WT and HNF4α-KO fed HFD. (G) Daily energy intake in HFD fed WT and HNF4α-KO mice. Means adjusted with body mass used as a covariate for energy intake. (H) Daily energy balance in HFD fed WT and HNF4α-KO mice. (I) Average body mass in WT and HNF4α-KO mice during transition from normal chow to HFD. Gray background indicates dark cycle time points. Values are means ± SEM. Statistical significance determined by one-way ANOVA with * indicating significance with $p < 0.05$ between WT and HNF4α-KO.

Table 4.4.3: Body composition, food consumption, and blood glucose data for WT and HNF4α-KO mice subjected to acute HFD challenge. HFD body mass was measured when the mice started to feed on HFD. End body mass was measured after 4 days of HFD feeding and immediately before euthanasia. Consumption of HFD represents the total amount consumed throughout the HFD feeding period and are presented as absolute values. Fat mass was measured before euthanasia. Change in fat mass was calculated for each mouse by subtracting the fat mass measured before indirect calorimetry analysis from the fat mass measured before euthanasia. Fat free mass was calculated by subtracting fat mass from body mass using the values obtained immediately before euthanasia. Blood glucose was measured immediately before euthanasia. Values are means ± SEM. Statistical significance determined by Student's t-test with * indicating significance with $p < 0.05$ between WT and HNF4α-KO.

	WT	KO
HFD Body Mass (g)	21.83 ± 1.74	20.90 ± 1.14
End Body Mass (g)	23.50 ± 1.62	19.60 ± 0.77
Difference between HFD Body Mass and End Body Mass (g)	1.68 (7.7%) ± 0.33	-1.30 (-6.2%) ± 0.45*
HFD Consumed (g)	11.70 ± 0.51	9.30 ± 0.78*
Fat Mass (g)	2.84 ± 0.44	1.40 ± 0.11*
Change in Fat Mass (g)	1.03 ± 0.51	0.17 ± 0.18
Fat Free Mass (g)	20.66 ± 1.19	18.20 ± 0.72
Blood Glucose (mg/dL)	200.00 ± 32.97	112.00 ± 6.36*

4.4.5. Changes in Serum Lipids and Hepatic Gene Expression in WT and HNF4α-KO Mice Across Feeding Conditions.

To understand the metabolic phenotype characterized using indirect calorimetry, we measured serum lipids, ketones and hepatic expression of lipid and carbohydrate metabolism genes in WT and HNF4α-KO mice during fed, fasted and HFD conditions. Serum triglycerides and serum free fatty acids were significantly lower in HNF4α-KO animals in all conditions (Table 4.4.3A). No significant differences in serum ketones were observed between WT and HNF4α-KO mice (Table 4.4.3A). Gene expression for the rate limiting enzymes in gluconeogenesis (G6Pase, PEPCK) were decreased in HNF4α-KO mice in all conditions as expected given their lower glucose levels (Table 4.4.3B). PDK4, an enzyme involved in conservation of glucose and upregulation of lipid utilization, was elevated in HNF4α-KO mice in all conditions (Table 4.4.3B). CPT1, the rate limiting enzyme for fatty acid entry into the mitochondria and subsequent β-oxidation, was suppressed in HNF4α-KO mice in all conditions (Table 4.4.3C). Expression of the hepatic lipid importer CD36 was elevated in HNF4α-KO mice in all conditions (Table 4.4.3C). Expression of the apolipoprotein packaging enzyme MTTP was suppressed in HNF4α-KO mice in all conditions (Table 4.4.3C). Thus, gene expression profiles of the livers from the HNF4α-KO are suggestive of impaired gluconeogenesis and enhanced lipid uptake paired with reduced capacity to oxidize and export lipids.

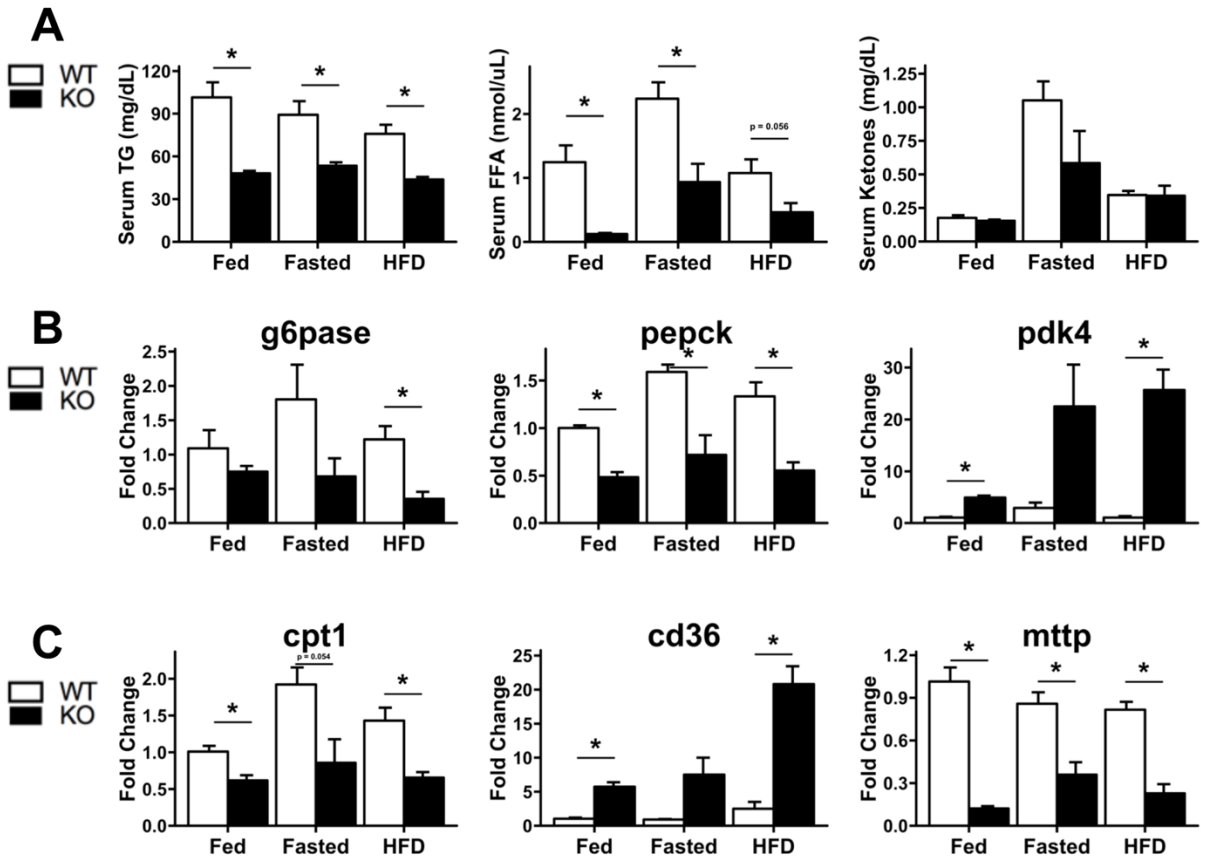

Figure 4.4.5. Changes in serum lipids and hepatic gene expression in WT and HNF4α-KO mice across feeding conditions. (A) Serum quantification of (left to right) triglycerides (TG), free fatty acids (FFA) and β-hydroxybutyrate (Ketones). Hepatic expression of genes involved in (B) glucose metabolism and (C) lipid metabolism and trafficking. Gene expression expressed as fold change compared to WT mice fed normal chow. Values are means ± SEM. Statistical significance determined by one-way ANOVA with * indicating significance with $p < 0.05$ between WT and HNF4α-KO.

4.5. Discussion

The role of HNF4α in hepatocyte differentiation and quiescence is well recognized (Duncan et al., 1994; Kyrmizi et al., 2006; J. Li et al., 2000; Morimoto et al., 2017; Parviz et al., 2003). HNF4α regulates several liver specific functions including lipid and carbohydrate metabolism, but our understanding of the role of HNF4α in metabolism is limited to its role in regulating hepatic gene expression and hepatic nutrient storage. Whether HNF4α mediated regulation of hepatic metabolism results in changes to systemic energetics has not been studied, which was the focus of these studies.

The major finding of this study was that deletion of HNF4α from hepatocytes results in decreased resting energy expenditure during fed conditions. Additionally, hypoglycemia, body mass decrease, and decreased adiposity were observed in HNF4α-KO mice in all feeding conditions. The origin of these phenotypes was directly linked to decreased hepatic HNF4α levels by examining mice during a 7-day time course of hepatic HNF4α deletion. The differences in energy expenditure between WT and HNF4α-KO mice were exaggerated during HFD feeding, with HNF4α-KO mice exhibiting significant decreases in total, resting, and non-resting energy expenditure as well as decreased spontaneous activity.

Reductions in energy expenditure caused by hepatic HNF4α deletion cannot be attributed to decreased energy intake. HNF4α-KO mice exhibited positive energy balance that was similar to WT energy balance during all feeding conditions. Despite exhibiting positive energy balance,

HNF4α-KO mice consistently exhibited decreases in body mass which were caused by depletion of fat mass. While it is not clear how HNF4α-KO mice lose body mass while maintaining positive energy balance, it could be explained by poor intestinal lipid absorption due to decreased bile acid production. It is well known that HNF4α regulates genes involved in bile acid synthesis, conjugation and transport (Hayhurst et al., 2001; Y. Inoue et al., 2004; Y. Inoue, Yu, et al., 2006). Cyp7a1, Cyp27a1 and Cyp8b1 are all positively regulated by HNF4α and exhibit decreased expression in HNF4α-KO mice (Y. Inoue, Yu, et al., 2006). As a result, HNF4α-KO mice synthesize fewer bile acids and excrete fewer bile acids in feces (Y. Inoue, Yu, et al., 2006). Basal expression of Cyp7a1 requires HNF4α and LRH-1 (Kir et al., 2012). Like HNF4α, LRH-1 also regulates Cyp8b1 and liver specific deletion of LRH-1 decreases Cyp8b1 expression resulting in decreased bile acid production and poor intestinal lipid absorption (Mataki et al., 2007). It is highly probable that decreased bile acid synthesis in HNF4α-KO mice produces a similar phenotype of reduced intestinal lipid absorption. This would cause HNF4α-KO mice to have increased dependence on endogenous adipose stores for lipid fuel molecules. This is supported by the increased lipolysis observed in HNF4α-KO mice throughout all experiments, including HFD challenge, which was so severe that adipose tissue from epididymal fat pads could not be collected from HNF4α-KO mice. Impaired availability of dietary lipids and dependence on endogenous lipids would also explain the dramatic reductions in HNF4α-KO energy expenditure and activity observed when the majority of dietary caloric intake was available as lipids during the HFD challenge, as well as their resistance to HFD-induced increases in adiposity. Decreased lipid absorption would result in an overestimation of energy intake in HNF4α-KO mice since energy intake was calculated using the mass of food consumed.

If the energy actually absorbed by the intestines could be calculated, HNF4α-KO energy balance would likely be negative and reflect the observed loss in body mass.

Decreased availability of dietary lipids for energy production could affect metabolic activity in peripheral lean tissue. Serum triglycerides and free fatty acids were decreased in HNF4α-KO mice in all feeding conditions consistent with previous publications (Hayhurst et al., 2001; Martinez-Jimenez et al., 2010; L. Yin et al., 2011). These studies attribute decreased VLDL secretion in HNF4α-KO mice to decreased expression of MTTP and ApoB, which we also observed in all feeding conditions. Decreased hepatic VLDL secretion, combined with depletion of adipose tissue after long term HNF4α deletion, would effectively starve peripheral lean tissue of lipid energy molecules, resulting in decreased energy expenditure.

Additional explanations exist for why we observed decreased energy expenditure after hepatic HNF4α deletion. HNF4α regulates hepatic CPT1a, the enzyme involved in the rate limiting step of fatty acid oxidation, during fed and fasted conditions (Martinez-Jimenez et al., 2010). CPT1a was downregulated in HNF4α-KO mice across all feeding challenges in the current study. It has been estimated that liver accounts for 20% of total EE (Ramsey, Harper, & Weindruch, 2000), so decreased capacity for hepatic β-oxidation could result in a detectable reduction in whole body energy expenditure. Decreased hepatic β-oxidation would increase RQ, opposite of what was observed in HNF4α-KO mice. However, this increase in RQ is likely masked the decreased RQ of peripheral tissues which would be forced to metabolize lipids in a hypoglycemic environment.

It has been shown that during cold exposure, activation of HNF4α is required for hepatic synthesis of acyl-carnitines which are used as fuel in brown fat thermogenesis (Simcox et al., 2017). The mice in our study were housed at 24°C. While this is not cold exposure, it could be considered a source of minor thermoregulatory stress (Tschop et al., 2011). If hepatic HNF4α deletion results in reduced acyl-carnitine synthesis, brown adipose tissue in HNF4α-KO mice would be starved of energy molecules required for thermogenesis and therefore be less metabolically active, resulting in decreased energy expenditure.

A previously unknown phenotype of hepatocyte-specific HNF4α deletion was reduction in fat mass. In all experiments with normal chow fed mice, depletion of adipose in HNF4α-KO mice drove a decrease in body mass. Additionally, HNF4α-KO mice were resistant to HFD-induced increases in body mass and adiposity. Increased lipolysis was likely caused by decreased availability of dietary lipids, but could also be caused by increased glucagon signaling in the hypoglycemic HNF4α-KO mice. Long term, this could result in near total lipolysis of adipose therefore preventing a fasting induced increase in serum FFA, such as what was observed in fasted HNF4α-KO mice. White adipose tissue is metabolically active itself and it has been shown to increase energy expenditure in lean tissue via leptin signaling (Kaiyala et al., 2010). Because HNF4α-KO mice are leaner, leptin signaling is likely lower, which would decrease energy expenditure in lean tissue.

Peripheral tissues of HNF4α-KO mice had decreased access to lipid energy molecules, but were also starved of glucose which could contribute to decreased energy expenditure. In all conditions, HNF4α-KO mice were significantly hypoglycemic. HNF4α is required for PGC1α mediated gluconeogenesis by co-activating PEPCK and G6Pase (Rhee et al., 2003; Yoon et al., 2001). Moreover, hepatic fat oxidation, which is impaired in HNF4α-KO mice due to decreased CPT1a expression, is necessary for fueling gluconeogenesis. Indeed, PEPCK and G6Pase expression decreased in all feeding conditions following HNF4α deletion. Hepatocyte-specific HNF4α-KO mice exhibit depletion of hepatic glycogen (Walesky, Edwards, et al., 2013) which is likely caused by failed gluconeogenesis. Since liver is the primary gluconeogenic organ and HNF4α is required for hepatic gluconeogenesis, diet must be the exclusive source of carbohydrate for HNF4α-KO mice. Furthermore, if intestinal lipid absorption is impaired in HNF4α-KO mice, dietary carbohydrates would be especially important for energy production. This is supported by the decreases in total energy expenditure in HNF4α-KO mice during the deletion time course which occurred almost exclusively during the light cycle when mice reduce food consumption. Further, when availability of dietary carbohydrates was reduced, such as during HFD challenge, energy expenditure and activity are significantly reduced as HNF4α-KO mice must produce energy from a dwindling supply of endogenous lipid depots along with a liver exhibiting impaired gluconeogenesis.

Substrate utilization data supports the hypothesis that HNF4α-KO mice depend exclusively on diet as a source glucose. During fed conditions, HNF4α-KO mice exhibited nearly significant increased oscillation between light and dark cycle RQ. Close inspection of RQ in Figure 4.4.1A

suggests a trend of increased dark cycle RQ and decreased light cycle RQ. Decreased light cycle RQ was also observed in HNF4α-KO mice before initiation of HFD feeding (Figure 4.4.4C). Elevated dark cycle RQ in HNF4α-KO mice can be explained by metabolism of dietary glucose consumed during the dark cycle feeding period in an organism with impaired VLDL secretion and exhausted adipose stores. During the light cycle, HNF4α-KO mice stopped feeding and quickly exhausted stored glucose, forcing them to use stored adipose resulting in reduced light cycle RQ.

The most notable difference in substrate utilization between WT and HNF4α-KO mice was observed during the fasting challenge, where HNF4α-KO mice were slow to decrease RQ, suggesting a reluctance for HNF4α-KO mice to use lipids during caloric restriction. However, this was not supported by the HFD challenge, where HNF4α-KO did not have problems using lipids as a fuel source during HFD feeding and actually displayed lower RQ than WT mice during HFD feeding. The dependence on carbohydrates for fuel exhibited by fasted HNF4α-KO mice may not be caused by defective lipolysis or fatty acid oxidation, but rather be a product of deficient hepatic VLDL secretion and exhausted adipose stores following prolonged HNF4α deletion. This would force peripheral tissues to use any remaining carbohydrate for fuel during caloric restriction. As for substrate utilization during the HFD challenge, it is surprising that RQ was lower in HNF4α-KO mice considering dietary lipid absorption was likely reduced. HFD contained very low quantities of carbohydrates and gluconeogenesis was significantly inhibited in HNF4α-KO mice. Thus, options for energy sources in this scenario would be limited to endogenous lipids or residual intestinal lipid absorption. Also, increased ketogenesis could

explain the low RQ exhibited by HNF4α-KO mice during HFD feeding (Schutz & Ravussin, 1980). Previous studies have shown increased ketosis in HNF4α-KO mice (Martinez-Jimenez et al., 2010), but we observed no differences between WT and HNF4α-KO serum β-hydroxybutyrate. It is possible that ketone production was higher in HNF4α-KO mice during some phases of the dark cycle when RQ was below 0.7 but was not detectable in our samples which were collected during the light cycle. Another explanation could be the decrease in activity of HNF4α-KO mice fed HFD. While HNF4α-KO mice did not consume less energy than WT mice, reduced ambulatory activity during the feeding period translated into fewer dark cycle feeding bouts, which could result in lower RQ.

Hypoglycemia and transient hepatic steatosis are well-known metabolic changes which occur after PH (J. Huang & Rudnick, 2014), but countering either can lead to inhibited liver regeneration. Several studies have shown that inhibiting hepatic steatosis after PH reduces hepatocyte proliferation (Fernandez et al., 2006; Kohjima et al., 2013; Shteyer et al., 2004) because accumulation of hepatic triglycerides is required to fuel β-oxidation in the regenerating liver (Bellet et al., 2016; Kachaylo et al., 2017; Kohjima et al., 2013; Mukherjee et al., 2017). Studies have also shown that inhibition of transient steatosis impairs liver regeneration by increasing expression of the HNF4α target gene p21 (Gazit et al., 2010; Weymann et al., 2009). These lipids come from lipolysis of adipose depots, and regeneration in lipid dystrophic mice which have decreased adipose stores, exhibit decreased hepatic steatosis and impaired liver regeneration (Gazit et al., 2010). This lipolysis is triggered by hypoglycemia, and supplementation with dextrose or glucose inhibits liver regeneration (Caruana, Whalen,

Anthony, Sunby, & Ciechoski, 1986; Weymann et al., 2009). However, besides one study which has shown an increase in lipid utilization during liver regeneration with indirect calorimetry in mice (Kachaylo et al., 2017), little is known about how these metabolic conditions can affect total energy expenditure or respiratory quotient. The preliminary results presented here have reproduced these findings, as we found WT mice to exhibit low RQ following PH. While none of the HNF4α-KO died in the 7 day regeneration time course of this study, noticeably lower energy expenditure throughout regeneration followed by a significant decline at the end of the time course provides further evidence that the mortality observed in these mice after PH is caused by failure of nutrient homeostasis due to decompensating liver. Further studies are needed to confirm these results.

In conclusion, this study uses indirect calorimetry and targeted hepatic HNF4α deletion in adult mice to address unanswered questions regarding the role of hepatic HNF4α on systemic metabolic homeostasis and energy flux. Hepatocyte-specific HNF4α deletion reduces peripheral availability of energy molecules likely by reducing lipid absorption, hepatic VLDL secretion, and gluconeogenesis resulting in decreased resting energy expenditure. This study demonstrates how changes in hepatic HNF4α, a condition common in disease human liver (Baciu et al., 2017; Xu et al., 2015), can significantly impact whole body energy expenditure and availability of energy stores. This data will inform future attempts to target or modulate hepatic HNF4α by demonstrating its role in metabolism outside of the liver. Our findings reveal for the first time the impact of hepatic HNF4α on systemic energy flux and highlight the importance of liver as a central metabolic organ.

Chapter 5. Summary and Future Directions

Previous studies have shown HNF4α plays a central role in maintenance of hepatocyte function and suppression of hepatocyte proliferation. Decreased HNF4α expression and activity in the progression of liver disease makes it a promising target for therapeutic intervention. However, several questions about HNF4α biology had remained unanswered, which could be summarized as follows: Does HNF4α contribute to regulation of hepatocyte proliferation during liver regeneration? Does perturbed HNF4α activity during this process contribute to the initiation and advancement of liver disease? Is there a way to accurately measure the components of HNF4α activity which are relevant to the progression of liver disease? Can understanding HNF4α activity be used to accurately stage and prognosticate various forms of liver disease? If therapeutic targeting of hepatic HNF4α is performed, what are there consequences beyond the liver? Do changes to hepatic HNF4α during hepatocyte proliferation or during liver disease progression contribute to metabolic disturbances observed in these conditions? The studies presented in this dissertation were designed to answer these questions. While diverse methods and models were used, together our results provide new understanding of the role of HNF4α in liver biology and disease.

5.1. HNF4α Required For Liver Regeneration

Despite the well-recognized role of HNF4α in hepatocyte differentiation and quiescence, detailed studies on the role of HNF4α during liver regeneration were not performed. Using partial hepatectomy as a model of liver regeneration, we identified changes in nuclear HNF4α expression and activity during the initiation of liver regeneration. These changes occurred without changes to HNF4α transcription, repeating the findings of a previous study (Flodby et

al., 1993). This suggested regulation of HNF4α during liver regeneration was occurring at the post-translational level. Src kinase is known to phosphorylate HNF4α on Tyrosine-277 and 279 and induce cytoplasmic translocation and proteasomal degradation in enterocytes (Chellappa, Jankova, et al., 2012). Indeed, inhibition of SRC increased nuclear levels of HNF4α after PH, suggesting that this is the mechanism by which HNF4α is regulated during liver regeneration. However, it is not clear what the impact of Src inhibition would be on proliferation over the regenerative time course or if other kinases could compensate for Src inhibition. Numerous examples of HNF4α regulation by PTMs exist outside of liver regeneration. HNF4α phosphorylation, ubiquitination and acetylation has been identified, and phosphorylation and acetylation has been shown to inhibit HNF4a transcriptional activity (Z. Wang et al., 2011; Yokoyama et al., 2011). Src is not the only kinase capable of phosphorylating HNF4α. Phosphorylation of HNF4α by Protein kinase C (PKC) on serine-78 in HepG2 cells decreases HNF4α nuclear localization, transcriptional activity and protein stability (K. Sun et al., 2007). Phosphorylation of HNF4a at serine 78 by PKC also occurs during the development of hepatic steatosis in HFD fed mice (Yu et al., 2018). Protein kinase A (PKA) can phosphorylate HNF4α at serine-142 and decreased DNA binding (Viollet, Kahn, & Raymondjean, 1997; Z. Wang et al., 2011). Treatment of HepG2 cells with thyroid stimulating hormone activates PKA leading to phosphorylation of HNF4α and decreased nuclear localization and transcriptional activity (Y. Song et al., 2015). In mice, loss of prostaglandin E_2 (PGE_2) signaling in the liver leads to overactivation of PKA, phosphorylation of HNF4α at serine-143, leading to decreased CYP7A1 expression and decreased bile acid synthesis (Yan et al., 2017). Future studies are needed to examine the expression and activity of these kinases during liver regeneration. Experiments using transgenic mice will determine the role of these kinases in liver regeneration. Transgenic

mice expressing phospho-null or phosphomimetic mutated HNF4α will be used to see if this changes HNF4α activity after partial hepatectomy or the regenerative process.

Deletion of HNF4α prevented hepatocytes from redifferentiating after PH providing evidence that death in these mice was due to hepatic failure. PH is used to study signals and mechanisms behind the innate ability of hepatocytes to proliferate. An advantage of this model is these signals can be studied without needing to consider toxicant-specific effects present in models of liver regeneration after acute chemical injury. This means the model may have more relevance to the abnormal hepatocyte proliferation, wound healing responses and changes in differentiation present during the progression of liver disease. Failure of hepatocytes to compensate for HNF4α deletion during regeneration is another demonstration of HNF4α as the central regulator in hepatocyte differentiation. Previous work has demonstrated cirrhotic decompensation is associated with decreased expression of several hepatic transcription factors (FoxA2, HNF1α, Cebpα, HNF4α). Reexpression of HNF4α alone is enough to restore expression of these transcription factors and restore hepatic function and reversing hepatic failure. Interestingly, expression of HNF4α from the reexpression vector was only temporary, but this was enough to reactivate the endogenous HNF4α gene permanently (T. Nishikawa et al., 2015). Our results suggest that decreased hepatic function is a normal part of the regenerative process, but it occurs only for a short time. If the liver is injured in pathologic conditions, the regenerative process may never fully terminate, resulting in permanently compromised hepatic function. Reexpression of HNF4α may be a good strategy to restore expression of not just HNF4α targets, but all genes targeted by hepatic transcription factors.

5.2. HNF4α Gene Signature and Disease Progression

Numerous studies have reported decreased expression of HNF4α being associated with the progression of liver disease, specifically the development and advancement of HCC. While the quest for drugs or other methods to restore HNF4α expression in diseased livers is ongoing, we hypothesized that a tool which could measure HNF4α activity would have significant use in the diagnosis and prognosis of liver disease. Other gene signatures have been developed for similar uses which use a specific pathological feature or changes in expression of known oncogene targets to identify the genes to be included in the signature. We took a more hypothesis driven approach. Our method was blinded to these outcomes and instead was based on the hypothesis that HNF4α activity could be measured based on expression of its direct target genes, and that a subset of these genes would be specifically downregulated in carcinogenesis. Instead of relying on detection of specific staining patterns or expression of canonical carcinogenic genes, this signature provided a more robust, global approach towards detecting HNF4α activity. Also, by centering our gene signature around a specific transcription factor, any sample the signature determines exhibits low HNF4α activity could conceivably be treated with a therapy restoring HNF4α. In this way the signature could be used to prescribe therapy to targeting the molecular drivers specific to a patient's disease.

The workflow we used to identify genes in the HNF4α signature could also be used to identify signatures for other transcription factors in other diseases. Generation of other signatures depicting the activity of a targetable transcription factor could be used in conjunction with the

HNF4α signature and lead to more accurate prognosis, staging and treatment of multiple disease states. The role of HNF4α in hepatic metabolism and its role in regulating gene expression of secreted proteins allows for potential for generation of a signature to measure HNF4α activity based on metabolites and biological material found in serum. This would allow for less invasive ways to measure HNF4α activity and could be used as an easily obtained biomarker of HCC or other liver conditions from a simple blood draw.

Our study tested the signature in cirrhotic and HCC samples, but more studies are needed to determine if the signature could also be used to predict which cases of less advanced liver disorders (NAFLD, NASH, mild fibrosis) will progress into more severe forms. As detailed in the introduction, decreased expression of HNF4α occurs early on in these liver diseases. While mechanisms by which decreased HNF4α contributes to the pathogenesis of these diseases are known, it is not known if further downregulation of HNF4α is a mechanism pushing these conditions to a more advance stage of disease.

Finally, the methods used to measure HNF4α activity in human and mouse tissues rely on a comparison between diseased samples and normal or less advanced tissues. While this is required for establishing our initial understanding of how the signature works, clinical use of the signature would ideally be able to determine HNF4α activity based on the information contained in a single sample. Preliminary work done by the bioinformatics core has identified multiple internal reference genes for each of the 44 signature genes, and machine learning techniques

have been used to quantify HNF4α activity based on the relationships between each signature gene and its reference genes. This is a promising approach which could lead to practical clinical application.

5.3. Hepatic HNF4α in Systemic Metabolism and Energetics

Our understanding of the role of HNF4α in metabolism has been limited to its effects on the liver and serum chemistries. Deletion of HNF4α causes hepatic steatosis by decreasing hepatic lipid export and increasing hepatic lipid import while depletion of hepatic glycogen occurs through inhibited hepatic gluconeogenesis. These observations are adequate for understanding HNF4α's role in hepatic metabolism, but its broader impact on systemic metabolism is not as well understood. The studies performed using indirect calorimetry have demonstrated how metabolic regulation by hepatic HNF4α is central to energy homeostasis and how disruption of HNF4α has significant consequences for metabolism in the entire organism.

Hypoglycemia and transient hepatic steatosis are well-known metabolic changes which occur after PH (J. Huang & Rudnick, 2014), but countering either can lead to inhibited liver regeneration. Several studies have shown that inhibiting hepatic steatosis after PH reduces hepatocyte proliferation (Fernandez et al., 2006; Kohjima et al., 2013; Shteyer et al., 2004) because accumulation of hepatic triglycerides is required to fuel β-oxidation in the regenerating liver (Bellet et al., 2016; Kachaylo et al., 2017; Kohjima et al., 2013; Mukherjee et al., 2017). Studies have also shown that inhibition of transient steatosis impairs liver regeneration by

increasing expression of the HNF4α target gene p21 (Gazit et al., 2010; Weymann et al., 2009). These lipids come from lipolysis of adipose depots, and regeneration in lipid dystrophic mice which have decreased adipose stores, exhibit decreased hepatic steatosis and impaired liver regeneration (Gazit et al., 2010). This lipolysis is triggered by hypoglycemia, and supplementation with dextrose or glucose inhibits liver regeneration (Caruana et al., 1986; Weymann et al., 2009). Only one study has used indirect calorimetry to examine liver regeneration after PH (Kachaylo et al., 2017). This dissertation has demonstrated the role of HNF4α in liver regeneration and has uncovered significant effects on energy expenditure following hepatic HNF4α deletion. Future studies will use indirect calorimetry and other techniques to examine how HNF4α regulates metabolism during liver regeneration.

Endoplasmic Reticulum (ER) stress is known to cause hepatic steatosis and reduced serum lipids (Rutkowski et al., 2008; Yamamoto et al., 2010; Zhang et al., 2011). ER stress-induced hepatic steatosis involves changes in the expression of many genes involved in lipid metabolism. ER stress can downregulate HNF4α which decreases expression of β-oxidation and VLDL genes (Arensdorf, Dezwaan McCabe, Kaufman, & Rutkowski, 2013; Piccolo et al., 2017). Decreased β-oxidation and VLDL secretion contributes to fatty liver during early ER stress, but with prolonged ER stress, mice become hypoglycemic and increased adipose lipolysis becomes a major contributor to hepatic steatosis (DeZwaan-McCabe et al., 2017). This phenotype (decreased β-oxidation, decreased VLDL secretion, hypoglycemia, increased adipose lipolysis) is very similar to what we observed in HNF4α-KO mice. Knowing the role decreased HNF4α plays in progression of liver disease, it would be interesting to examine if similar mechanisms

drive mouse models of liver disease. Indirect calorimetry analysis would allow us to test if interventions to restore metabolic homeostasis can reverse or attenuate these diseases, or improve survival. Already it has been shown in mice that increased β-oxidation following fibrate treatment increases energy expenditure and prevents hepatic steatosis, despite higher ER stress (Chan et al., 2013). In humans, L-carnitine supplementation in cirrhotic patients exhibiting protein-energy malnutrition, can improve respiratory quotient values (Sakai et al., 2016), a marker with prognostic value (H. Nishikawa et al., 2017). Indirect calorimetry would allow us to investigate how disruptions in HNF4α-regulated metabolism contributes to these diseases.

Finally, chemicals known as perfluoroalkyl acids are known to cause hepatic steatosis and are capable of targeting HNF4α (Beggs et al., 2016). These compounds are also known to produce some obesogenic effects (Domazet, Grontved, Timmermann, Nielsen, & Jensen, 2016; Liu et al., 2018). While the toxic effects of compounds are often described by their effects on individual tissues, indirect calorimetry would allow us to determine if the net toxic effects of a chemical would be likely to cause obesity by creating a long term positive energy balance.

References

Alpern, D., Langer, D., Ballester, B., Le Gras, S., Romier, C., Mengus, G., & Davidson, I. (2014). TAF4, a subunit of transcription factor II D, directs promoter occupancy of nuclear receptor HNF4A during post-natal hepatocyte differentiation. *Elife, 3*, e03613. doi:10.7554/eLife.03613

Appikonda, S., Thakkar, K. N., & Barton, M. C. (2016). Regulation of gene expression in human cancers by TRIM24. *Drug Discov Today Technol, 19*, 57-63. doi:10.1016/j.ddtec.2016.05.001

Apte, U., Singh, S., Zeng, G., Cieply, B., Virji, M. A., Wu, T., & Monga, S. P. (2009). Beta-catenin activation promotes liver regeneration after acetaminophen-induced injury. *Am J Pathol, 175*(3), 1056-1065. doi:10.2353/ajpath.2009.080976

Arensdorf, A. M., Dezwaan McCabe, D., Kaufman, R. J., & Rutkowski, D. T. (2013). Temporal clustering of gene expression links the metabolic transcription factor HNF4alpha to the ER stress-dependent gene regulatory network. *Front Genet, 4*, 188. doi:10.3389/fgene.2013.00188

Armartmuntree, N., Murata, M., Techasen, A., Yongvanit, P., Loilome, W., Namwat, N., . . . Thanan, R. (2018). Prolonged oxidative stress down-regulates Early B cell factor 1 with inhibition of its tumor suppressive function against cholangiocarcinoma genesis. *Redox Biol, 14*, 637-644. doi:10.1016/j.redox.2017.11.011

Armour, S. M., Remsberg, J. R., Damle, M., Sidoli, S., Ho, W. Y., Li, Z., . . . Lazar, M. A. (2017). An HDAC3-PROX1 corepressor module acts on HNF4alpha to control hepatic triglycerides. *Nat Commun, 8*(1), 549. doi:10.1038/s41467-017-00772-5

Baciu, C., Pasini, E., Angeli, M., Schwenger, K., Afrin, J., Humar, A., . . . Bhat, M. (2017). Systematic integrative analysis of gene expression identifies HNF4A as the central gene in pathogenesis of non-alcoholic steatohepatitis. *PLoS One, 12*(12), e0189223. doi:10.1371/journal.pone.0189223

Baker, M. E. (2008). Trichoplax, the simplest known animal, contains an estrogen-related receptor but no estrogen receptor: Implications for estrogen receptor evolution. *Biochem Biophys Res Commun, 375*(4), 623-627. doi:10.1016/j.bbrc.2008.08.047

Battistelli, C., Sabarese, G., Santangelo, L., Montaldo, C., Gonzalez, F. J., Tripodi, M., & Cicchini, C. (2018). The lncRNA HOTAIR transcription is controlled by HNF4alpha-induced chromatin topology modulation. *Cell Death Differ*. doi:10.1038/s41418-018-0170-z

Beggs, K. M., McGreal, S. R., McCarthy, A., Gunewardena, S., Lampe, J. N., Lau, C., & Apte, U. (2016). The role of hepatocyte nuclear factor 4-alpha in perfluorooctanoic acid- and perfluorooctanesulfonic acid-induced hepatocellular dysfunction. *Toxicol Appl Pharmacol, 304*, 18-29. doi:10.1016/j.taap.2016.05.001

Bellet, M. M., Masri, S., Astarita, G., Sassone-Corsi, P., Della Fazia, M. A., & Servillo, G. (2016). Histone Deacetylase SIRT1 Controls Proliferation, Circadian Rhythm, and Lipid Metabolism during Liver Regeneration in Mice. *J Biol Chem, 291*(44), 23318-23329. doi:10.1074/jbc.M116.737114

Benet, M., Lahoz, A., Guzman, C., Castell, J. V., & Jover, R. (2010). CCAAT/enhancer-binding protein alpha (C/EBPalpha) and hepatocyte nuclear factor 4alpha (HNF4alpha) synergistically cooperate with constitutive androstane receptor to transactivate the human cytochrome P450 2B6 (CYP2B6) gene: application to the development of a metabolically

competent human hepatic cell model. *J Biol Chem, 285*(37), 28457-28471. doi:10.1074/jbc.M110.118364

Berasain, C., Herrero, J. I., Garcia-Trevijano, E. R., Avila, M. A., Esteban, J. I., Mato, J. M., & Prieto, J. (2003). Expression of Wilms' tumor suppressor in the liver with cirrhosis: relation to hepatocyte nuclear factor 4 and hepatocellular function. *Hepatology, 38*(1), 148-157. doi:10.1053/jhep.2003.50269

Bi, Y., Shi, X., Zhu, J., Guan, X., Garbacz, W. G., Huang, Y., . . . Xie, W. (2018). Regulation of Cholesterol Sulfotransferase SULT2B1b by Hepatocyte Nuclear Factor 4alpha Constitutes a Negative Feedback Control of Hepatic Gluconeogenesis. *Mol Cell Biol, 38*(7). doi:10.1128/MCB.00654-17

Boj, S. F., Servitja, J. M., Martin, D., Rios, M., Talianidis, I., Guigo, R., & Ferrer, J. (2009). Functional targets of the monogenic diabetes transcription factors HNF-1alpha and HNF-4alpha are highly conserved between mice and humans. *Diabetes, 58*(5), 1245-1253. doi:10.2337/db08-0812

Bonzo, J. A., Ferry, C. H., Matsubara, T., Kim, J. H., & Gonzalez, F. J. (2012). Suppression of hepatocyte proliferation by hepatocyte nuclear factor 4alpha in adult mice. *J Biol Chem, 287*(10), 7345-7356. doi:10.1074/jbc.M111.334599

Borude, P., Edwards, G., Walesky, C., Li, F., Ma, X., Kong, B., . . . Apte, U. (2012). Hepatocyte-specific deletion of farnesoid X receptor delays but does not inhibit liver regeneration after partial hepatectomy in mice. *Hepatology, 56*(6), 2344-2352. doi:10.1002/hep.25918

Briancon, N., Bailly, A., Clotman, F., Jacquemin, P., Lemaigre, F. P., & Weiss, M. C. (2004). Expression of the alpha7 isoform of hepatocyte nuclear factor (HNF) 4 is activated by HNF6/OC-2 and HNF1 and repressed by HNF4alpha1 in the liver. *J Biol Chem, 279*(32), 33398-33408. doi:10.1074/jbc.M405312200

Bruix, J., Han, K. H., Gores, G., Llovet, J. M., & Mazzaferro, V. (2015). Liver cancer: Approaching a personalized care. *J Hepatol, 62*(1 Suppl), S144-156. doi:10.1016/j.jhep.2015.02.007

Cai, S. H., Lu, S. X., Liu, L. L., Zhang, C. Z., & Yun, J. P. (2017). Increased expression of hepatocyte nuclear factor 4 alpha transcribed by promoter 2 indicates a poor prognosis in hepatocellular carcinoma. *Therap Adv Gastroenterol, 10*(10), 761-771. doi:10.1177/1756283X17725998

Cai, W. Y., Lin, L. Y., Hao, H., Zhang, S. M., Ma, F., Hong, X. X., . . . Li, B. A. (2017). Yes-associated protein/TEA domain family member and hepatocyte nuclear factor 4-alpha (HNF4alpha) repress reciprocally to regulate hepatocarcinogenesis in rats and mice. *Hepatology, 65*(4), 1206-1221. doi:10.1002/hep.28911

Caruana, J. A., Whalen, D. A., Jr., Anthony, W. P., Sunby, C. R., & Ciechoski, M. P. (1986). Paradoxical effects of glucose feeding on liver regeneration and survival after partial hepatectomy. *Endocr Res, 12*(2), 147-156.

Chan, S. M., Sun, R. Q., Zeng, X. Y., Choong, Z. H., Wang, H., Watt, M. J., & Ye, J. M. (2013). Activation of PPARalpha ameliorates hepatic insulin resistance and steatosis in high fructose-fed mice despite increased endoplasmic reticulum stress. *Diabetes, 62*(6), 2095-2105. doi:10.2337/db12-1397

Chandra, V., Huang, P., Potluri, N., Wu, D., Kim, Y., & Rastinejad, F. (2013). Multidomain integration in the structure of the HNF-4alpha nuclear receptor complex. *Nature, 495*(7441), 394-398. doi:10.1038/nature11966

Charos, A. E., Reed, B. D., Raha, D., Szekely, A. M., Weissman, S. M., & Snyder, M. (2012). A highly integrated and complex PPARGC1A transcription factor binding network in HepG2 cells. *Genome Res, 22*(9), 1668-1679. doi:10.1101/gr.127761.111

Chellappa, K., Deol, P., Evans, J. R., Vuong, L. M., Chen, G., Briancon, N., . . . Sladek, F. M. (2016). Opposing roles of nuclear receptor HNF4alpha isoforms in colitis and colitis-associated colon cancer. *Elife, 5*. doi:10.7554/eLife.10903

Chellappa, K., Jankova, L., Schnabl, J. M., Pan, S., Brelivet, Y., Fung, C. L., . . . Sladek, F. M. (2012). Src tyrosine kinase phosphorylation of nuclear receptor HNF4alpha correlates with isoform-specific loss of HNF4alpha in human colon cancer. *Proc Natl Acad Sci U S A, 109*(7), 2302-2307. doi:10.1073/pnas.1106799109

Chellappa, K., Robertson, G. R., & Sladek, F. M. (2012). HNF4alpha: a new biomarker in colon cancer? *Biomark Med, 6*(3), 297-300. doi:10.2217/bmm.12.23

Chen, W. S., Manova, K., Weinstein, D. C., Duncan, S. A., Plump, A. S., Prezioso, V. R., . . . Darnell, J. E., Jr. (1994). Disruption of the HNF-4 gene, expressed in visceral endoderm, leads to cell death in embryonic ectoderm and impaired gastrulation of mouse embryos. *Genes Dev, 8*(20), 2466-2477.

Chiba, H., Itoh, T., Satohisa, S., Sakai, N., Noguchi, H., Osanai, M., . . . Sawada, N. (2005). Activation of p21CIP1/WAF1 gene expression and inhibition of cell proliferation by overexpression of hepatocyte nuclear factor-4alpha. *Exp Cell Res, 302*(1), 11-21. doi:10.1016/j.yexcr.2004.08.014

Colletti, M., Cicchini, C., Conigliaro, A., Santangelo, L., Alonzi, T., Pasquini, E., . . . Amicone, L. (2009). Convergence of Wnt signaling on the HNF4alpha-driven transcription in controlling liver zonation. *Gastroenterology, 137*(2), 660-672. doi:10.1053/j.gastro.2009.05.038

Costa, R. H., Kalinichenko, V. V., Holterman, A. X., & Wang, X. (2003). Transcription factors in liver development, differentiation, and regeneration. *Hepatology, 38*(6), 1331-1347. doi:10.1016/j.hep.2003.09.034

Das, A. T., Tenenbaum, L., & Berkhout, B. (2016). Tet-On Systems For Doxycycline-inducible Gene Expression. *Curr Gene Ther, 16*(3), 156-167.

de Hoon, M. J., Imoto, S., Nolan, J., & Miyano, S. (2004). Open source clustering software. *Bioinformatics, 20*(9), 1453-1454. doi:10.1093/bioinformatics/bth078

Desai, S. S., Tung, J. C., Zhou, V. X., Grenert, J. P., Malato, Y., Rezvani, M., . . . Chang, T. T. (2016). Physiological ranges of matrix rigidity modulate primary mouse hepatocyte function in part through hepatocyte nuclear factor 4 alpha. *Hepatology, 64*(1), 261-275. doi:10.1002/hep.28450

Desert, R., Rohart, F., Canal, F., Sicard, M., Desille, M., Renaud, S., . . . Musso, O. (2017). Human hepatocellular carcinomas with a periportal phenotype have the lowest potential for early recurrence after curative resection. *Hepatology, 66*(5), 1502-1518. doi:10.1002/hep.29254

DeZwaan-McCabe, D., Sheldon, R. D., Gorecki, M. C., Guo, D. F., Gansemer, E. R., Kaufman, R. J., . . . Rutkowski, D. T. (2017). ER Stress Inhibits Liver Fatty Acid Oxidation while Unmitigated Stress Leads to Anorexia-Induced Lipolysis and Both Liver and Kidney Steatosis. *Cell Rep, 19*(9), 1794-1806. doi:10.1016/j.celrep.2017.05.020

Dhe-Paganon, S., Duda, K., Iwamoto, M., Chi, Y. I., & Shoelson, S. E. (2002). Crystal structure of the HNF4 alpha ligand binding domain in complex with endogenous fatty acid ligand. *J Biol Chem, 277*(41), 37973-37976. doi:10.1074/jbc.C200420200

Domazet, S. L., Grontved, A., Timmermann, A. G., Nielsen, F., & Jensen, T. K. (2016). Longitudinal Associations of Exposure to Perfluoroalkylated Substances in Childhood and Adolescence and Indicators of Adiposity and Glucose Metabolism 6 and 12 Years Later: The European Youth Heart Study. *Diabetes Care, 39*(10), 1745-1751. doi:10.2337/dc16-0269

Duncan, S. A., Manova, K., Chen, W. S., Hoodless, P., Weinstein, D. C., Bachvarova, R. F., & Darnell, J. E., Jr. (1994). Expression of transcription factor HNF-4 in the extraembryonic endoderm, gut, and nephrogenic tissue of the developing mouse embryo: HNF-4 is a marker for primary endoderm in the implanting blastocyst. *Proc Natl Acad Sci U S A, 91*(16), 7598-7602.

Duncan, S. A., Nagy, A., & Chan, W. (1997). Murine gastrulation requires HNF-4 regulated gene expression in the visceral endoderm: tetraploid rescue of Hnf-4(-/-) embryos. *Development, 124*(2), 279-287.

Eisen, M. B., Spellman, P. T., Brown, P. O., & Botstein, D. (1998). Cluster analysis and display of genome-wide expression patterns. *Proc Natl Acad Sci U S A, 95*(25), 14863-14868.

Erdmann, S., Senkel, S., Arndt, T., Lucas, B., Lausen, J., Klein-Hitpass, L., . . . Thomas, H. (2007). Tissue-specific transcription factor HNF4alpha inhibits cell proliferation and induces apoptosis in the pancreatic INS-1 beta-cell line. *Biol Chem, 388*(1), 91-106. doi:10.1515/BC.2007.011

Fabregat, I., Moreno-Caceres, J., Sanchez, A., Dooley, S., Dewidar, B., Giannelli, G., . . . Consortium, I.-L. (2016). TGF-beta signalling and liver disease. *FEBS J, 283*(12), 2219-2232. doi:10.1111/febs.13665

Fan, T. T., Hu, P. F., Wang, J., Wei, J., Zhang, Q., Ning, B. F., . . . Shi, B. (2013). Regression effect of hepatocyte nuclear factor 4alpha on liver cirrhosis in rats. *J Dig Dis, 14*(6), 318-327. doi:10.1111/1751-2980.12042

Fang, B., Mane-Padros, D., Bolotin, E., Jiang, T., & Sladek, F. M. (2012). Identification of a binding motif specific to HNF4 by comparative analysis of multiple nuclear receptors. *Nucleic Acids Res, 40*(12), 5343-5356. doi:10.1093/nar/gks190

Fernandez, M. A., Albor, C., Ingelmo-Torres, M., Nixon, S. J., Ferguson, C., Kurzchalia, T., . . . Pol, A. (2006). Caveolin-1 is essential for liver regeneration. *Science, 313*(5793), 1628-1632. doi:10.1126/science.1130773

Fletcher, J. A., Linden, M. A., Sheldon, R. D., Meers, G. M., Morris, E. M., Butterfield, A., . . . Thyfault, J. P. (2018). Fibroblast growth factor 21 increases hepatic oxidative capacity but not physical activity or energy expenditure in hepatic peroxisome proliferator-activated receptor gamma coactivator-1alpha-deficient mice. *Exp Physiol, 103*(3), 408-418. doi:10.1113/EP086629

Flodby, P., Antonson, P., Barlow, C., Blanck, A., Porsch-Hallstrom, I., & Xanthopoulos, K. G. (1993). Differential patterns of expression of three C/EBP isoforms, HNF-1, and HNF-4 after partial hepatectomy in rats. *Exp Cell Res, 208*(1), 248-256. doi:10.1006/excr.1993.1244

Fukuda, T., Fukuchi, T., Yagi, S., & Shiojiri, N. (2016). Immunohistochemical analyses of cell cycle progression and gene expression of biliary epithelial cells during liver regeneration after partial hepatectomy of the mouse. *Exp Anim, 65*(2), 135-146. doi:10.1538/expanim.15-0082

Gazit, V., Weymann, A., Hartman, E., Finck, B. N., Hruz, P. W., Tzekov, A., & Rudnick, D. A. (2010). Liver regeneration is impaired in lipodystrophic fatty liver dystrophy mice. *Hepatology, 52*(6), 2109-2117. doi:10.1002/hep.23920

Global, regional, and national age-sex specific all-cause and cause-specific mortality for 240 causes of death, 1990-2013: a systematic analysis for the Global Burden of Disease Study 2013. (2015). *Lancet, 385*(9963), 117-171. doi:10.1016/s0140-6736(14)61682-2

Godini, R., & Fallahi, H. (2018). Dynamics changes in the transcription factors during early human embryonic development. *J Cell Physiol*. doi:10.1002/jcp.27386

Gonzalez, F. J. (2008). Regulation of hepatocyte nuclear factor 4 alpha-mediated transcription. *Drug Metab Pharmacokinet, 23*(1), 2-7.

Grasso, L. C., Hayward, D. C., Trueman, J. W., Hardie, K. M., Janssens, P. A., & Ball, E. E. (2001). The evolution of nuclear receptors: evidence from the coral Acropora. *Mol Phylogenet Evol, 21*(1), 93-102. doi:10.1006/mpev.2001.0994

Gupta, R. K., Gao, N., Gorski, R. K., White, P., Hardy, O. T., Rafiq, K., . . . Kaestner, K. H. (2007). Expansion of adult beta-cell mass in response to increased metabolic demand is dependent on HNF-4alpha. *Genes Dev, 21*(7), 756-769. doi:10.1101/gad.1535507

Guzman-Lepe, J., Cervantes-Alvarez, E., Collin de l'Hortet, A., Wang, Y., Mars, W. M., Oda, Y., . . . Soto-Gutierrez, A. (2018). Liver-enriched transcription factor expression relates to chronic hepatic failure in humans. *Hepatol Commun, 2*(5), 582-594. doi:10.1002/hep4.1172

Habka, D., Mann, D., Landes, R., & Soto-Gutierrez, A. (2015). Future Economics of Liver Transplantation: A 20-Year Cost Modeling Forecast and the Prospect of Bioengineering Autologous Liver Grafts. *PLoS One, 10*(7), e0131764. doi:10.1371/journal.pone.0131764

Harries, L. W., Locke, J. M., Shields, B., Hanley, N. A., Hanley, K. P., Steele, A., . . . Hattersley, A. T. (2008). The diabetic phenotype in HNF4A mutation carriers is moderated by the expression of HNF4A isoforms from the P1 promoter during fetal development. *Diabetes, 57*(6), 1745-1752. doi:10.2337/db07-1742

Hatziapostolou, M., Polytarchou, C., Aggelidou, E., Drakaki, A., Poultsides, G. A., Jaeger, S. A., . . . Iliopoulos, D. (2011). An HNF4alpha-miRNA inflammatory feedback circuit regulates hepatocellular oncogenesis. *Cell, 147*(6), 1233-1247. doi:10.1016/j.cell.2011.10.043

Hayhurst, G. P., Lee, Y. H., Lambert, G., Ward, J. M., & Gonzalez, F. J. (2001). Hepatocyte nuclear factor 4alpha (nuclear receptor 2A1) is essential for maintenance of hepatic gene expression and lipid homeostasis. *Mol Cell Biol, 21*(4), 1393-1403. doi:10.1128/MCB.21.4.1393-1403.2001

Higgins, G., & Anderson, R. M. (1931). Experimental pathology of the liver. Restoration of the liver of the white rat following partial surgical removal. *Archives of Pathology, 12*, 186.

Hoffman, B. G., Robertson, G., Zavaglia, B., Beach, M., Cullum, R., Lee, S., . . . Hoodless, P. A. (2010). Locus co-occupancy, nucleosome positioning, and H3K4me1 regulate the functionality of FOXA2-, HNF4A-, and PDX1-bound loci in islets and liver. *Genome Res, 20*(8), 1037-1051. doi:10.1101/gr.104356.109

Hu, Y., Guo, X., Wang, J., Liu, Y., Gao, H., Fan, H., . . . Tang, H. (2018). A novel microRNA identified in hepatocellular carcinomas is responsive to LEF1 and facilitates proliferation and epithelial-mesenchymal transition via targeting of NFIX. *Oncogenesis, 7*(2), 22. doi:10.1038/s41389-017-0010-x

Huang, J., & Rudnick, D. A. (2014). Elucidating the metabolic regulation of liver regeneration. *Am J Pathol, 184*(2), 309-321. doi:10.1016/j.ajpath.2013.04.034

Huang, Q., Pu, M., Zhao, G., Dai, B., Bian, Z., Tang, H., . . . Tao, K. (2017). Tg737 regulates epithelial-mesenchymal transition and cancer stem cell properties via a negative feedback circuit between Snail and HNF4alpha during liver stem cell malignant transformation. *Cancer Lett, 402*, 52-60. doi:10.1016/j.canlet.2017.05.005

Huck, I., Gunewardena, S., Espanol-Suner, R., Willenbring, H., & Apte, U. (2018). Hepatocyte Nuclear Factor 4 alpha (HNF4alpha) Activation is Essential for Termination of Liver Regeneration. *Hepatology*. doi:10.1002/hep.30405

Huck, I., Morris, E. M., Thyfault, J. P., & Apte, U. (2018). Hepatocyte-Specific Hepatocyte Nuclear Factor 4 alpha (HNF4α) Deletion Decreases Resting Energy Expenditure By Disrupting Lipid and Carbohydrate Homeostasis. *bioRxiv*, 401802. doi:10.1101/401802

Hwang-Verslues, W. W., & Sladek, F. M. (2008). Nuclear receptor hepatocyte nuclear factor 4alpha1 competes with oncoprotein c-Myc for control of the p21/WAF1 promoter. *Mol Endocrinol, 22*(1), 78-90. doi:10.1210/me.2007-0298

Hwang-Verslues, W. W., & Sladek, F. M. (2010). HNF4alpha--role in drug metabolism and potential drug target? *Curr Opin Pharmacol, 10*(6), 698-705. doi:10.1016/j.coph.2010.08.010

Inoue, K., & Negishi, M. (2008). Nuclear receptor CAR requires early growth response 1 to activate the human cytochrome P450 2B6 gene. *J Biol Chem, 283*(16), 10425-10432. doi:10.1074/jbc.M800729200

Inoue, Y., Hayhurst, G. P., Inoue, J., Mori, M., & Gonzalez, F. J. (2002). Defective ureagenesis in mice carrying a liver-specific disruption of hepatocyte nuclear factor 4alpha (HNF4alpha). HNF4alpha regulates ornithine transcarbamylase in vivo. *J Biol Chem, 277*(28), 25257-25265. doi:10.1074/jbc.M203126200

Inoue, Y., Peters, L. L., Yim, S. H., Inoue, J., & Gonzalez, F. J. (2006). Role of hepatocyte nuclear factor 4alpha in control of blood coagulation factor gene expression. *J Mol Med (Berl), 84*(4), 334-344. doi:10.1007/s00109-005-0013-5

Inoue, Y., Yu, A. M., Inoue, J., & Gonzalez, F. J. (2004). Hepatocyte nuclear factor 4alpha is a central regulator of bile acid conjugation. *J Biol Chem, 279*(4), 2480-2489. doi:10.1074/jbc.M311015200

Inoue, Y., Yu, A. M., Yim, S. H., Ma, X., Krausz, K. W., Inoue, J., . . . Gonzalez, F. J. (2006). Regulation of bile acid biosynthesis by hepatocyte nuclear factor 4alpha. *J Lipid Res, 47*(1), 215-227. doi:10.1194/jlr.M500430-JLR200

Jia, Y., Viswakarma, N., & Reddy, J. K. (2014). Med1 subunit of the mediator complex in nuclear receptor-regulated energy metabolism, liver regeneration, and hepatocarcinogenesis. *Gene Expr, 16*(2), 63-75. doi:10.3727/105221614X13919976902219

Jiao, H., Zhu, Y., Lu, S., Zheng, Y., & Chen, H. (2015). An Integrated Approach for the Identification of HNF4alpha-Centered Transcriptional Regulatory Networks During Early Liver Regeneration. *Cell Physiol Biochem, 36*(6), 2317-2326. doi:10.1159/000430195

Jover, R., Moya, M., & Gomez-Lechon, M. J. (2009). Transcriptional regulation of cytochrome p450 genes by the nuclear receptor hepatocyte nuclear factor 4-alpha. *Curr Drug Metab, 10*(5), 508-519.

Juma, A. R., Damdimopoulou, P. E., Grommen, S. V., Van de Ven, W. J., & De Groef, B. (2016). Emerging role of PLAG1 as a regulator of growth and reproduction. *J Endocrinol, 228*(2), R45-56. doi:10.1530/JOE-15-0449

Kachaylo, E., Tschuor, C., Calo, N., Borgeaud, N., Ungethum, U., Limani, P., . . . Humar, B. (2017). PTEN Down-Regulation Promotes beta-Oxidation to Fuel Hypertrophic Liver Growth After Hepatectomy in Mice. *Hepatology, 66*(3), 908-921. doi:10.1002/hep.29226

Kaiyala, K. J., Morton, G. J., Leroux, B. G., Ogimoto, K., Wisse, B., & Schwartz, M. W. (2010). Identification of body fat mass as a major determinant of metabolic rate in mice. *Diabetes, 59*(7), 1657-1666. doi:10.2337/db09-1582

Kamiyama, Y., Matsubara, T., Yoshinari, K., Nagata, K., Kamimura, H., & Yamazoe, Y. (2007). Role of human hepatocyte nuclear factor 4alpha in the expression of drug-metabolizing enzymes and transporters in human hepatocytes assessed by use of small interfering RNA. *Drug Metab Pharmacokinet, 22*(4), 287-298.

Kawashima, S. (2006). Involvement of hepatocyte nuclear factor 4 in the different expression level between CYP2C9 and CYP2C19 in the human liver. *Drug Metabolism and Disposition*. doi:10.1124/dmd.106.009365

Kir, S., Zhang, Y., Gerard, R. D., Kliewer, S. A., & Mangelsdorf, D. J. (2012). Nuclear receptors HNF4alpha and LRH-1 cooperate in regulating Cyp7a1 in vivo. *J Biol Chem, 287*(49), 41334-41341. doi:10.1074/jbc.M112.421834

Kohjima, M., Tsai, T. H., Tackett, B. C., Thevananther, S., Li, L., Chang, B. H., & Chan, L. (2013). Delayed liver regeneration after partial hepatectomy in adipose differentiation related protein-null mice. *J Hepatol, 59*(6), 1246-1254. doi:10.1016/j.jhep.2013.07.025

Kyrmizi, I., Hatzis, P., Katrakili, N., Tronche, F., Gonzalez, F. J., & Talianidis, I. (2006). Plasticity and expanding complexity of the hepatic transcription factor network during liver development. *Genes Dev, 20*(16), 2293-2305. doi:10.1101/gad.390906

Larroux, C., Fahey, B., Liubicich, D., Hinman, V. F., Gauthier, M., Gongora, M., . . . Degnan, B. M. (2006). Developmental expression of transcription factor genes in a demosponge: insights into the origin of metazoan multicellularity. *Evol Dev, 8*(2), 150-173. doi:10.1111/j.1525-142X.2006.00086.x

Lazarevich, N. L., Cheremnova, O. A., Varga, E. V., Ovchinnikov, D. A., Kudrjavtseva, E. I., Morozova, O. V., . . . Duncan, S. A. (2004). Progression of HCC in mice is associated with a downregulation in the expression of hepatocyte nuclear factors. *Hepatology, 39*(4), 1038-1047. doi:10.1002/hep.20155

Lee, D. H., Park, J. O., Kim, T. S., Kim, S. K., Kim, T. H., Kim, M. C., . . . Lim, D. S. (2016). LATS-YAP/TAZ controls lineage specification by regulating TGFbeta signaling and Hnf4alpha expression during liver development. *Nat Commun, 7*, 11961. doi:10.1038/ncomms11961

Leung, A., Parks, B. W., Du, J., Trac, C., Setten, R., Chen, Y., . . . Schones, D. E. (2014). Open chromatin profiling in mice livers reveals unique chromatin variations induced by high fat diet. *J Biol Chem, 289*(34), 23557-23567. doi:10.1074/jbc.M114.581439

Li, J., Ning, G., & Duncan, S. A. (2000). Mammalian hepatocyte differentiation requires the transcription factor HNF-4alpha. *Genes Dev, 14*(4), 464-474.

Li, T., Chanda, D., Zhang, Y., Choi, H. S., & Chiang, J. Y. (2010). Glucose stimulates cholesterol 7alpha-hydroxylase gene transcription in human hepatocytes. *J Lipid Res, 51*(4), 832-842. doi:10.1194/jlr.M002782

Li, T., & Chiang, J. Y. (2005). Mechanism of rifampicin and pregnane X receptor inhibition of human cholesterol 7 alpha-hydroxylase gene transcription. *Am J Physiol Gastrointest Liver Physiol, 288*(1), G74-84. doi:10.1152/ajpgi.00258.2004

Li, T., & Chiang, J. Y. (2007). A novel role of transforming growth factor beta1 in transcriptional repression of human cholesterol 7alpha-hydroxylase gene. *Gastroenterology, 133*(5), 1660-1669. doi:10.1053/j.gastro.2007.08.042

Li, T., Jahan, A., & Chiang, J. Y. (2006). Bile acids and cytokines inhibit the human cholesterol 7 alpha-hydroxylase gene via the JNK/c-jun pathway in human liver cells. *Hepatology, 43*(6), 1202-1210. doi:10.1002/hep.21183

Liu, G., Dhana, K., Furtado, J. D., Rood, J., Zong, G., Liang, L., . . . Sun, Q. (2018). Perfluoroalkyl substances and changes in body weight and resting metabolic rate in response to weight-loss diets: A prospective study. *PLoS Med, 15*(2), e1002502. doi:10.1371/journal.pmed.1002502

Livak, K. J., & Schmittgen, T. D. (2001). Analysis of relative gene expression data using real-time quantitative PCR and the 2(-Delta Delta C(T)) Method. *Methods, 25*(4), 402-408. doi:10.1006/meth.2001.1262

Llovet, J. M., Bru, C., & Bruix, J. (1999). Prognosis of hepatocellular carcinoma: the BCLC staging classification. *Semin Liver Dis, 19*(3), 329-338. doi:10.1055/s-2007-1007122

Llovet, J. M., Burroughs, A., & Bruix, J. (2003). Hepatocellular carcinoma. *The Lancet, 362*(9399), 1907-1917. doi:10.1016/s0140-6736(03)14964-1

Llovet, J. M., Zucman-Rossi, J., Pikarsky, E., Sangro, B., Schwartz, M., Sherman, M., & Gores, G. (2016). Hepatocellular carcinoma. *Nat Rev Dis Primers, 2*, 16018. doi:10.1038/nrdp.2016.18

Louet, J. F., Hayhurst, G., Gonzalez, F. J., Girard, J., & Decaux, J. F. (2002). The coactivator PGC-1 is involved in the regulation of the liver carnitine palmitoyltransferase I gene expression by cAMP in combination with HNF4 alpha and cAMP-response element-binding protein (CREB). *J Biol Chem, 277*(41), 37991-38000. doi:10.1074/jbc.M205087200

Lu, H., Gonzalez, F. J., & Klaassen, C. (2010). Alterations in hepatic mRNA expression of phase II enzymes and xenobiotic transporters after targeted disruption of hepatocyte nuclear factor 4 alpha. *Toxicol Sci, 118*(2), 380-390. doi:10.1093/toxsci/kfq280

Lucas, B., Grigo, K., Erdmann, S., Lausen, J., Klein-Hitpass, L., & Ryffel, G. U. (2005). HNF4alpha reduces proliferation of kidney cells and affects genes deregulated in renal cell carcinoma. *Oncogene, 24*(42), 6418-6431. doi:10.1038/sj.onc.1208794

Ludtke, T. H., Christoffels, V. M., Petry, M., & Kispert, A. (2009). Tbx3 promotes liver bud expansion during mouse development by suppression of cholangiocyte differentiation. *Hepatology, 49*(3), 969-978. doi:10.1002/hep.22700

Malato, Y., Naqvi, S., Schurmann, N., Ng, R., Wang, B., Zape, J., . . . Willenbring, H. (2011). Fate tracing of mature hepatocytes in mouse liver homeostasis and regeneration. *J Clin Invest, 121*(12), 4850-4860. doi:10.1172/JCI59261

Martinez-Jimenez, C. P., Kyrmizi, I., Cardot, P., Gonzalez, F. J., & Talianidis, I. (2010). Hepatocyte nuclear factor 4alpha coordinates a transcription factor network regulating hepatic fatty acid metabolism. *Mol Cell Biol, 30*(3), 565-577. doi:10.1128/MCB.00927-09

Mataki, C., Magnier, B. C., Houten, S. M., Annicotte, J. S., Argmann, C., Thomas, C., . . . Schoonjans, K. (2007). Compromised intestinal lipid absorption in mice with a liver-

specific deficiency of liver receptor homolog 1. *Mol Cell Biol, 27*(23), 8330-8339. doi:10.1128/MCB.00852-07

Matsuo, S., Ogawa, M., Muckenthaler, M. U., Mizui, Y., Sasaki, S., Fujimura, T., . . . Inoue, Y. (2015). Hepatocyte Nuclear Factor 4alpha Controls Iron Metabolism and Regulates Transferrin Receptor 2 in Mouse Liver. *J Biol Chem, 290*(52), 30855-30865. doi:10.1074/jbc.M115.694414

Michalopoulos, G. K. (2017). Hepatostat: Liver regeneration and normal liver tissue maintenance. *Hepatology, 65*(4), 1384-1392. doi:10.1002/hep.28988

Moore, B. D., Khurana, S. S., Huh, W. J., & Mills, J. C. (2016). Hepatocyte nuclear factor 4alpha is required for cell differentiation and homeostasis in the adult mouse gastric epithelium. *Am J Physiol Gastrointest Liver Physiol, 311*(2), G267-275. doi:10.1152/ajpgi.00195.2016

Morimoto, A., Kannari, M., Tsuchida, Y., Sasaki, S., Saito, C., Matsuta, T., . . . Inoue, Y. (2017). An HNF4alpha-microRNA-194/192 signaling axis maintains hepatic cell function. *J Biol Chem, 292*(25), 10574-10585. doi:10.1074/jbc.M117.785592

Morris, E. M., Jackman, M. R., Johnson, G. C., Liu, T. W., Lopez, J. L., Kearney, M. L., . . . Thyfault, J. P. (2014). Intrinsic aerobic capacity impacts susceptibility to acute high-fat diet-induced hepatic steatosis. *Am J Physiol Endocrinol Metab, 307*(4), E355-364. doi:10.1152/ajpendo.00093.2014

Mortensen, K. E., & Revhaug, A. (2011). Liver regeneration in surgical animal models - a historical perspective and clinical implications. *Eur Surg Res, 46*(1), 1-18. doi:10.1159/000321361

Mukherjee, S., Chellappa, K., Moffitt, A., Ndungu, J., Dellinger, R. W., Davis, J. G., . . . Baur, J. A. (2017). Nicotinamide adenine dinucleotide biosynthesis promotes liver regeneration. *Hepatology, 65*(2), 616-630. doi:10.1002/hep.28912

Nedumaran, B., Hong, S., Xie, Y. B., Kim, Y. H., Seo, W. Y., Lee, M. W., . . . Choi, H. S. (2009). DAX-1 acts as a novel corepressor of orphan nuclear receptor HNF4alpha and negatively regulates gluconeogenic enzyme gene expression. *J Biol Chem, 284*(40), 27511-27523. doi:10.1074/jbc.M109.034660

Ning, B. F., Ding, J., Liu, J., Yin, C., Xu, W. P., Cong, W. M., . . . Xie, W. F. (2014). Hepatocyte nuclear factor 4alpha-nuclear factor-kappaB feedback circuit modulates liver cancer progression. *Hepatology, 60*(5), 1607-1619. doi:10.1002/hep.27177

Ning, B. F., Ding, J., Yin, C., Zhong, W., Wu, K., Zeng, X., . . . Xie, W. F. (2010). Hepatocyte nuclear factor 4 alpha suppresses the development of hepatocellular carcinoma. *Cancer Res, 70*(19), 7640-7651. doi:10.1158/0008-5472.CAN-10-0824

Nishikawa, H., Enomoto, H., Iwata, Y., Kishino, K., Shimono, Y., Hasegawa, K., . . . Nishiguchi, S. (2017). Prognostic significance of nonprotein respiratory quotient in patients with liver cirrhosis. *Medicine (Baltimore), 96*(3), e5800. doi:10.1097/MD.0000000000005800

Nishikawa, T., Bell, A., Brooks, J. M., Setoyama, K., Melis, M., Han, B., . . . Fox, I. J. (2015). Resetting the transcription factor network reverses terminal chronic hepatic failure. *J Clin Invest, 125*(4), 1533-1544. doi:10.1172/JCI73137

O'Donnell, K. A., Keng, V. W., York, B., Reineke, E. L., Seo, D., Fan, D., . . . Boeke, J. D. (2012). A Sleeping Beauty mutagenesis screen reveals a tumor suppressor role for Ncoa2/Src-2 in liver cancer. *Proc Natl Acad Sci U S A, 109*(21), E1377-1386. doi:10.1073/pnas.1115433109

Odom, D. T., Dowell, R. D., Jacobsen, E. S., Nekludova, L., Rolfe, P. A., Danford, T. W., . . . Young, R. A. (2006). Core transcriptional regulatory circuitry in human hepatocytes. *Mol Syst Biol, 2*, 2006 0017. doi:10.1038/msb4100059

Odom, D. T., Zizlsperger, N., Gordon, D. B., Bell, G. W., Rinaldi, N. J., Murray, H. L., . . . Young, R. A. (2004). Control of pancreas and liver gene expression by HNF transcription factors. *Science, 303*(5662), 1378-1381. doi:10.1126/science.1089769

Palanker, L., Tennessen, J. M., Lam, G., & Thummel, C. S. (2009). Drosophila HNF4 regulates lipid mobilization and beta-oxidation. *Cell Metab, 9*(3), 228-239. doi:10.1016/j.cmet.2009.01.009

Palu, R. A., & Thummel, C. S. (2016). Sir2 Acts through Hepatocyte Nuclear Factor 4 to maintain insulin Signaling and Metabolic Homeostasis in Drosophila. *PLoS Genet, 12*(4), e1005978. doi:10.1371/journal.pgen.1005978

Paranjpe, S., Bowen, W. C., Mars, W. M., Orr, A., Haynes, M. M., DeFrances, M. C., . . . Michalopoulos, G. K. (2016). Combined systemic elimination of MET and epidermal growth factor receptor signaling completely abolishes liver regeneration and leads to liver decompensation. *Hepatology, 64*(5), 1711-1724. doi:10.1002/hep.28721

Parviz, F., Matullo, C., Garrison, W. D., Savatski, L., Adamson, J. W., Ning, G., . . . Duncan, S. A. (2003). Hepatocyte nuclear factor 4alpha controls the development of a hepatic epithelium and liver morphogenesis. *Nat Genet, 34*(3), 292-296. doi:10.1038/ng1175

Piccolo, P., Annunziata, P., Soria, L. R., Attanasio, S., Barbato, A., Castello, R., . . . Brunetti-Pierri, N. (2017). Down-regulation of hepatocyte nuclear factor-4alpha and defective zonation in livers expressing mutant Z alpha1-antitrypsin. *Hepatology, 66*(1), 124-135. doi:10.1002/hep.29160

Ramsey, J. J., Harper, M. E., & Weindruch, R. (2000). Restriction of energy intake, energy expenditure, and aging. *Free Radic Biol Med, 29*(10), 946-968.

Reich, M., Liefeld, T., Gould, J., Lerner, J., Tamayo, P., & Mesirov, J. P. (2006). GenePattern 2.0. *Nat Genet, 38*(5), 500-501. doi:10.1038/ng0506-500

Rhee, J., Inoue, Y., Yoon, J. C., Puigserver, P., Fan, M., Gonzalez, F. J., & Spiegelman, B. M. (2003). Regulation of hepatic fasting response by PPARgamma coactivator-1alpha (PGC-1): requirement for hepatocyte nuclear factor 4alpha in gluconeogenesis. *Proc Natl Acad Sci U S A, 100*(7), 4012-4017. doi:10.1073/pnas.0730870100

Rieck, S., Zhang, J., Li, Z., Liu, C., Naji, A., Takane, K. K., . . . Kaestner, K. H. (2012). Overexpression of hepatocyte nuclear factor-4alpha initiates cell cycle entry, but is not sufficient to promote beta-cell expansion in human islets. *Mol Endocrinol, 26*(9), 1590-1602. doi:10.1210/me.2012-1019

Rutkowski, D. T., Wu, J., Back, S. H., Callaghan, M. U., Ferris, S. P., Iqbal, J., . . . Kaufman, R. J. (2008). UPR pathways combine to prevent hepatic steatosis caused by ER stress-mediated suppression of transcriptional master regulators. *Dev Cell, 15*(6), 829-840. doi:10.1016/j.devcel.2008.10.015

Sakai, Y., Nishikawa, H., Enomoto, H., Yoh, K., Iwata, Y., Hasegawa, K., . . . Nishiguchi, S. (2016). Effect of L-Carnitine in Patients With Liver Cirrhosis on Energy Metabolism Using Indirect Calorimetry: A Pilot Study. *J Clin Med Res, 8*(12), 863-869. doi:10.14740/jocmr2734w

Sangiovanni, A., Del Ninno, E., Fasani, P., De Fazio, C., Ronchi, G., Romeo, R., . . . Colombo, M. (2004). Increased survival of cirrhotic patients with a hepatocellular carcinoma

detected during surveillance☆. *Gastroenterology, 126*(4), 1005-1014. doi:10.1053/j.gastro.2003.12.049

Santangelo, L., Marchetti, A., Cicchini, C., Conigliaro, A., Conti, B., Mancone, C., . . . Tripodi, M. (2011). The stable repression of mesenchymal program is required for hepatocyte identity: a novel role for hepatocyte nuclear factor 4alpha. *Hepatology, 53*(6), 2063-2074. doi:10.1002/hep.24280

Schmidt, D., Wilson, M. D., Ballester, B., Schwalie, P. C., Brown, G. D., Marshall, A., . . . Odom, D. T. (2010). Five-vertebrate ChIP-seq reveals the evolutionary dynamics of transcription factor binding. *Science, 328*(5981), 1036-1040. doi:10.1126/science.1186176

Schutz, Y., & Ravussin, E. (1980). Respiratory quotients lower than 0.70 in ketogenic diets. *Am J Clin Nutr, 33*(6), 1317-1319. doi:10.1093/ajcn/33.6.1317

Sel, S., Ebert, T., Ryffel, G. U., & Drewes, T. (1996). Human renal cell carcinogenesis is accompanied by a coordinate loss of the tissue specific transcription factors HNF4 alpha and HNF1 alpha. *Cancer Lett, 101*(2), 205-210.

Shteyer, E., Liao, Y., Muglia, L. J., Hruz, P. W., & Rudnick, D. A. (2004). Disruption of hepatic adipogenesis is associated with impaired liver regeneration in mice. *Hepatology, 40*(6), 1322-1332. doi:10.1002/hep.20462

Simcox, J., Geoghegan, G., Maschek, J. A., Bensard, C. L., Pasquali, M., Miao, R., . . . Villanueva, C. J. (2017). Global Analysis of Plasma Lipids Identifies Liver-Derived Acylcarnitines as a Fuel Source for Brown Fat Thermogenesis. *Cell Metab, 26*(3), 509-522 e506. doi:10.1016/j.cmet.2017.08.006

Sladek, F. M. (2011). What are nuclear receptor ligands? *Mol Cell Endocrinol, 334*(1-2), 3-13. doi:10.1016/j.mce.2010.06.018

Sladek, F. M., Zhong, W. M., Lai, E., & Darnell, J. E., Jr. (1990). Liver-enriched transcription factor HNF-4 is a novel member of the steroid hormone receptor superfamily. *Genes Dev, 4*(12b), 2353-2365.

Song, K. H., Li, T., & Chiang, J. Y. (2006). A Prospero-related homeodomain protein is a novel co-regulator of hepatocyte nuclear factor 4alpha that regulates the cholesterol 7alpha-hydroxylase gene. *J Biol Chem, 281*(15), 10081-10088. doi:10.1074/jbc.M513420200

Song, Y., Zheng, D., Zhao, M., Qin, Y., Wang, T., Xing, W., . . . Zhao, J. (2015). Thyroid-Stimulating Hormone Increases HNF-4alpha Phosphorylation via cAMP/PKA Pathway in the Liver. *Sci Rep, 5*, 13409. doi:10.1038/srep13409

Speakman, J. R., Fletcher, Q., & Vaanholt, L. (2013). The '39 steps': an algorithm for performing statistical analysis of data on energy intake and expenditure. *Dis Model Mech, 6*(2), 293-301. doi:10.1242/dmm.009860

Stanulovic, V. S., Kyrmizi, I., Kruithof-de Julio, M., Hoogenkamp, M., Vermeulen, J. L., Ruijter, J. M., . . . Lamers, W. H. (2007). Hepatic HNF4alpha deficiency induces periportal expression of glutamine synthetase and other pericentral enzymes. *Hepatology, 45*(2), 433-444. doi:10.1002/hep.21456

Sun, K., Montana, V., Chellappa, K., Brelivet, Y., Moras, D., Maeda, Y., . . . Sladek, F. M. (2007). Phosphorylation of a conserved serine in the deoxyribonucleic acid binding domain of nuclear receptors alters intracellular localization. *Mol Endocrinol, 21*(6), 1297-1311. doi:10.1210/me.2006-0300

Sun, L., Beggs, K., Borude, P., Edwards, G., Bhushan, B., Walesky, C., . . . Apte, U. (2016). Bile acids promote diethylnitrosamine-induced hepatocellular carcinoma via increased

inflammatory signaling. *Am J Physiol Gastrointest Liver Physiol, 311*(1), G91-G104. doi:10.1152/ajpgi.00027.2015

Takashima, Y., Horisawa, K., Udono, M., Ohkawa, Y., & Suzuki, A. (2018). Prolonged inhibition of hepatocellular carcinoma cell proliferation by combinatorial expression of defined transcription factors. *Cancer Sci*. doi:10.1111/cas.13798

Tanaka, T., Jiang, S., Hotta, H., Takano, K., Iwanari, H., Sumi, K., . . . Kodama, T. (2006). Dysregulated expression of P1 and P2 promoter-driven hepatocyte nuclear factor-4alpha in the pathogenesis of human cancer. *J Pathol, 208*(5), 662-672. doi:10.1002/path.1928

Tirona, R. G., Lee, W., Leake, B. F., Lan, L. B., Cline, C. B., Lamba, V., . . . Kim, R. B. (2003). The orphan nuclear receptor HNF4alpha determines PXR- and CAR-mediated xenobiotic induction of CYP3A4. *Nat Med, 9*(2), 220-224. doi:10.1038/nm815

Torre, L. A., Bray, F., Siegel, R. L., Ferlay, J., Lortet-Tieulent, J., & Jemal, A. (2015). Global cancer statistics, 2012. *CA Cancer J Clin, 65*(2), 87-108. doi:10.3322/caac.21262

Torres-Padilla, M. E., Fougere-Deschatrette, C., & Weiss, M. C. (2001). Expression of HNF4alpha isoforms in mouse liver development is regulated by sequential promoter usage and constitutive 3' end splicing. *Mech Dev, 109*(2), 183-193.

Torres-Padilla, M. E., Sladek, F. M., & Weiss, M. C. (2002). Developmentally regulated N-terminal variants of the nuclear receptor hepatocyte nuclear factor 4alpha mediate multiple interactions through coactivator and corepressor-histone deacetylase complexes. *J Biol Chem, 277*(47), 44677-44687. doi:10.1074/jbc.M207545200

Tsagianni, A., Mars, W. M., Bhushan, B., Bowen, W. C., Orr, A., Stoops, J., . . . Michalopoulos, G. K. (2018). Combined Systemic Disruption of MET and Epidermal Growth Factor Receptor Signaling Causes Liver Failure in Normal Mice. *Am J Pathol*. doi:10.1016/j.ajpath.2018.06.009

Tschop, M. H., Speakman, J. R., Arch, J. R., Auwerx, J., Bruning, J. C., Chan, L., . . . Ravussin, E. (2011). A guide to analysis of mouse energy metabolism. *Nat Methods, 9*(1), 57-63. doi:10.1038/nmeth.1806

Vandesompele, J., De Preter, K., Pattyn, F., Poppe, B., Van Roy, N., De Paepe, A., & Speleman, F. (2002). Accurate normalization of real-time quantitative RT-PCR data by geometric averaging of multiple internal control genes. *Genome Biol, 3*(7), Research0034.

Villanueva, A., Hoshida, Y., Toffanin, S., Lachenmayer, A., Alsinet, C., Savic, R., . . . Llovet, J. M. (2010). New strategies in hepatocellular carcinoma: genomic prognostic markers. *Clin Cancer Res, 16*(19), 4688-4694. doi:10.1158/1078-0432.CCR-09-1811

Viollet, B., Kahn, A., & Raymondjean, M. (1997). Protein kinase A-dependent phosphorylation modulates DNA-binding activity of hepatocyte nuclear factor 4. *Mol Cell Biol, 17*(8), 4208-4219.

Vuong, L. M., Chellappa, K., Dhahbi, J. M., Deans, J. R., Fang, B., Bolotin, E., . . . Sladek, F. M. (2015). Differential Effects of Hepatocyte Nuclear Factor 4alpha Isoforms on Tumor Growth and T-Cell Factor 4/AP-1 Interactions in Human Colorectal Cancer Cells. *Mol Cell Biol, 35*(20), 3471-3490. doi:10.1128/MCB.00030-15

Walesky, C., Edwards, G., Borude, P., Gunewardena, S., O'Neil, M., Yoo, B., & Apte, U. (2013). Hepatocyte nuclear factor 4 alpha deletion promotes diethylnitrosamine-induced hepatocellular carcinoma in rodents. *Hepatology, 57*(6), 2480-2490. doi:10.1002/hep.26251

Walesky, C., Gunewardena, S., Terwilliger, E. F., Edwards, G., Borude, P., & Apte, U. (2013). Hepatocyte-specific deletion of hepatocyte nuclear factor-4alpha in adult mice results in

increased hepatocyte proliferation. *Am J Physiol Gastrointest Liver Physiol, 304*(1), G26-37. doi:10.1152/ajpgi.00064.2012

Wang, Y., Matye, D., Nguyen, N., Zhang, Y., & Li, T. (2018). HNF4alpha regulates CSAD to couple hepatic taurine production to bile acid synthesis in mice. *Gene Expr*. doi:10.3727/105221618X15277685544442

Wang, Z., Salih, E., & Burke, P. A. (2011). Quantitative analysis of cytokine-induced hepatocyte nuclear factor-4alpha phosphorylation by mass spectrometry. *Biochemistry, 50*(23), 5292-5300. doi:10.1021/bi200540w

Wattanavanitchakorn, S., Rojvirat, P., Chavalit, T., MacDonald, M. J., & Jitrapakdee, S. (2018). CCAAT-enhancer binding protein-alpha (C/EBPalpha) and hepatocyte nuclear factor 4alpha (HNF4alpha) regulate expression of the human fructose-1,6-bisphosphatase 1 (FBP1) gene in human hepatocellular carcinoma HepG2 cells. *PLoS One, 13*(3), e0194252. doi:10.1371/journal.pone.0194252

Wei, L., Dai, Y., Zhou, Y., He, Z., Yao, J., Zhao, L., . . . Yang, L. (2017). Oroxylin A activates PKM1/HNF4 alpha to induce hepatoma differentiation and block cancer progression. *Cell Death Dis, 8*(7), e2944. doi:10.1038/cddis.2017.335

Weir, J. B. (1949). New methods for calculating metabolic rate with special reference to protein metabolism. *J Physiol, 109*(1-2), 1-9.

Weng, M.-Z., Zhuang, P.-Y., Hei, Z.-Y., Lin, P.-Y., Chen, Z.-S., Liu, Y.-B., . . . Tang, Z.-H. (2014). ZBTB20 is involved in liver regeneration after partial hepatectomy in mouse. *Hepatobiliary & Pancreatic Diseases International, 13*(1), 48-54. doi:10.1016/s1499-3872(14)60006-0

Weymann, A., Hartman, E., Gazit, V., Wang, C., Glauber, M., Turmelle, Y., & Rudnick, D. A. (2009). p21 is required for dextrose-mediated inhibition of mouse liver regeneration. *Hepatology, 50*(1), 207-215. doi:10.1002/hep.22979

Wolfe, A., Thomas, A., Edwards, G., Jaseja, R., Guo, G. L., & Apte, U. (2011). Increased activation of the Wnt/beta-catenin pathway in spontaneous hepatocellular carcinoma observed in farnesoid X receptor knockout mice. *J Pharmacol Exp Ther, 338*(1), 12-21. doi:10.1124/jpet.111.179390

Wurmbach, E., Chen, Y. B., Khitrov, G., Zhang, W., Roayaie, S., Schwartz, M., . . . Llovet, J. M. (2007). Genome-wide molecular profiles of HCV-induced dysplasia and hepatocellular carcinoma. *Hepatology, 45*(4), 938-947. doi:10.1002/hep.21622

Xie, Z., Zhang, H., Tsai, W., Zhang, Y., Du, Y., Zhong, J., . . . Zhang, W. J. (2008). Zinc finger protein ZBTB20 is a key repressor of alpha-fetoprotein gene transcription in liver. *Proc Natl Acad Sci U S A, 105*(31), 10859-10864. doi:10.1073/pnas.0800647105

Xu, Y., Zalzala, M., Xu, J., Li, Y., Yin, L., & Zhang, Y. (2015). A metabolic stress-inducible miR-34a-HNF4alpha pathway regulates lipid and lipoprotein metabolism. *Nat Commun, 6*, 7466. doi:10.1038/ncomms8466

Yamamoto, K., Takahara, K., Oyadomari, S., Okada, T., Sato, T., Harada, A., & Mori, K. (2010). Induction of liver steatosis and lipid droplet formation in ATF6alpha-knockout mice burdened with pharmacological endoplasmic reticulum stress. *Mol Biol Cell, 21*(17), 2975-2986. doi:10.1091/mbc.E09-02-0133

Yan, S., Tang, J., Zhang, Y., Wang, Y., Zuo, S., Shen, Y., . . . Yu, Y. (2017). Prostaglandin E2 promotes hepatic bile acid synthesis by an E prostanoid receptor 3-mediated hepatocyte nuclear receptor 4alpha/cholesterol 7alpha-hydroxylase pathway in mice. *Hepatology, 65*(3), 999-1014. doi:10.1002/hep.28928

Yang, J. D., Larson, J. J., Watt, K. D., Allen, A. M., Wiesner, R. H., Gores, G. J., . . . Leise, M. D. (2017). Hepatocellular Carcinoma Is the Most Common Indication for Liver Transplantation and Placement on the Waitlist in the United States. *Clin Gastroenterol Hepatol, 15*(5), 767-775 e763. doi:10.1016/j.cgh.2016.11.034

Yang, X., Fu, Y., Hu, F., Luo, X., Hu, J., & Wang, G. (2018). PIK3R3 regulates PPARalpha expression to stimulate fatty acid beta-oxidation and decrease hepatosteatosis. *Exp Mol Med, 50*(1), e431. doi:10.1038/emm.2017.243

Yanger, K., Zong, Y., Maggs, L. R., Shapira, S. N., Maddipati, R., Aiello, N. M., . . . Stanger, B. Z. (2013). Robust cellular reprogramming occurs spontaneously during liver regeneration. *Genes Dev, 27*(7), 719-724. doi:10.1101/gad.207803.112

Yildiz, G., Arslan-Ergul, A., Bagislar, S., Konu, O., Yuzugullu, H., Gursoy-Yuzugullu, O., . . . Ozturk, M. (2013). Genome-wide transcriptional reorganization associated with senescence-to-immortality switch during human hepatocellular carcinogenesis. *PLoS One, 8*(5), e64016. doi:10.1371/journal.pone.0064016

Yin, C., Lin, Y., Zhang, X., Chen, Y. X., Zeng, X., Yue, H. Y., . . . Xie, W. F. (2008). Differentiation therapy of hepatocellular carcinoma in mice with recombinant adenovirus carrying hepatocyte nuclear factor-4alpha gene. *Hepatology, 48*(5), 1528-1539. doi:10.1002/hep.22510

Yin, C., Wang, P. Q., Xu, W. P., Yang, Y., Zhang, Q., Ning, B. F., . . . Zhang, X. (2013). Hepatocyte nuclear factor-4alpha reverses malignancy of hepatocellular carcinoma through regulating miR-134 in the DLK1-DIO3 region. *Hepatology, 58*(6), 1964-1976. doi:10.1002/hep.26573

Yin, L., Ma, H., Ge, X., Edwards, P. A., & Zhang, Y. (2011). Hepatic hepatocyte nuclear factor 4alpha is essential for maintaining triglyceride and cholesterol homeostasis. *Arterioscler Thromb Vasc Biol, 31*(2), 328-336. doi:10.1161/ATVBAHA.110.217828

Yokoyama, A., Katsura, S., Ito, R., Hashiba, W., Sekine, H., Fujiki, R., & Kato, S. (2011). Multiple post-translational modifications in hepatocyte nuclear factor 4alpha. *Biochem Biophys Res Commun, 410*(4), 749-753. doi:10.1016/j.bbrc.2011.06.033

Yoon, J. C., Puigserver, P., Chen, G., Donovan, J., Wu, Z., Rhee, J., . . . Spiegelman, B. M. (2001). Control of hepatic gluconeogenesis through the transcriptional coactivator PGC-1. *Nature, 413*(6852), 131-138. doi:10.1038/35093050

Yu, D., Chen, G., Pan, M., Zhang, J., He, W., Liu, Y., . . . Xu, B. (2018). High fat diet-induced oxidative stress blocks hepatocyte nuclear factor 4alpha and leads to hepatic steatosis in mice. *J Cell Physiol, 233*(6), 4770-4782. doi:10.1002/jcp.26270

Yuan, X., Ta, T. C., Lin, M., Evans, J. R., Dong, Y., Bolotin, E., . . . Sladek, F. M. (2009). Identification of an endogenous ligand bound to a native orphan nuclear receptor. *PLoS One, 4*(5), e5609. doi:10.1371/journal.pone.0005609

Yue, H. Y., Yin, C., Hou, J. L., Zeng, X., Chen, Y. X., Zhong, W., . . . Xie, W. F. (2010). Hepatocyte nuclear factor 4alpha attenuates hepatic fibrosis in rats. *Gut, 59*(2), 236-246. doi:10.1136/gut.2008.174904

Zaret, K. S., & Grompe, M. (2008). Generation and regeneration of cells of the liver and pancreas. *Science, 322*(5907), 1490-1494. doi:10.1126/science.1161431

Zhang, K., Wang, S., Malhotra, J., Hassler, J. R., Back, S. H., Wang, G., . . . Kaufman, R. J. (2011). The unfolded protein response transducer IRE1alpha prevents ER stress-induced hepatic steatosis. *EMBO J, 30*(7), 1357-1375. doi:10.1038/emboj.2011.52